Validation of the novel label-free dynamic mass redistribution technology and its application for functional analysis of G protein-coupled receptors

Dissertation

zur

Erlangung des Doktorgrades (Dr. rer. nat.)

der

Mathematisch-Naturwissenschaftlichen Fakultät

der

Rheinischen Friedrich-Wilhelms-Universität Bonn

vorgelegt von

Ralf Schröder

aus

Schleiden

Bonn 2010

Angefertigt mit der Genehmigung der Mathematischen-Naturwissenschaftlichen Fakultät der Rheinischen Friedrich-Wilhelms-Universität Bonn

1. Gutachter: Prof. Dr. E. Kostenis

2. Gutachter: Prof. Dr. G. M. König

Tag der Promotion: 31.05.2011

Erscheinungsjahr: 2011

Die vorliegende Arbeit wurde angefertigt in der Zeit von Oktober 2006 bis August 2010 im Institut für Pharmazeutische Biologie der Rheinischen Friedrich-Wilhelms-Universität Bonn unter der Leitung von Frau Prof. Dr. rer. nat. Evi Kostenis.

Table of contents

1. Introduction

1.1 G protein coupled receptors

One of the largest and most diverse families in the mammalian genome is represented by the G protein coupled receptor (GPCR) superfamily. Around 800 genes encode for GPCRs which share a common membrane topology: an intracellular C-terminus, an extracellular N-terminus, and seven transmembrane (TM) helices, connected by three intracellular loops (ICLs) and three extracellular loops (ECLs) (Lander, et al., 2001, Venter, et al., 2001, Fredriksson, et al., 2003). A salient feature of GPCRs is to sense signals outside the cell and activate signal transduction within the cell, ultimately leading to cellular responses. Most GPCRs signal by activation of heterotrimeric guanosin-5'-triphosphate (GTP) binding proteins (G proteins), but progressive research indicates an increasing number of G protein-independent signaling events. Thus GPCRs are also referred to with the more general term 7TM receptors (Pierce, et al., 2002, Fredriksson, et al., 2003).

GPCRs, responsible for 80% of signal transduction across the cell membrane, are activated by a wide range of stimuli including photons, ions, small organic compounds, odorants, amino acids, lipids, fatty acids, eicosanoids, peptides and nucleotides and contribute to a host of physiological processes. They are involved in visual and smell senses, behavioral and mood regulation, immune and nervous system, and in general the body homeostasis (Millar and Newton, 2010). Also involved in pathological processes, GPCRs are important pharmacological drug targets, which is illustrated by the fact that about one third of all current therapeutics are active on GPCRs (Overington, et al., 2006, Millar and Newton, 2010). Drugable GPCRs are relevant in diseases including stroke, asthma, schizophrenia, cancer, neurological pain, migraine, allergies, gastric ulcer, diabetes, obesity and hypertension (Jacoby, et al., 2006, Chung, et al., 2008).

The GPCR superfamily is phylogenetically classified into 5 main branches: (i) the rhodopsin like receptors (672 members), (ii) the secretin receptors (15 members), (iii) the adhesion receptors (33 members), (iv) the glutamate receptors (22 members) and the (v) frizzled/taste receptors (11/25 members). Presently, there are still approximately 100 orphan GPCRs whose endogenous ligands are not identified yet, thus their role in health and disease is still to be unveiled (Fredriksson, et al., 2003, Lagerström and Schioth, 2008).

1.2 GPCRs and signaling

In a classical view GPCR signal transduction is initiated by agonist binding, leading to conformational changes of the receptor molecule accompanied by a transition from an inactive to an active state. That in turn activates the receptor bound heterotrimeric G protein, which now dissociates from the receptor and modulates downstream effector molecules (Samama, et al., 1993, Kenakin, T., 1995, Cabrera-Vera, et al., 2003).

G proteins are composed of the three subunits Gα, Gβ and Gγ and their functional principle depends on the capability of Gα to cycle between an inactive and an active conformation. In the inactive state Gα is bound to GDP and able to bind to a receptor and the Gβγ subunits. Due to GPCR activation Gα in turn is activated resulting in conformational changes that induce an exchange of GDP for GTP. In this active state the Gα molecule dissociates from the receptor and the Gβγ subunits. Now both, Gα as well as the Gβγ subunits are able to bind to corresponding effector molecules. The Gα subunit possesses a GTPase domain, which hydrolyses GTP to GDP resulting in self-inactivation, enabling Gα again to bind to a receptor and Gβγ subunits. Hence, the activation process can start again (Sprang, 1997, Oldham and Hamm, 2008).

Although the GPCR superfamily is large, the number of individual interacting G proteins is relatively small. In humans there are at least 16 Gα subunits, 5 Gβ subunits and 14 Gγ subunits. Since there are more different GPCRs than G protein families, each is generally able to interact with many different receptors. G protein heterotrimers are typically divided into four classes based on the primary sequence similarity of the Gα subunit and their functional properties: $G\alpha_s$, $G\alpha_{i/o}$, $G\alpha_{q/11}$, $G\alpha_{12/13}$ (Simon, et al., 1991, Milligan and Kostenis, 2006, Oldham and Hamm, 2008).

$G\alpha_s$ proteins are known to bind to and stimulate adenylyl cyclase (Northup, et al., 1980, Ross, E. M. and Gilman, 1980), leading to an increase of intracellular cAMP levels. This signal is further transduced by activation of protein kinase A (PKA), the exchange protein directly activated by cAMP (Epac) or the transcription factor CREB (cAMP response element binding). Further downstream targets are members of the Src family of tyrosin protein kinases (PKs) and the GTPase of tubulin (Ma, et al., 2000, Milligan and Kostenis, 2006, Woehler and Ponimaskin, 2009, Gloerich and Bos, 2010).

$G\alpha_{i/o}$ proteins are characterized by inhibition of adenylyl cylase (Bokoch, et al., 1984, Sternweis and Robishaw, 1984), resulting in a decrease of cellular cAMP levels. Downstream targets are tyrosin PKs and GTPase activating proteins (GAPs), GTPase of tubulin, and in addition $G\alpha_i$ proteins and in particular the corresponding Gβγ subunits, liberated upon $G\alpha_i$

activation also modulate ion channels like G protein activated inward rectifying potassium channel (GIRK) and calcium channels (Woehler and Ponimaskin, 2009).

$G\alpha_{q/11}$ is predominantly known to activate the phospholipase C (PLC) (Cockcroft and Gomperts, 1985), which hydrolyses phosphatidylinositol 4,5-bisphospate (PIP_2) resulting in inositol triphosphate (IP_3) and diacylglycerol (DAG). DAG can activate protein kinase C (PKC), while IP_3 acts on receptors in the endoplasmatic reticulum, resulting in release of calcium from intracellular stores. In addition $G\alpha_q$-dependent activation of potassium channels and downstream signaling towards serine and tyrosin PKs, guanine nucleotide exchange factors (GEFs) and tubulin is described (Milligan and Kostenis, 2006, Woehler and Ponimaskin, 2009).

The $G\alpha_{12/13}$ pathway (Strathmann and Simon, 1991) is lacking a distinct second messenger as there are IP3 and calcium for $G\alpha_q$ and cAMP for $G\alpha_s$- and $G\alpha_i$-mediated signaling. Best characterized downstream effectors of $G\alpha_{12/13}$ are RhoGEF-mediated activation of RhoA that in turn might activate Rho kinases (ROCK) leading to formation of stress fibers and certain downstream pathways like activation of serum response transcription factor (SRF), ultimately regulating gene expression. In some cases also calcium release via PLC was (Ross, R. A., 2009). Further, members of the family of small GTPases like Rho, Rac and Cdc42 can likewise be activated mediating various cellular effects. Additionally a variety of other interaction partners for G12/13 including cadherins and protein phosphatases and kinases, phospholipases, GAPs and GEFs have been reported (Worzfeld, et al., 2008, Ross, R. A., 2009, Siehler, 2009, Woehler and Ponimaskin, 2009).

For $G\beta\gamma$ subunits a host of effectors is described mostly associated with calcium release via channels or PLC, but also diverse kinases and nucleotide exchange factors may be affected, among others (Milligan and Kostenis, 2006, Oldham and Hamm, 2008).

GPCRs are often characterized by the G proteins binding to them but these have not to belong to one single class of G proteins. For an increasing number of receptors promiscuity of G protein coupling was demonstrated and context-dependency of these coupling events indicates a more complex and dynamic signaling system than expected many years before (Galandrin, et al., 2007, Kenakin, T., 2010).

As more downstream signaling events mitogen-activated protein kinases (MAPK) can be activated by several different pathways. GPCRs are known to activate each of the three known mammalian MAP kinases: extracellular-regulated kinases 1/2 (ERK1/2), the c-Jun amino terminal kinases (JNKs) and the p38 MAPKs, ultimately leading to regulation at the gene expression level (Pierce, et al., 2002, Woehler and Ponimaskin, 2009).

GPCRs are also able to mediate G protein-independent signaling events. Best known is the β-arrestin2-dependent signaling (Pierce and Lefkowitz, 2001, Wei, et al., 2003, Lefkowitz, 2007) targeting MAP kinases, Src and AKT among others. But also Janus protein kinase/signal transducers and activators of transcription (JAK/STAT), the Src-protein family, tyrosine kinases, GPCR kinases (GRKs), and PDZ domain-containing proteins have been suggested to directly relay signals from GPCRs independent of G proteins (Galandrin, et al., 2007, Millar and Newton, 2010).

Signaling activity of GPCRs can be regulated and modulated by a lot of cellular mechanisms including control of expression levels, phosphorylation and internalization. Commonly, signaling of activated receptors is regulated by desensitization mechanisms to avoid exaggerated responses. In many cases, receptors are phosphorylated by GRKs which in turn enables binding of β-arrestin proteins. This initiates the association of clathrin and adaptor protein 2 (AP-2) leading to receptor endocytosis. Subsequently, the receptor molecule may be degraded intracellularly or recycled back to the cell surface raring again for signaling (Sorkin and von Zastrow, 2009a).

For an increasing number of receptors further features are reported, which can modulate GPCR-mediated signaling including biased agonism (i.e. ligation of different agonists to one receptor activates one or more different signaling pathways), differential receptor phosphorylation inducing variable signaling events, receptor crosstalk with or without homo- and heterodimerisation affecting signaling properties, and recent advances are made for the detection of sustained signaling events after receptor internalization (Galandrin, et al., 2007, Kenakin, T. P., 2009, Milligan, 2009, Mullershausen, et al., 2009, Calebiro, et al., 2010, Prezeau, et al., 2010).

The complexity of possible GPCR behaviors and phenomena including inverse agonism, allosteric modulation and biased agonism, also referred to as functional selectivity or pluridimensional efficacy, is no longer explainable by a simple two state receptor model that switches between an inactive and an active state only. It seems that receptors might rather oscillate between multiple conformations, which can be differentially stabilized by ligands and in turn permit access to the whole or only a subset of the complete receptor signaling repertoire (Galandrin, et al., 2007, Kenakin, T. P., 2009, Kenakin, T., 2010).

The rising complexity in the known GPCR/7TM receptor signaling behavior seems to require detection systems with complex readouts improving access to the plasticity of receptor-mediated signaling behavior.

1.3 Detection of receptor interactions and functionality

In the field of GPCR research a lot of techniques for detection of GPCR-ligand interactions, receptor activation and downstream signaling events are established.

Binding assays are necessary to investigate the direct ligand-receptor interaction, and in this manner the affinity of a ligand towards a receptor binding site can be determined. Receptor efficacy on the other hand is determined by functional assays. [^{35}S]GTPSγS assays capture direct activation of G proteins in closest proximity to the receptor, but this method is particularly amenable for $G\alpha_i$-coupled receptors and not in living cells (Milligan, 2003). Most current cell-based assays are second messenger assays for cAMP and IP3 (or IP1) or calcium, capturing specific events of $G\alpha_s$-, $G\alpha_i$- and $G\alpha_q$-dependent pathways, usually performed as endpoint assays including cell lysis. Very popular is the detection of intracellular calcium release, which can be recorded in real time, using calcium sensitive fluorescence dyes. Mainly signaling by $G\alpha_q$ is captured this way but in some cases also other pathways namely $G\alpha_i$ are linked to mobilization of intracellular calcium. Furthermore, success was achieved designing promiscuous G proteins, able to funnel $G\alpha_s$- or $G\alpha_i$-coupled receptors to $G\alpha_q$ and thus getting access to their signaling by detection of calcium release (Conklin, et al., 1993, Kostenis, et al., 2005b, Heilker, et al., 2009).

The lack of a specific second messenger complicates the measurement of $G\alpha_{12/13}$-dependent signaling. RhoA activation by RhoA-GTP immunoblot detection is practiced and also direct detection of $G\alpha_{12/13}$ activation by immunoprecipitation (IP) is possible, but these techniques are less suited for pharmacological studies. In high content screen (HCS) approaches (see below) fluorescent biosensors for activated RhoA are available and cellular translocation of RhoGEF can be observed by green fluorescence protein (GFP) tagged p115-Rho-GEF (Meyer, et al., 2008, Siehler, 2009).

Direct activation of far downstream effectors is detectable by phosphorylation assays as performed for MAP kinases and reporter gene assays are also used for various pathways, where certain signaling events trigger expression of a cotransfected luciferase reporter gene (Liu and Wu, 2004). Microscopy techniques, using colors or fluorescent labels are mainstay for internalization and trafficking studies (Hein, et al., 1997, Whistler, et al., 2002).

Other approaches to detect receptor and signaling behavior are intermolecular fluorescence resonance energy transfer (FRET) and bioluminescence resonance energy transfer (BRET) techniques for detection of interplay between signaling cascade components like interactions between G protein subunits and receptors or beneath each other as well as for other interacting molecules like β-arrestins. Intramolecular FRET at receptor molecules was also shown for

muscarinic receptors gaining access to real time receptor activation studies (Hoffmann, et al., 2005, Marullo and Bouvier, 2007).

All these techniques provide valuable information and contribute to the present knowledge about GPCRs and their comprehensive behavioral repertoire and impact in complex signaling events. Indispensable as these techniques are, they usually require manipulations or molecular engineering of cells, such as overexpression of the target GPCRs, loading of dyes or fluorescent molecules, cotransfection with promiscuous G proteins or tagged signal cascade components. Due to their invasive nature - manipulations may alter the cellular physiology - the risk of causing artificial results may have to be taken into account (Lee, et al., 2008, Kenakin, T. P., 2009).

Recent approaches to get access to complex receptor functions and signaling properties are on the one hand high content screens (HCS) and on the other hand label-free technologies. HCS deals also with invasive techniques and represents a combination of high resolution fluorescence microscopy with automated image analysis in a microtiterplate format. By using diverse fluorescent labels many GPCR functions including ligand binding, internalization, second messenger generation and downstream signaling events are detectable, some of them in real time (Heilker, et al., 2009). Label-free cell based assays on the other hand provide access to receptor efficacy in a non-invasive and holistic manner by impedance-based or optical-based biosensors (Heilker, et al., 2009, Kenakin, T. P., 2009, Rocheville and Jerman, 2009).

1.4 Label-free methods

In contrast to the invasive techniques mentioned above, during the last years label-free assay platforms emerged which allow detection of functional receptor activity and properties in living cells, in real time and without interventions in the investigated cells, and a single detection system is capable to capture various responses of GPCRs that couple to different pathways.

At time label-free detection of GPCR-mediated cellular responses are possible with three different methods: optical-based biosensors, impedance-based biosensors and acidification-based microphysiometry. The latter detects changes in the extracellular acidification rate (ECAR) as a reflection of GPCR mediated Na^+/H^+ exchange (NHE) (McConnell, et al., 1992, Kramarenko, et al., 2009). Whereas acidification-based systems so far do not have found

broad application in GPCR research, optical- and impedance-based systems are apparently widely employed in the pharmaceutical industry (Peters, et al., 2009, Scott and Peters, 2010).
Impedance-based instruments utilize interdigitated electrodes embedded within each well of a microtiter plate. Cells plated on these electrodes resist the flow of a small, applied current. Even subtile changes in cell shape, adhesion and cell-cell interaction alters impedance. GPCRs induce those cellular changes through different signaling pathways and in this way changes in impedances can be used as efficacy readout (Heilker, et al., 2009, Scott and Peters, 2010).
Optical-based instruments detect and quantify the index of refraction near the surface of a microtiter plate, which therefore contains an optical grating surface, serving as biosensor, in each well. Cells are cultivated directly on the biosensor and GPCR-induced cellular changes lead to movement of cellular matters, herein referred to as dynamic mass redistributions (DMR). DMR in turn might alter optical density near the surface and is detectable this way (Fang and Ferrie, 2007, Lee, et al., 2008, Scott and Peters, 2010). This technology was originally developed for biochemical binding assays and subsequently shown to be capable of detecting GPCR-induced mass redistribution in cells.

1.4.1 Label-free dynamic mass redistribution technology

The Corning® Epic® System used in the present study represents an optical-based instrument for cell based label-free detection of GPCR-mediated responses by DMR measurements. Ligand-induced activation of a receptor might lead to a plethora of cellular events and responses including movement and rearrangement of signaling cascade components, dynamic interaction with regulatory proteins (e.g. β-arrestins and GRKs), internalization, cytoskeleton rearrangements and changes in cell shape. All these (intra-) cellular movements may contribute to dynamic mass redistribution, ultimately leading to changes in optical density, which in turn is detected by the biosensor.
For experiments within the scope of this thesis, a beta version of the Corning® Epic® System was used, consisting of a temperature control unit, an optical detection unit, an on-board robotic liquid handling device and an affiliated incubator. For measurement of DMR cells were grown on a 384-well Epic® microplate which contains a resonant waveguide grating biosensor in the bottom of each well.
Functional principle (see also **Fig. 1**): the microplate underside is illuminated with polarized broadband light centered at 830 nm, and light of a given wavelength is guided to travel parallel through the bottom of each microwell. The electromagnetic field of the light extends

into the adjacent cells, and depending on the optical density in this area, the light loses energy, is reflected and wavelength is measured. In response to cell function-affecting interventions (e.g. ligand-induced G-protein signaling) cellular components are relocated, leading to changes of local index of refraction, which in turn results in a shift of the reflected wavelength. The magnitude of wavelength shift is proportional to the amount of DMR. Increase of mass contributes positively and decrease negatively to the overall response. For the Epic system penetration depth is 150 nm i.e. DMR that takes place within this penetration depth can be detected.

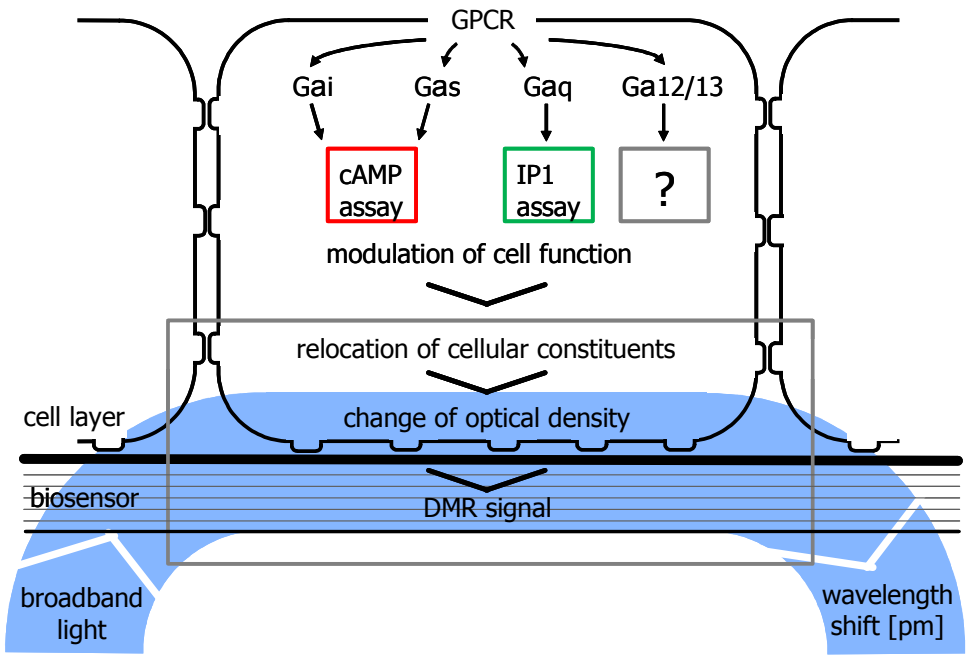

Figure 1: Sketch of dynamic mass redistribution (DMR) measurement. Activation of the four major G protein dependent pathways leads to modulation of cell function accompanied by relocation of cellular constituents and ultimately to changes of optical density which is detected by the induced wavelength shift. Second messenger generation allows detection of $G\alpha_i$, $G\alpha_s$ and G_q signaling by conventional assays via detection of cAMP and IP1 generation, whereas for $G\alpha_{12/13}$ signaling (?) a conventional second messenger assay is not known (figure adapted from Schröder et.al. (2010)).

DMR technology is of interest for and used by pharmaceutical companies in drug screening approaches including high throughput screening (HTS), but it might provide more than a sensitive, label-free readout for various pathways. DMR measurements enable monitoring of GPCR-mediated cellular responses in real time, resulting in a holistic readout that may display the integrated efficacy of complex signaling behavior. This might also be of high value for basic GPCR research as it provides access to complex and intertwined cellular

responses (Fang, 2007, Fang and Ferrie, 2007, Lee, et al., 2008, Schröder, et al., 2009, Schröder, et al., 2010).

1.5 Signaling pathway modulators

G protein coupling specificity of GPCRs can be investigated by the use of specific toxins and other pathway-affecting substances.

Pertussis toxin (PTX)

This toxin is a hexameric protein derived from the bacterium *Bordetella pertussis* and was found to irreversibly ADP-ribosylate $G\alpha_{i/o}$ and $G\alpha_t$ proteins (Kaslow, et al., 1987). As a result $G\alpha_{i/o}$ proteins remain locked in their inactive GDP-bound state, unable to be activated and to inhibit adenylyl cyclase activity. $G\alpha_t$ (transducin) is involved in the visual process and not relevant for the topics explored herein.

Cholera toxin (CTX)

The pentameric CTX protein is derived from *Vibrio cholerae* and irreversibly ADP-ribosylates the $G\alpha_s$ subunit of heterotrimeric G proteins, resulting in inhibition of GTPase activity (Gill and Meren, 1978). In contrast to the action of PTX does CTX lead to a permanent activation of the corresponding G protein. This results in a durable activation of adenylyl cyclase accompanied by increased cAMP levels. Since for $G\alpha_s$ proteins no selective inhibitor is known to date, CTX is used for investigation of the $G\alpha_s$ pathway: prestimulation of adenyly cyclase and the accompanied sustained cAMP increase causes that further $G\alpha_s$ activation is no more detectable and therefore masked. Due to its stimulatory character investigations with CTX have to be considered with care, because the sustained cAMP level elevation is likely to alter the cell's responsiveness and receptor functions.

Forskolin

Direct activation of adenylyl cyclase is mediated by forskolin (de Souza, et al., 1983) and therefore used in inhibitory cAMP second messenger assays. It can also be used for investigations at the $G\alpha_s$ pathway through its masking effect by prestimulation, similar to CTX.

YM-254890

The cyclic peptide YM-254890 is producd by *Chromobabacterium sp.* and found as potent and selective inhibitor for the $G\alpha_{q/11}$ pathway (Takasaki, et al., 2004). The suggested point of action is at the receptor $G\alpha_{q/11}$ interaction or the subsequent guanine nucleotide exchange step (Nishimura, et al., 2010).

Amuminiumfluoride (AlF_4^-)

AlF_4^- ions, herein referred to as AlF, are capable to interact with G proteins of all coupling classes resulting in a pan-activation (Bigay, et al., 1987). This effect may be useful in connection with the issue of G-protein dependence of signaling events.

Up to date, no inhibitor for $G\alpha_{12/13}$ proteins is known, thus identification of $G\alpha_{12/13}$ proteins as trigger of cellular response has to be explored by other methods including dominant negative G proteins, siRNA or approaches using antibodies against these proteins.

1.6 Eicosanoids, prostanoids and prostaglandins

Eicosanoids are generated from twenty carbon essential fatty acids and represent signaling molecules that exert complex control over many body systems. Prostanoids represent a subclass of eicosanoids and are classified according to their precursor dihomo-γ-linolenic acid (DHGLA) (20:3(n-6)) as 1-series, arachidonic acid (AA) (20:4(n-6)) as 2-series and eicosapentaenoic acid (EPA) (20:5(n-3)) as 3-series of prostanoids. The 1-series and the 3-series are predominantly described as anti-inflammatory, whereas a huge number of pathophysiological processes are correlated with increased amounts of the 2-series eicosanoids (Bell, et al., 1994, Smyth, et al., 2009).

Arachidonic acid is produced from membrane phospholipids by the action of phospholipase A_2 (PLA_2) and can be converted into different eicosanoid subfamilies. Enzymatical conversion by cyclooxygenases (COX) leads to prostanoids, with lipoxygenases (LOX) to leukotriens and lipoxins and with cytochrome P450 to hydroxyeicosatetraenoic acids (HETEs). COX-1 and COX-2 catalyzed oxidation of AA leads to prostaglandin (PG) G_2 (PGG_2), which is immediately reduced to PGH_2, that in turn serves as a substrate for the prostanoid synthase enzymes responsible for the generation of five principle bioactive prostanoids of the 2-series: prostaglandin D_2 (PGD_2), prostaglandin E_2 (PGE_2), prostaglandin $F_2\alpha$ ($PGF_2\alpha$), prostacyclin I_2 (PGI_2) and thromboxane A_2 (TXA_2) (**Fig. 2**). In addition a host

of further converted metabolites with biological activity are detectable (Bell, et al., 1994, Levin, et al., 2002, Hata and Breyer, 2004, Smyth, et al., 2009).

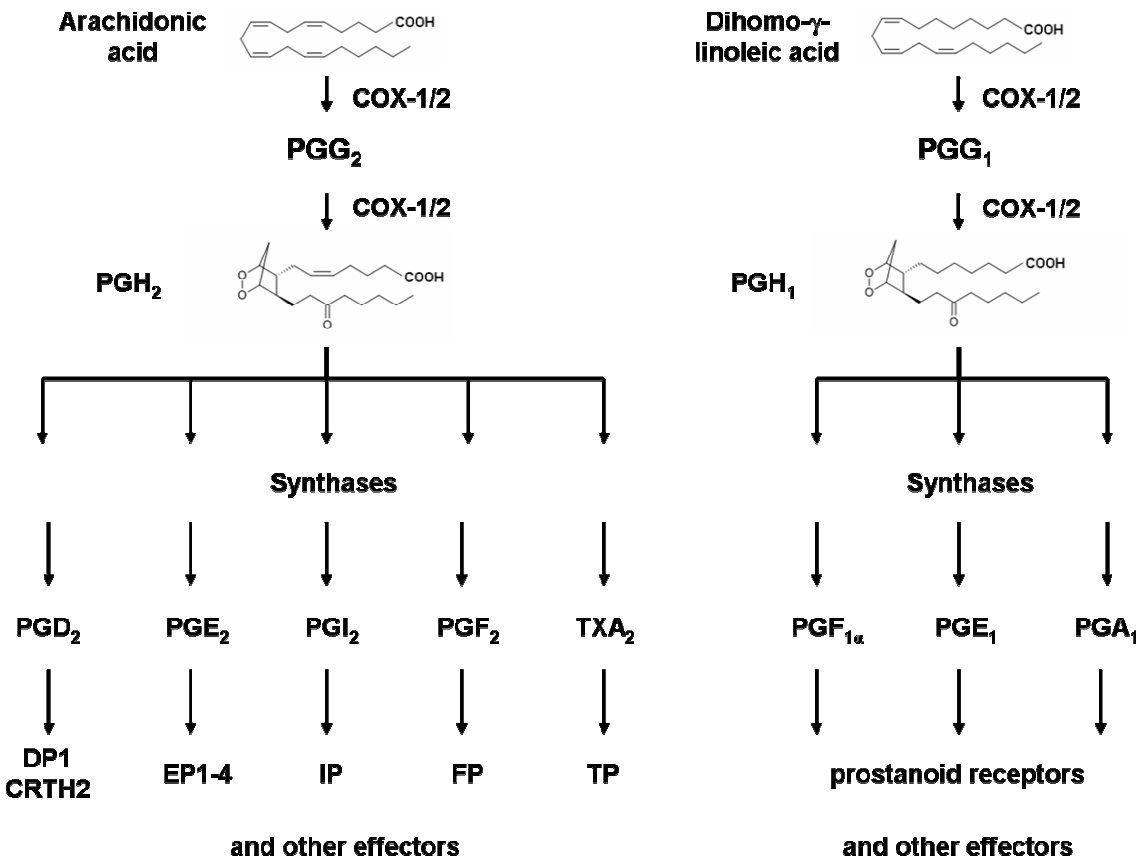

Fig 2: Prostanoid biosynthesis
Archaidonic acid and dihomo-γ-linolenic acid are converted by cyclooxygenase 1 and 2 (COX-1/2) to prostaglandin (PG) H_2 (PGH_2) and H_1 (PGH_1) respectively, the common precursor of four principal prostaglandins and one thromboxane (TX). Specific synthases including PGD synthase (PGDS) and PGE synthase (PGES) catalyze the formation of prostanoids, which in turn interact with the corresponding receptors as D-prostanoid receptor (DP1), chemo attractant-receptor homologous molecule expressed on T-helper type 2 cells (CRTH2), E-prostanoid receptor (EP), I-prostanoid receptor (IP), F-prostanoid receptor (FP) and thromboxane receptor (TP), or other effectors.

Prostanoids are ubiquitously produced and elicit a diverse set of pharmacological effects in modulating physiological systems like the CNS, cardiovascular, gastrointestinal, genitourinary, endocrine, respiratory and immune systems. A broad array of diseases is correlated to prostaglandin synthesis like inflammation and pain, hypertension, cardiovascular diseases and cancer. Generally 2-series prostanoids are considered to be potent pro-inflammatory mediators, indicated by the great market of pharmacological therapeutics that block prostaglandin biosyntheses like COX inhibitors. However, anti-inflammatory effects

were also observed, indicating a complex interaction of mediators, and effectors. Conversion of DHGLA by COX-1/2 generates PGH_1, which is converted to the 1-series of prostaglandins (**Fig. 2**). Further metabolites like PGE_1 and PGA_1 are mainly referred to as anti-inflammatory, and moreover no leukotriens are generated by this pathway (Zurier and Quagliata, 1971, Kunkel, et al., 1979, Zurier, 1982, Rossi, et al., 2000, Levin, et al., 2002, Hata and Breyer, 2004, Mandal, et al., 2005, Smyth, et al., 2009). This is reflected in nutrition recommendations for diets enriched with ω-3 fatty acids and γ-linolenic (GLA) acid, which, among other effects, are supposed to lead to increased levels of DHGLA resulting in formation of anti-inflammatory mediators (Chilton, et al., 2008).

1.7 Prostanoid receptors

Mediators of physiological prostanoid effects are G protein-coupled prostanoid receptors. To date nine receptors are known, which all belong to the class of rhodopsin like receptors: four E-prostanoid receptors (EP_1-EP_4), the F-prostanoid receptor (FP), the I-prostanoid receptor (IP), the thromboxane receptor (TP) and the D-prostanoid receptors 1 and 2 (DP1 and DP2).DP2 is also referred to as chemoattractant receptor homologous molecule expressed on T-helper type 2 (Th2) cells (CRTH2) (Hata and Breyer, 2004).

1.7.1 Chemoattractant receptor homologous molecule expressed on T-helper type 2 cells

PGD_2 is the major agonist of two pharmacologically distinct G protein-coupled receptors: The D-prostanoid 1 (DP1) receptor (Boie, et al., 1995) and CRTH2, representing the most recently discovered prostanoid receptor. CRTH2 was initially identified as a Th2 cell-specific surface receptor and subsequently demonstrated to bind PGD_2 with approximately equal affinity in a nanomolar range compared to that observed for the DP1 receptor (Nagata, et al., 1999a, Nagata, et al., 1999b, Hirai, et al., 2001). Phylogenetic studies revealed that CRTH2 shares only little similarity to the other known prostanoid receptors and is more related to chemoattractant receptors like the leukotrien receptors (BLTR and CysLTR), anaphylatoxin C3a and C5a receptors and N-formyl peptide receptors (FPR) (Nagata, et al., 1999a, Hata and Breyer, 2004). CRTH2 is expressed in various human tissues whereas significant levels of mRNA were detected in blood leucocytes/lymphocytes such as Th2 cells (but not in Th1 cells), eosinophils and basophils, as well as in brain, heart, stomach and other tissues (Marchese, et al., 1999, Nagata, et al., 1999b).

Activation of CRTH2 leads to inhibition of cAMP via $G\alpha_i$ proteins, but signaling via $G\beta\gamma$ protein subunits has also been reported and results in intracellular calcium mobilization in a variety of cell types like Th2 cells and eosinophils (Hirai, et al., 2001, Sawyer, et al., 2002, Kostenis and Ulven, 2006). PTX sensitivity was also observed for activation of phosphatidylinositol-3-kinase (PI3K), PLC and MAP kinases in eosinophils (Stubbs, et al., 2002). G protein-independent signaling via β-arrestin 2 was shown (Mathiesen, et al., 2005) whereas internalization occurs in a β-arrestin 2-independent manner and the receptor molecule is not phosphorylated upon agonist stimulation (Schröder, et al., 2009). The C terminus of CRTH2 constrains Gαi signaling, which may compensate for the absence of the classical phosphorylation-dependent signal attenuation (Schröder, et al., 2009). Downstream signaling of CRTH2 results in PI3K-dependent phosphorylation of AKT, phosphorylation of glycogen synthase kinase-3β (GSK-3β) and nuclear translocation of NFAT (Xue, et al., 2007). CRTH2 appears to play an import role in inflammation, allergic diseases and asthma and is predominantly described as pro-inflammatory. In this context it is worth to mention that the $G\alpha_s$-coupled DP1 receptor is also involved in inflammatory reactions, and in many cases it seems to exhibit functions contrary to CRTH2 (Kostenis and Ulven, 2006, Pettipher, 2008).

Activation of CRTH2 can lead to a plethora of biological effects that include shape change, chemotaxis, respiratory burst and degranulation of eosinophils (Gervais, et al., 2001, Hirai, et al., 2001, Monneret, et al., 2001, Heinemann, et al., 2003), chemotaxis and histamine release by basophils (Hirai, et al., 2001, Yoshimura-Uchiyama, et al., 2004) and chemotaxis, release of pro-inflammatory cytokines from Th2 cell and it counteracts apoptosis of Th2 cells (Xue, et al., 2005, Xue, et al., 2009). Several studies in mice have shown that CRTH2 antagonists can ameliorate allergen-induced cutaneous, pulmonary and upper respiratory inflammation (Böhm, et al., 2004, Uller, et al., 2007, Lukacs, et al., 2008, Nomiya, et al., 2008, Shiraishi, et al., 2008). In humans sequence variants of the CRTH2 gene are associated with asthma and allergic phenotypes (Huang, et al., 2004, Cameron, et al., 2009). Recent data suggest that CRTH2 is also expressed on monocytes and macrophages and mediates their migration induced by PGD2 and endotoxin (Tajima, et al., 2008, Shirasaki, et al., 2009) and CRTH2 expression levels are elevated in patients with allergic dermatitis (Yahara, et al., 2010).

A hallmark of CRTH2 is that it is not only activated by PGD_2 but also by other endogenous ligands including several PGD_2 metabolites and other prostanoids not only from the D-type. Endogenous ligands are the PGD_2 metabolites 13,14-dihydro-15-keto-PGD_2 (DK-PGD2), Δ^{12}-PGD_2, 15-deoxy-$\Delta^{12,14}$-PGD_2 (15d-PGD_2) and also metabolites with J-rings as PGJ_2, Δ^{12}-PGJ_2, 15-deoxy-$\Delta^{12,14}$-PGJ_2 (15d-PGJ_2) or F-rings as 11β-$PGF_2\alpha$ (Hirai, et al., 2001,

Monneret, et al., 2002, Sawyer, et al., 2002, Heinemann, et al., 2003, Gazi, et al., 2005, Sandig, et al., 2006). Interestingly, also PGs generated independently from PGD synthase were found to be active at CRTH2 like $PGF_2\alpha$ (Sandig, et al., 2006), 11-dehydro Thromboxane B2 (11d-TXB2) (Böhm, et al., 2004) and recently the precursor of the 2-series of prostanoids PGH_2 (Schuligoi, et al., 2009) (relevant structural formulas are depicted in chapter 2.2.3, **table 1a,b** and chapter 3.4, **Fig. 37**).

Being involved in inflammation and allergic diseases, CRTH2 is an attractive therapeutic target and a large number of structurally diverse antagonists have meanwhile become available from both academic and industrial researchers (Ulven and Kostenis, 2010).

1.7.2 E-prostanoid receptors

Four different GPCRs are predominantly activated by ligation of E-prostanoids and are therefore classified as E-prostanoid (EP) receptors and designated as EP1 through EP4.

EP2 and EP4 are $G\alpha_s$-coupled whereas EP4 is additionaly described to activate PI3K, but$G\alpha_i$ coupling has also been reported in a recent study (Leduc, et al., 2009). EP1 signals via calcium increase by an unknown mechanism (Sugimoto and Narumiya, 2007). For EP3 at least three isoforms, EP3α, β and γ were found, all predominantly coupling to $G\alpha_i$ proteins. However, EP3α and β additionally couple to $G\alpha_{12}$ proteins leading to IP3 formation and calcium release, whereas EP3γ might also activate $G\alpha_s$ proteins, but in addition IP3 and calcium release has been described. EP receptors exhibit different tissue distributions and are involved in a host of physiological and pathophysiological processes including ovulation and fertilization, bone formation and duodenal secretion, but also inflammation, fever, pain and some cancer diseases (Hata and Breyer, 2004, Sugimoto and Narumiya, 2007, Smyth, et al., 2009).

PGE_2 and PGE_1 are described to induce different physiological effects. Whereas PGE_2 is predominantly associated with pathological effects, for PGE_1 mainly anti-inflammatory properties are described. PGE_1 seems to prefer EP2 and EP4 receptors and is therefore associated with cAMP elevation. PGE_1 and its synthetic derivative misoprostol are used as therapeutics in gynecology and obstetrics, for diabetic kidney disease, erectile dysfunction, cutaneous diseases and wound healing (Levin, et al., 2002, Boulvain, et al., 2008, Murota, et al., 2008, Eardley, et al., 2010, Wang, et al., 2010).

1.8 Aim and scope

The present study is based on the validation and utilization of the recently developed label-free DMR assay technology (Corning® Epic® system) as a novel cell based GPCR functional assay system. Up to date, this technique has been predominantly used for high throughput screening and pharmacological ligand profiling in pharmaceutical companies and at the beginning of this study, validation of this novel technology platform has been performed on a rather empirical basis aimed to provide feasibility for drug screening approaches.

- The first objective was to explore the usability of DMR technology for GPCR basic research, with regard to precise allocation of signaling pathway origins to the captured response profiles. Of particular interest in this context was the $G\alpha_{12/13}$ pathway, which is not accessible by conventional second messenger assays. The pursued strategy was to choose GPCRs from the four main coupling classes and to examine their response profiles regarding the corresponding pathways by a panel of toxins, inhibitors and pathway affecting agents. For comparison, traditional second messenger assays were included.

- A further aim was to explore the sensitivity of DMR technology with regard to detection of endogenously expressed receptors, even in primary cells, which are known to display lower receptor expression levels as compared with recombinant cell systems. Primary and immortalized human keratinocytes were chosen as cellular model system and the known cAMP elevating agent PGE_1 was selected as stimulus and examined using both the novel DMR assay platform as well as traditional cAMP second messenger assays for comparison.

- As DMR technology validation was successful, a ligand screening approach at CRTH2 stably expressed in HEK293 cells was conducted. Since CRTH2 is activated by a plethora of endogenous prostanoid ligands, two main questions arose: (i) do additional prostanoid ligands exist with bioactivity on CRTH2 and (ii) do CRTH2 ligands differ regarding their induced signaling behavior? If so, this might be detectable by a holistic readout provided by the DMR assay system. In order to provide a comprehensive overview, the DMR-supported ligand screening at CRTH2 was designed with 2-series prostanoids known to activate CRTH2, as well as with the main representatives of the 1-series of PGs, including the corresponding biosynthetic precursors.

2. Results

2.1 Validation of DMR technology as functional assay for GPCR characterization

The first part of the presented study deals with the exploration and validation of the recently developed label-free dynamic mass redistribution (DMR) technology (Epic® system, Corning®) (chapter 1.4.1), with regard to the origins of GPCR mediated signaling events. This was accomplished by utilizing the receptors CRTH2, EP2/EP4, FFA1 and GPR55 as representatives of GPCRs linked to G proteins of the four main coupling classes $G\alpha_{i/0}$, $G\alpha_{s}$, $G\alpha_{q/11}$ and $G\alpha_{12/13}$ respectively.

2.1.1 DMR reflects $G\alpha_i$-dependent CRTH2 response

The DMR technology validation study was initiated by examinations of CRTH2, referred to as $G\alpha_i$-coupled, leading to inhibition of cAMP levels, and for some cells also PTX-sensitive calcium signaling is described (Hirai, et al., 2001, Sawyer, et al., 2002, Kostenis and Ulven, 2006) (see also chapter 1.7.1). In addition, signaling via β-arrestin2 in a G protein-independent manner was also observed (Mathiesen, et al., 2005). Known for its weak functional responses compared to other $G\alpha_i$-coupled receptors (Schröder, et al., 2009), it was of interest to determine whether CRTH2-dependent signaling is detectable at all and if so, which signaling events are responsible for the detected signals.

In order to explore this, HEK293 cells stably expressing CRTH2 (CRTH2-HEK) and native HEK293 (HEK) cells were seeded onto Epic® biosensor microplates and cultivated for ~24 h to reach confluent monolayers. During DMR assay performance, cells were challenged with various concentrations of the CRTH2 specific agonist DK-PGD_2 (Hirai, et al., 2001, Kostenis and Ulven, 2006), and the resulting wavelength shift was detected and recorded as a measure of receptor activation over time. The captured responses are depicted in **figure 3a,b** and subsequently they will be referred to as signatures or traces.

CRTH2-HEK cells responded with robust and concentration-dependent signals to challenging with DK-PGD_2 (**Fig. 3a**), whereas native HEK cells were unaffected by this treatment (**Fig. 3b**). In **figure 3a** the timepoint of agonist addition is denoted by an arrow, indicating

that the captured response appeared immediately after compound application. This was generally observed for all receptors and the corresponding traces examined in this study.

The response of DK-PGD_2-induced traces in CRTH2-HEK cells exhibited a characteristic shape: a rapid increase, reaching a point of maximum response, which was followed by a steep decrease. Usually the traces did not touch the base line (zero) but after about 1200 s they declined only very slowly and appeared to reach a plateau phase paralleling the x-axis.

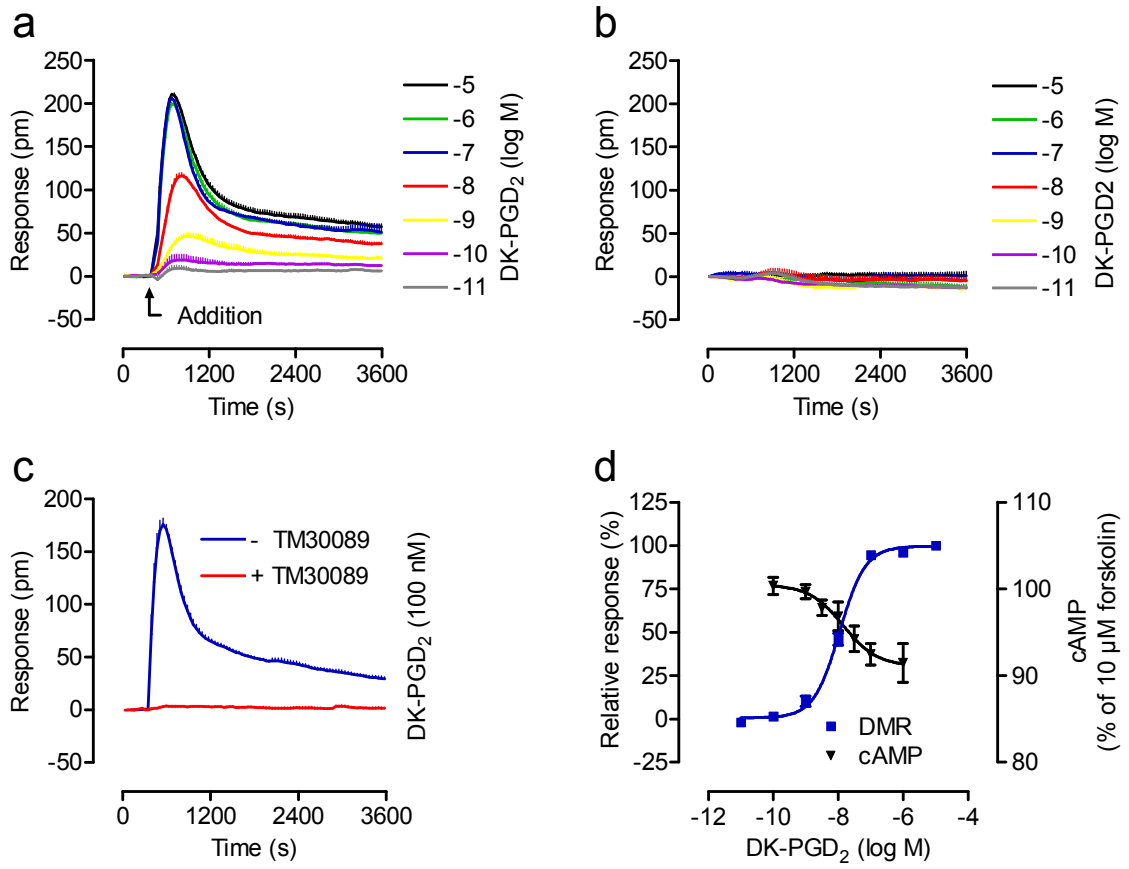

Figure 3: DMR enables measurement of CRTH2. HEK293 cells stably expressing CRTH2 (**a**) and native HEK293 cells (**b**) were challenged with the indicated concentrations of the specific CRTH2 agonist DK-PGD2, and wavelength shift was monitored over time. Shown are representative data (mean + SEM) out of six (**a**) or four (**b**) independent experiments. (**c**) The signal of DK-PGD2 in stable CRTH2 transfectants was inhibited by pretreatment with 1 µM of the CRTH2 specific antagonist TM30089. (**d**) Concentration effect curves of DMR data were generated by the maximum response between 300 and 1200 s. CRTH-mediated decrease of intracellular cAMP is calculated as percent inhibition of adenylyl cyclase stimulated with 10 µM forskolin. Calculated molar pEC_{50} values are: DMR: 7.96 ± 0.04, cAMP: 7.85 ± 0.34. Data are mean ± SEM of at least three independent experiments, each performed in triplicates.

To further confirm that induced signaling induced by DK-PGD_2 was CRTH2-dependent (**Fig. 3a**), CRTH2-HEK cells were pretreated for 1 h with 1 µM of the CRTH2 specific antagonist TM30089 (Mathiesen, et al., 2005) or assay buffer as a control, both containing equal amounts of DMSO, before agonist addition. TM30089 pretreatment led to a total inhibition

compared with the signature generated by addition of 100 nM DK-PGD_2 to buffer-pretreated cells (**Fig. 3c**). By this it was verified that CRTH2 was responsible for the captured traces. Additionally, Schild plots were performed, which are depicted in a later context (chapter 2.1.5.2 (**Fig. 15**)). Quantification of the DMR-derived traces for the generation of concentration effect curves was performed by gathering the maximum responses in the range of 300 and 1200 s (chapter 5.4.8). The results are depicted in **figure 3d**. Additionally, the effect of DK-PGD_2 at CRTH2-HEK cells was determined by traditional inhibitory cAMP accumulation assays, where accessorily to the indicated agonist concentrations, 10 µM forskolin was added (**Fig. 3d**) in order to stimulate adenylyl cyclase. The comparison of concentration effect curves obtained by DMR and cAMP assays revealed that calculated molar pEC_{50} values were very similar (**Fig. 3**, legend). However, the resulting assay windows were quite different. The forskolin induced cAMP level was decreased less than 10%, which is generally in agreement with the observation that DK-PGD2 is a partial agonist at CRTH2 (Hirai, et al., 2001, Kostenis and Ulven, 2006). But obviously, the cAMP assay offered only a small assay window in contrast to the DMR measurements, which provided robust signals and small sized error bars.

These results demonstrated that DMR technology enables the detection of CRTH2-dependent signaling in a recombinant HEK293 expression system. The signals were regarded as specific for CRTH2 because (i) a CRTH2 specific agonist was used (DK-PGD_2), (ii) only CRTH2-HEK and not HEK cells responded to DK-PGD_2 and (iii) the obtained signatures were totally inhibited in the presence of the CRTH2 specific antagonist TM30089.

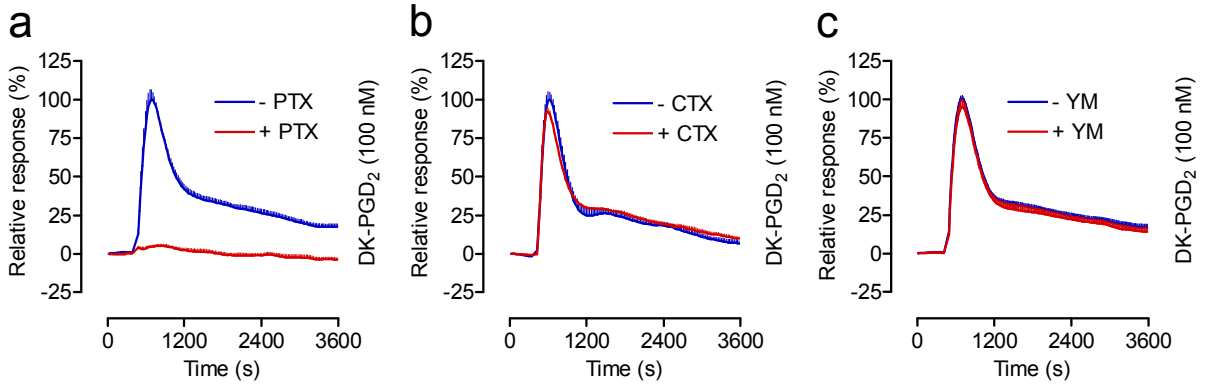

Figure 4: The CRTH2-mediated DMR trace is triggered by Gα_i proteins. The CRTH2-mediated DMR response of DK-PGD2 in HEK293 cells stably expressing CRTH2 is blocked by (**a**) pretreatment with 5 ng/ml of pertussis toxin (PTX) but not with (**b**) 100 ng/ml of cholera toxin (CTX) or (**c**) 300 nM YM25890 (YM). Shown are representative data (mean + SEM) of four to six independent experiments.

To explore which signaling events are reflected in the cumulative DMR response profile, CRTH2-HEK cells were pretreated for 18 h with the $G\alpha_i$ inhibitor pertussis toxin (PTX). Moreover, in parallel approaches the cells were pretreated for 2.5 h with the $G\alpha_q$ inhibitor YM25890 (YM) or for 18 h with the $G\alpha_s$ activator cholera toxin (CTX) (chapter 1.5). Pretreatment with PTX resulted in virtually total inhibition of the response obtained from 100 nM DK-PGD_2. However, neither CTX nor YM pretreatment did affect the CRTH2-dependent signatures (**Fig. 4**), excluding an involvement of the $G\alpha_s$ or $G\alpha_q$ pathway in receptor signaling. A very weak response remained after PTX pretreatment, when compared to antagonist-pretreated cells (**Fig. 3c**). This slight difference was observed during most assays and may be due to non $G\alpha_i$ protein-dependent events. But the difference appeared to be too small to be suitable for further exploration.

These results demonstrated the fact, that $G\alpha_i$ proteins were the upstream post receptor triggers for the CRTH2-mediated traces and that additional signaling was not detectable.

2.1.2 DMR captures $G\alpha_s$ response of endogenous EP2/EP4 receptors

First of all, $G\alpha_s$-mediated signaling is characterized by its property to increase the intracellular cAMP level. For this reason, the suitability of DMR technology to detect this signaling event was explored in HEK cells challenged with prostaglandin E_1 (PGE_1) (**Fig. 5a**), which was described as cAMP elevating agent acting via endogenous E-prostanoid receptors (Levin, et al., 2002).

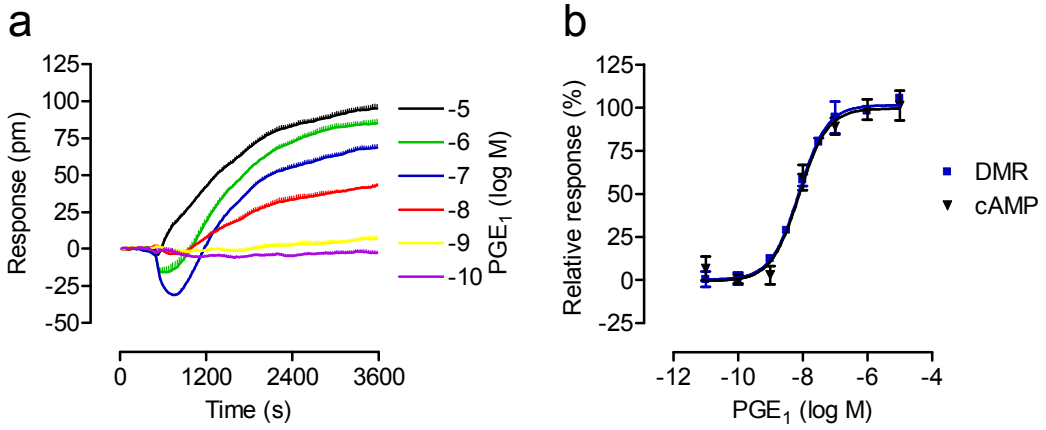

Figure 5: DMR technology captures PGE_1 induced response in native HEK cells. (**a**) HEK293 cells were challenged with various concentrations of PGE_1, and DMR was detected. Shown are representative data (mean + SEM) of four independent experiments. (**b**) DMR data were calculated by the area under the curve (AUC) between 0 and 3600 s, and concentration effect curves are superimposable to those derived from cAMP accumulation assays. Calculated molar pEC_{50} values are: DMR: 8.11 ± 0.07, cAMP: 8.11 ± 0.12. Data are means and SEM of at least three independent experiments, each performed in triplicates.

The monitored signatures were concentration-dependent and their shape was obviously different from those obtained from DK-PGD_2 at CRTH2-HEK cells (chapter 2.1.1, **Fig. 3a**). In contrast to the latter, the traces exhibited a much slower increase and aspired towards a stable maximum response. At some concentrations, an initial negative response was observed, which might also be a characteristic feature of a defined cellular process, however these initial negative DMR responses were not explored any further since a clear concentration effect relationship was lacking. Since there was no defined point of maximum response, the quantification of these signatures was performed by determination of the area under the curve (AUC) (chapter 5.4.8). In parallel, traditional cAMP accumulation assays were carried out, verifying that cAMP generation occurs. The resulting concentration effect curves were compared with those obtained from DMR measurements (**Fig. 5b**) and found to be superimposable with nearly equal molar pEC_{50} values.

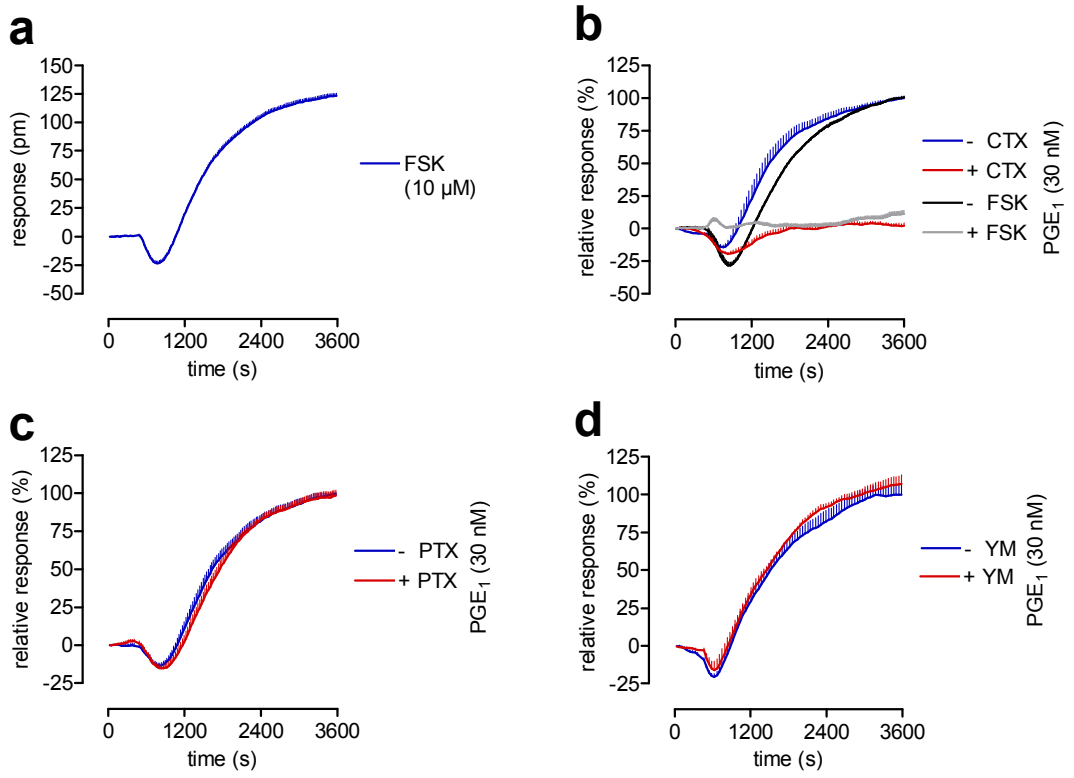

Figure 6: PGE_1 response in HEK cells is masked by CTX or forskolin. (**a**) Forskolin (Fsk) induced traces similar to those obtained by PGE_1 addition. PGE_1 response was invisible after (**b**) pretreatment with 100 ng/ml cholera toxin (CTX) or 10 µM forskolin, but not with (**c**) 5 ng/ml pertussis toxin (PTX) or (**d**) 300 nM YM254890 (YM). Shown are representative data (mean + SEM) of three to four independent experiments, each performed in triplicates.

When the cellular cAMP concentration was increased by addition of forskolin (Fsk) (**Fig. 5a**), which directly activates the adenylyl cyclase, a signature, very similar to the PGE_1 signal was recorded (**Fig. 6a**). Pretreatment of HEK cells with either forskolin (1.5 h) or CTX (18 h)

inhibited the PGE_1 signals as shown in **figure 5b**, whereas the PGE_1-induced traces were not affected by pretreatment with PTX or YM (**Fig. 5c,d**), although recently for EP4 also $G\alpha_i$ signaling was described. In conclusion, it can be stated that the optical traces, generated by PGE_1 in HEK293 cells, were caused by $G\alpha_s$ protein activation.

The use of PGE_1 as an agonist suggested EP2 and EP4 receptors as cellular targets for the captured response profiles. To further corroborate this assumption, HEK cells were pretreated with the EP2 and EP4 receptor antagonists AH6809 and L161,982, respectively. As demonstrated in **figure 7**, only a combination of the antagonists was suitable to block the signals (**Fig. 7a**), whereas each compound alone was hardly effective (**Fig. 7b**). This indicates that both receptors are expressed in HEK cells. While L161,982 is a specific EP4 receptor antagonist, the EP2 receptor antagonist AH6809 additionally acts at EP1 and EP3 receptors. Unfortunately, for these studies no antagonist with exclusive EP2 receptor-specificity was available. However, EP1 might be excluded as target involved in the DMR-captured responses, since signaling via calcium release is described for this receptor and no cAMP elevating properties are known (Sugimoto and Narumiya, 2007). EP3 on the other hand was predominantly referred to as $G\alpha_i$ coupled, although, for some EP3 isoforms signaling via $G\alpha_s$ might occur in addition (Sugimoto and Narumiya, 2007). However, additional $G\alpha_i$ signaling due to EP3 might be excluded herein, since the signatures were not sensitive towards PTX and the fact that DMR measurements would have detected simultaneous $G\alpha_i$ and $G\alpha_s$ signaling (chapter 2.2.3, **Fig. 23** and chapter 2.2.4, **Fig. 25**). This indicates that EP3 is not involved in PGE_1-induced signaling. Thus, PGE_1-induced signaling in HEK cells is suggested as exclusively mediated by EP2 and EP4.

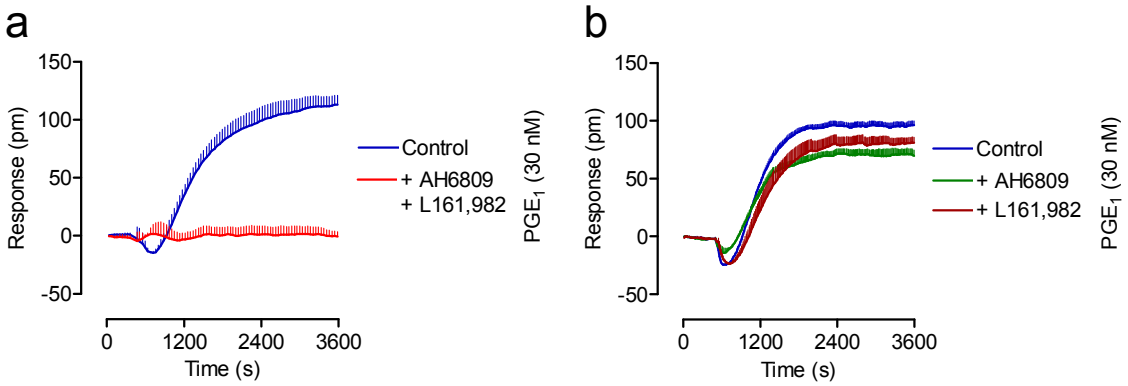

Figure 7: PGE_1 activates EP2 and EP4 receptors in HEK293 cells. The signal of 30 nM PGE_1 is inhibited by a combination of the EP2 and EP4 receptor antagonists AH6809 and L161,982 respectively (10 µM each) (**a**) but not when these antagonists are applied alone (**b**). Shown are representative data (mean + SEM) of four (**a**) or three (**b**) independent experiments, each preformed in triplicates.

2.1.3 DMR unveiles additional $G\alpha_i$ signaling for the $G\alpha_q$-linked FFA1 receptor

The free fatty acid receptor 1 (FFA1, GPR40), previously classified as $G_{q/11}$ sensitive (Brisco, 2003; Itho, 2003; Stoddart, 2007) was chosen to explore the detection of $G\alpha_q$ coupling events. HEK293-Flp-In™ T-Rex™ cells stably transfected with FFA1 (FFA1-HEK) were induced to express FFA1 by pretreatment with doxycyclin. As a control, cells were not induced. Receptor activation was stimulated by application of the small molecule agonist TUG424 (Christiansen, et al., 2008), resulting in strong DMR responses (**Fig. 8a**). FFA1 specificity of the captured traces was verified by the absence of signaling in FFA1-HEK cells not treated with doxycyclin and therefore not expressing the receptor (**Fig. 8b**). DMR traces mediated by FFA1 were concentration-dependent and different in shape from those obtained from the $G\alpha_i$-coupled CRTH2 (**Fig. 3a**) or the $G\alpha_s$-coupled EP2/EP4 receptors (**Fig. 5a**). The captured signatures were characterized by a steep initial increase, comparable to those obtained from $G\alpha_i$ signaling generated by CRTH2 (**Fig. 3a**), but in contrast to the latter, the DMR response remained at an elevated level and proceeded further nearly in parallel to the x-axis.

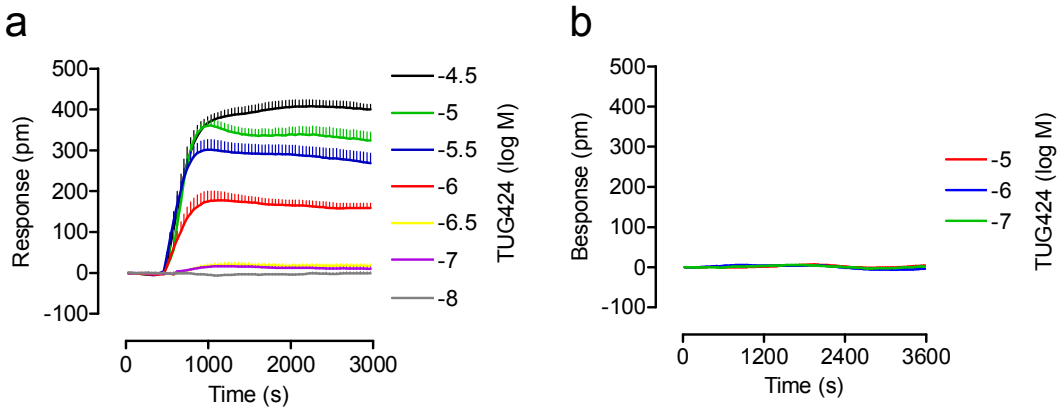

Figure 8: DMR technology captures TUG424 induced response of FFA1. (**a**) FFA1-HEK induced with doxycycline to express FFA1 responded with concentration-dependent DMR traces when treated with various concentrations of TUG424. (**b**) Non-induced FFA1-HEK cells did not respond to TUG424. Shown are representative data (mean + SEM) of at least three independent experiments.

To test the $G\alpha_q$ origin of the signatures, FFA1-HEK cells were pretreated with the $G\alpha_q$ specific inhibitor YM and DMR was monitored. Unlike what would be expected for a $G\alpha_q$ coupled receptor, the FFA1-mediated DMR response was only partly sensitive towards the inhibitory effect of YM (**Fig. 9a**, compare black and blue trace), but in addition, partial sensitivity towards PTX was also found (**Fig. 9a**, compare black and grey trace). Only the combination of YM and PTX was sufficient and required for complete erasure of the FFA1 response (**Fig. 9a**, compare black and red trace)**.**

Due to the partial inhibition by YM, it was of interest to examine the ability of YM to inhibit $G\alpha_q$-dependent signaling in HEK293 cells in another assay. To address this issue, IP1 accumulation assays were performed as shown in **figure 9b**. Stimulation of FFA1-HEK by TUG424 resulted in an increase of cellular IP1 concentrations in comparison to the negative control (**Fig. 9b**, first and third bar). Pretreatment with 300 nM YM (**Fig. 9b,** second and fourth bar) led to a considerable decrease of the cellular IP1 level compared to the negative control, irrespective of additionally challenged with TUG424 or not. This means that the endogenous IP1 generation, conceivable by constitutive $G\alpha_q$ signaling events, as well as the TUG424-induced $G\alpha_q$ activation, were lowered by YM to the same level, indicating sufficient inhibition of $G\alpha_q$ proteins by YM.

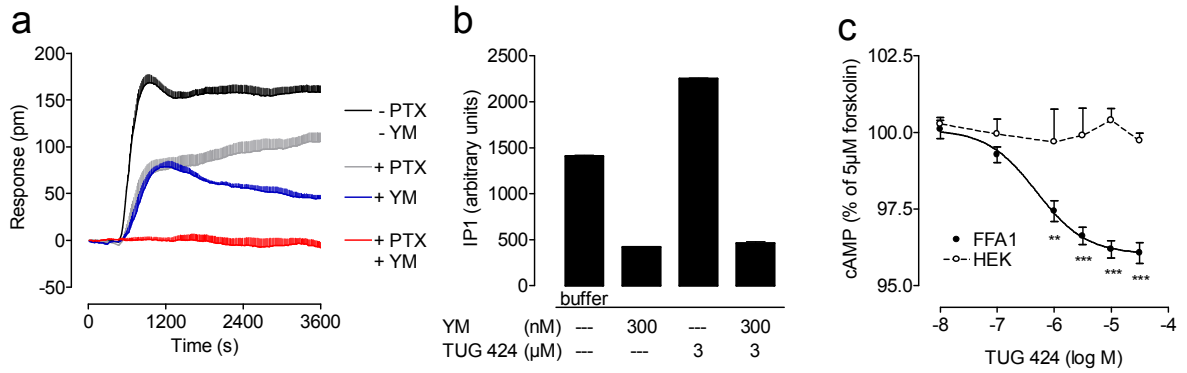

Figure 9: FFA1 is linked to $G\alpha_q$ and $G\alpha_i$ proteins. (**a**) The DMR signature obtained with 3 µM of the agonist TUG424 was partly sensitive to pretreatment of FFA1-HEK cells with 300 nM YM254890 (YM) or 5 ng/ml of pertussis toxin (PTX) but completely inhibited in the presence of a combination of PTX and YM. Shown are representative data (mean + SEM) of at least six independent experiments. (**b**) FFA1 mediated production of the second messenger IP1 was totally blunted by 300 nM YM. (**c**) FFA1 activation of the $G\alpha_i$ signaling pathway was statistically significant in cAMP inhibition assays. FFA1-HEK induced to express FFA1 (FFA1) or HEK control cells were stimulated with 5 µM forskolin and cAMP inhibition was quantified by a cAMP accumulation assay. (**b** and **c**) Shown are mean values and SEM of three to six independent experiments. (**c**) For statistical analysis, individual concentrations were compared by two-way analysis of variance (ANOVA) with Bonferroni's correction for multiple comparisons; ** $p < 0.01$, *** $p < 0.001$. (**b** and **c**) Data were kindly provided by Johannes Schmidt, Institute of Pharmaceutical Biology, University of Bonn, Germany.

Since PTX sensitivity of the DMR response indicated additional $G\alpha_i$-dependent signaling, this was probed by inhibitory cAMP second messenger assays (**Fig. 9c**). Although the inhibition was less than 5% of forskolin-stimulated adenylyl cyclase, the differences between cells expressing FFA1 and control cells were concentration-dependent and significant. These results confirm the partial PTX sensitivity observed in the DMR measurements, and demonstrate again the superiority of DMR technology for detection of $G\alpha_i$ signaling events.

Finally, it can be stated that DMR technology, since endowed with the advantages of a holistic approach, was not only competent to gather $G\alpha_q$-dependent responses, moreover it

was able to detect $G\alpha_q$ and $G\alpha_i$ effects simultaneously. This results in the discovery of the signaling promiscuity of FFA1 towards $G\alpha_q$ and $G\alpha_i$ proteins.

2.1.4 Signaling along the $G\alpha_{12/13}$ pathway is captured by DMR measurement

So far, it was demonstrated that DMR technology is suitable to detect signaling along the $G\alpha_i$, the $G\alpha_s$ and the $G\alpha_q$ pathways. For these pathways second messenger assays are well established. But how about the fourth Gα protein family, the $G\alpha_{12/13}$ proteins? Until now, no specific second messenger is known and therefore, apart from high content screen (HCS) approaches and detection of far downstream events like reporter gene assays (chapter 1.3 and 1.4) (Henstridge, et al., 2009, Henstridge, et al., 2010), no direct assays, which are sufficient for pharmacological characterizations, are available.

The atypical cannabinoid receptor GPR55 was chosen to probe whether DMR technology is able to capture signaling along this pathway. GPR55 is the only GPCR known to date with exclusive bias towards the $G\alpha_{12/13}$ pathway (Ryberg, et al., 2007, Henstridge, et al., 2009, Ross, R. A., 2009). AD-HEK293 cells (AD-HEK) and AD-HEK cells stably expressing GPR55 (GPR55-AD-HEK) were challenged with L-α-lysophosphatidylinositol (LPI), currently the most suitable GPR55 agonist (Henstridge, et al., 2010) (Fig 10). Captured response profiles displayed concentration-dependent traces (**Fig. 10a,b**), whereas AD-HEK cells not expressing GPR55, did not show any response (**Fig. 10c**).

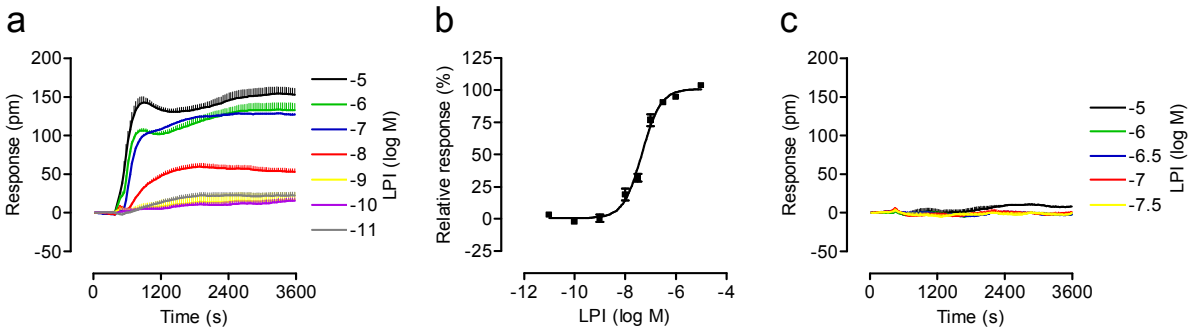

Figure 10: DMR measurement captures signaling of GPR55. GPR55-AD-HEK cells (**a**) or native AD-HEK cells (**c**) were stimulated with the indicated concentrations of L-α-lysophosphatidylinositol (LPI) and wavelength shift was detected over time. Shown are representative data (mean + SEM) of at least three independent experiments. (**b**) Concentration effect curve for LPI in GPR55-AD-HEK cells resulting from DMR traces of three independent experiments (mean ± SEM). The calculated molar pEC_{50} value is 7.34 ± 0.05.

By visual inspection, GPR55-derived traces display some similarity to the mixed $G\alpha_q/G\alpha_i$ traces obtained from FFA1. However, pretreatment with YM, PTX or CTX did not lead to inhibition of the signals, indicating an origin that is not derived from $G\alpha_q$, $G\alpha_i$ or $G\alpha_s$ proteins (**Fig. 11a**). To examine whether the captured traces were G protein-dependent at all, the pan G protein activator aluminium fluoride (AlF_4^- herein referred to as AlF) was used. **Figure 11b** showns, that the GPR55-mediated response was completely silenced by pretreatment with 300 µM AlF. For control purposes, the effect of AlF addition itself was measured, leading to an obvious response as depicted in **figure 11c**. The principle of silencing by AlF depends on activation of all Gα proteins (Bigay, et al., 1987). This causes that additional activation via Gα proteins is no longer detectable and therefore masked, similar to the action of CTX masking $G\alpha_s$ signaling. Critically, the inhibition of GPR55-mediated response by AlF can not be explained by a general blunting of cell responsiveness in DMR assays, because pretreatment with AlF did not prevent additional G protein-independent DMR changes to occur in response to growth factor containing serum (**Fig. 11d**).

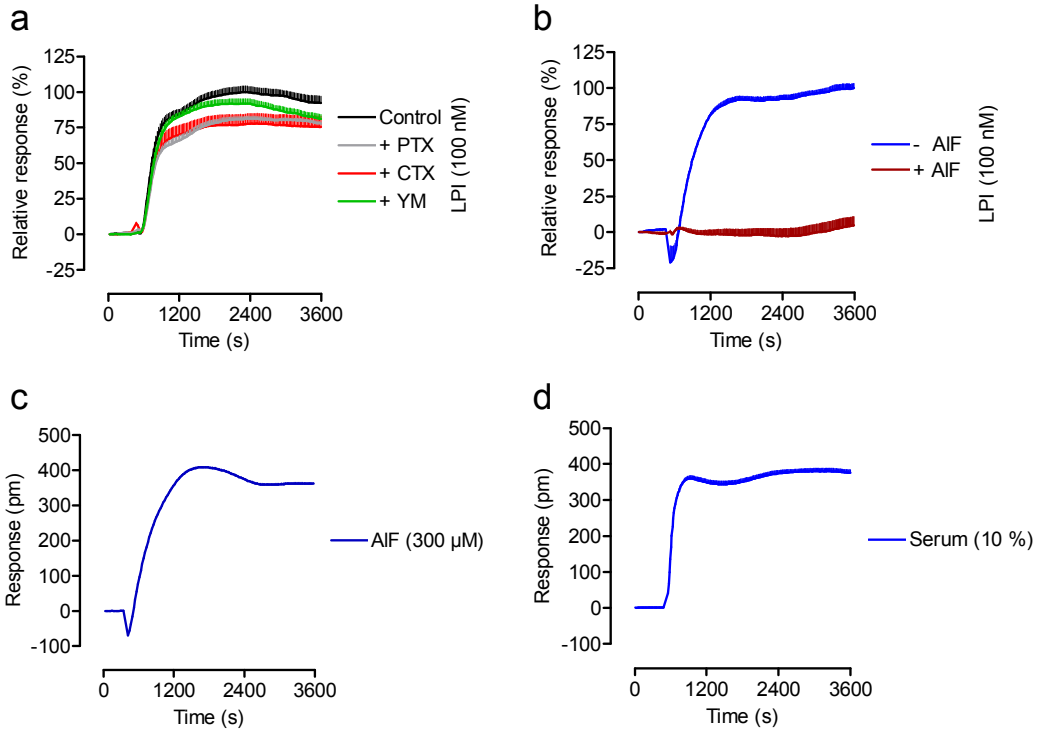

Figure 11: The GPR55 traces are of G protein origin but independent of $G\alpha_i$, $G\alpha_s$ or $G\alpha_q$ proteins. (**a**) LPI-mediated DMR in GPR55 cells was not blunted by pretreatment with 5 ng/ml pertussis toxin (PTX), 100 ng/ml of cholera toxin (CTX) or 300 nM YM254890 (YM), but (**b**) was sensitive to preincubation of cells with 300 µM pan G protein agonist AlF_4^- (AlF). (**c**) Treatment of cells with AlF caused robust DMR changes on its own. (**d**) GPR55-HEK cells pretreated for 1.5 h with 300 µM AlF were still responsive to serum to promote growth factor activation. Shown are representative data (mean + SEM) of at least three independent experiments.

These results suggest that the GPR55 mediated DMR response was generated by G proteins in general, but not by $G\alpha_q$, $G\alpha_i$ or $G\alpha_s$ proteins. This was additionally examined by second messenger assays. Neither an increase of cAMP levels could be observed, nor the inhibition of forskolin-stimulated adenylyl cyclase was detectable, and also IP1 accumulation was not altered to a significant extent (**Fig. 10a,b**). Thus, these pathways could be excluded, which was a strong hint towards involvement of $G\alpha_{12/13}$ proteins.

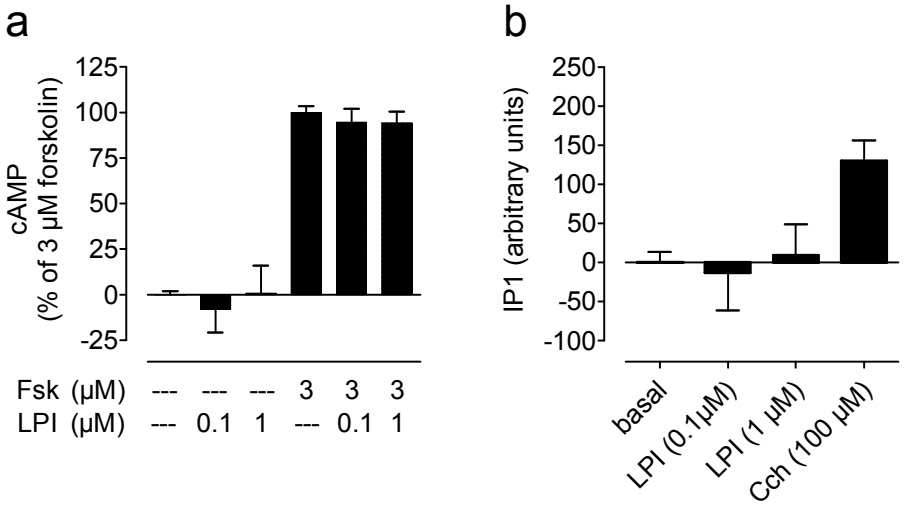

Figure 12: Second messenger levels in GPR55-HEK cells are not affected by LPI. (**a**) GPR55-HEK293 cells stimulated with L-α-lysophosphatidylinositol (LPI) displayed neither increased cAMP accumulation nor inhibition of forskolin (FSK)-stimulated cAMP production. (**b**) No relevant IP1 accumulation was detectable for GPR55-HEK cells stimulated with the indicated concentrations of LPI. Cells were stimulated with carbachol (Cch) for control. Data shown are mean values and SEM of three to four independent experiments, each performed in triplicates.

To investigate the specificity of GPR55-AD-HEK-mediated signaling in DMR assays, a dominant negative form of the $G\alpha_{13}$ protein ($G\alpha_{13}$dn, Q226L,D294N) was utilized. The mutations at the Gα13 protein lead to a combined effect of constitutive activity and a switch of selectivity from guanine nucleotides to xanthine nucleotides (Barren and Artemyev, 2007). The structural reasons for a dominant negative phenotype are not fully elucidated, but the $G\alpha_{13}$dn protein is now competent to sequester a respective GPCR without Gβγ binding and despite of an empty nucleotide pocket. Since $G\alpha_{13}$dn is not able to bind guanine nucleotides and since xanthine nucleotides are not available in the cells, the protein is bound tightly to the receptor. Thus, by blocking wild type proteins from binding to the activated GPCR, the G protein activation cycle is interrupted (Yu and Simon, 1998, Barren and Artemyev, 2007). GPR55-AD-HEK cells were transiently transfected by an electroporation method using either $G\alpha_{13}$dn or empty vector as a control. DMR assays were performed 48 h after transfection and

LPI-induced responses were considerably diminished in GPR55-HEK cells transfected with $G\alpha_{13}$dn compared to vector transfected cells (**Fig. 13a**). As a control, carbachol (Cch), an agonist of endogenously expressed $G\alpha_q$- and $G\alpha_i$-coupled muscarinic receptors, was applied to $G\alpha_{13}$dn and vector transfected cells and the resulting DMR traces were found virtually unaffected (**Fig. 13b**). Concentration sequences of LPI, applied at both cell samples, displayed a concentration-dependent effect with a consistent rank order, whereas the efficacy of $G\alpha_{13}$dn transfected cells was significantly diminished in comparison with vector transfected control cells (**Fig. 13c**).

To examine whether the signal reduction may not possibly be caused by different receptor surface expression levels, enzyme linked immunosorbent assays (ELISAs) were performed. This was carried out in parallel to the DMR assays, using the same transfectants. ELISA data demonstrate that the surface expression of GPR55 was not altered by transfection of $G\alpha_{13}$dn in comparison to vector transfected cells (**Fig. 13d**).

These data verified that the LPI-induced signatures in GPR55-AD-HEK cells were triggered by activation of $G\alpha_{12/13}$ proteins. Thus, the DMR technology represents a method to explore the functionality of GPCRs linked to G proteins of all four main coupling classes.

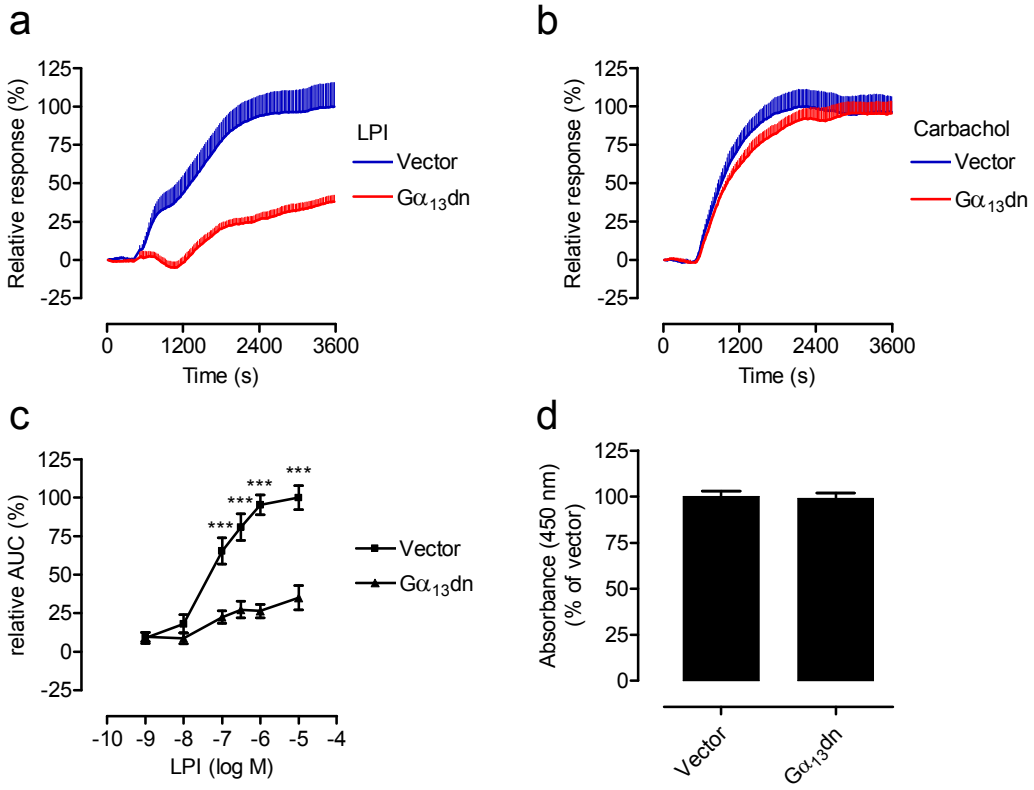

Figure 13: The $G\alpha_{12/13}$ pathway is captured by DMR measurements. Depicted are DMR responses and ELISA data of GPR55-AD-HEK cells cotransfected with a dominant negative form of $G\alpha_{13}$ ($G\alpha_{13}$dn, G13Q226L,D294N) or empty pcDNA3.1+ vector as control. (**a**) DMR response of $G\alpha_{13}$dn transfectants is substantially diminished compared with vector-transfected cells when treated with L-α-lysophosphatidylinositol (LPI) (**b**) but not when treated with 100 µM carbachol (Cch). Shown are representative data (mean + SEM) of five independent experiments. (**c**) Concentration effect relationship of LPI induced DMR responses at the GPR55-AD-HEK transfectants. (**d**) Parallel ELISA assays detected the same surface expressions of GPR55 for $G\alpha_{13}$dn and vector transfected cells. Data were buffer corrected and normalized. Shown are mean ± SEM of five (**c**) and three (**d**) independent experiments, each performed in triplicates. For statistical analysis, individual concentrations were compared by two-way ANOVA with Bonferroni's correction for multiple comparisons; *** $p < 0.001$.

2.1.5 Exploring DMR technology to interrogate features of agonist and antagonist pharmacology

Activation of the Gαi pathway can be detected by cAMP accumulation assays as mentioned above (chapter 1.3 and 2.1.1). However, because of its inhibitory character, the measurement of Gαi activation by detection of decreasing cAMP levels is more complicated and artificial than the detection of Gαs and Gαq signaling. In addition to the use of 3-isobutyl-1-methylxanthine (IBMX), that protects cAMP against enzymatic degradation by inhibition of the phosphodiesterase activity, the adenylyl cyclase has to be activated by forskolin to enable the detection of its inhibition. Thus, the non-invasive DMR technology is supposed to be a more sensitive and comfortable method to detect and examine Gαi-dependent signaling events. Its practicability was investigated using CRTH2 with regard to (i) detection of full and partial agonism, (ii) discrimination of different modes of pharmacological antagonist behavior and (iii) comparison of signaling efficacy and receptor expression levels.

2.1.5.1 Examination of full and partial agonism

The investigations at CRTH2 presented so far were performed utilizing DK-PGD_2 that is described to be a specific but also a partial agonist at the receptor. In contrast, prostaglandin D_2 (PGD_2), the major agonist of CRTH2, exerts full agonism properties (Hirai, et al., 2001, Kostenis and Ulven, 2006). To address the question whether these pharmacological properties will be reflected in DMR assays, PGD_2 and DK-PGD_2 were applied in parallel to CRTH2-HEK cells in both DMR and cAMP assays.

When CRTH2-HEK cells were challenged with PGD_2, the captured response profiles were found very similar to those derived from DK-PGD_2 (compare **Fig. 12a** and **Fig. 3a**). These responses were CRTH2-dependent, since HEK cells not expressing CRTH2 did not display any effect, except for occasionally appearing weak signals at 10 µM PGD_2. These might be attributable to unspecific activation of endogenous receptors by this high PGD_2 concentration (**Fig. 12b**). As observed for DK-PGD_2 before, pretreatment with PTX blunted the signal of PGD_2, indicating that also in this case only $G\alpha_i$ signaling was detected (**Fig. 12c**).

Comparing the DMR-derived concentration effect curves of PGD_2 and DK-PGD_2, it is noticeable, that the molar pEC_{50} values of both compounds are nearly equal. But unlike what would be expected, the detected efficacies were not considerably different (**Fig. 14d**). However, in cAMP assays, PGD_2 led to a decrease of cellular cAMP levels of about 40 %, whereas for DK-PGD_2 a reduction of less than 10% was observed, reflecting that DK-PGD_2 is

a partial agonist at CRTH2. These results indicate that DMR technology may be limited in its capacity to discriminate between partial and full agonism as pharmacological agonist characteristics.

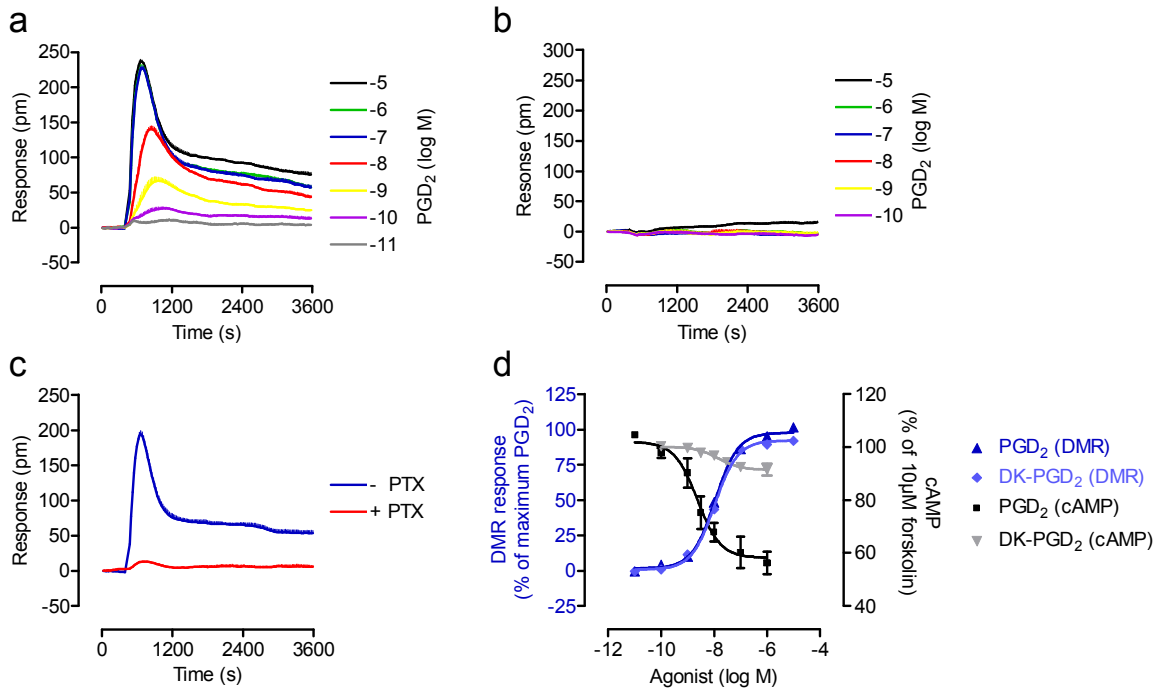

Figure 14: Partial agonism at CRTH2 is hardly detectable in DMR assays. DMR response was induced by PGD_2 in CRTH2-HEK cells (**a**) but not in native HEK cells (**b**). (**c**) The response of 100 nM PGD_2 was inhibited by pretreatment with 50 ng/ml of pertussis toxin (PTX). Shown are representative data (mean + SEM) of four (**c**) or six (**a**,**b**) independent experiments. (**d**) Comparison of concentration effect curves of PGD_2 and DK-PGD_2 derived from DMR and cAMP assays. For DMR assays the compared values of PGD_2 and DK-PGD_2 were obtained from the same measurement and were normalized to the respective maximum response of PGD_2, which was set to 100%. cAMP values were calculated as per cent inhibition of 10 µM forskolin. For DK-PGD_2 calculated molar pEC_{50} values are: DMR: 7.96 ± 0.04, cAMP: 7.85 ± 0.34, and for PGD_2: DMR: 7.97 ± 0.04, cAMP: 8.62 ± 0.17. Data are mean ± SEM of at least three independent experiments, each performed in triplicates.

2.1.5.2 Discrimination of surmountable and insurmountable antagonists

Substances with specific antagonistic properties towards receptors are important pharmacological tools and crucial for investigations at endogenously expressed receptors in both immortalized and primary cells. Since full and partial agonism hardly could be discriminated by DMR technology (chapter 2.1.5.1), it was of interest in how far different antagonistic behaviors would be reflected. To explore this, two CRTH2 specific antagonists with different pharmacological properties were chosen: on the one hand TM30642, described as an antagonist with competitive behavior and referred to as surmountable antagonist and on

the other hand TM30089, described as an insurmountable antagonist (Mathiesen, et al., 2005). CRTH2-HEK cells were pretreated with different concentrations of TM30642 or TM30089 and incubated for 1 h. Subsequently, cells were challenged with various concentrations of PGD_2 and wavelength shift was monitored over time (**Fig. 15**).

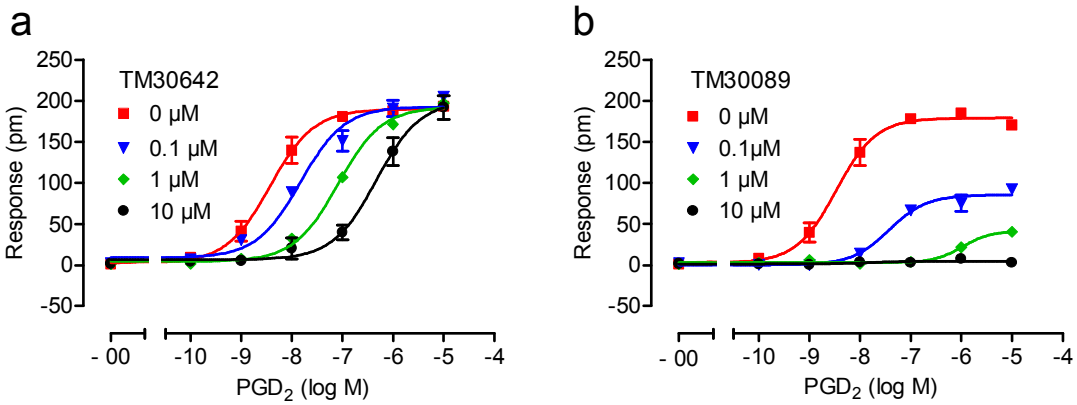

Figure 15: DMR technology accurately discriminates surmountable and insurmountable antagonism. CRTH2-HEK cells were pretreated for 1 h with the indicated antagonists before being challenged with PGD_2. (**a**) Increasing concentrations of TM30642 caused a right-ward shift of PGD_2 concentration effect curves, compatible with surmountable antagonism. The calculated pA_2 value for TM300642 is: 7.50 (± 0.14), slope 0.99 (± 0.11) (**b**) Increasing concentrations of TM30089 caused both, right-ward shift and depressed maximal PGD_2 efficacy, compatible with insurmountable antagonism. (**a,b**) Shown are representative data (mean ± SEM) of at least three independent experiments, each performed in triplicates.

As depicted in **figure 15a** it could be observed that increasing concentrations of TM30642 caused a right-ward shift of the PGD_2 concentration effect curves. However, the absolute maximum response was not decreased. This means that the effect could be compensated by increasing agonist concentrations and represents a competitive antagonist mechanism, which is also referred to as surmountable antagonism. The calculated pA_2 value for TM300642 is 7.50 (± 0.14) and the corresponding slope of 0.99 (± 0.10) substantiates a competitive mechanism. These results are in accordance with data presented by Mathiesen et al. (2009), where for TM30642 in [^{35}S]GTPSγS assays (at membranes from CHO cells stably expressing CRTH2) the determined pA_2 value was 7.72 (± 0.13) with a corresponding slope of 0.89 (± 0.08). Pretreatment with TM30089 induced an antagonistic effect which differs from the observation for TM30642. Increasing antagonist concentrations resulted also in right-wards shifts of PGD_2 concentration effect curves, but additionally the absolute maximum responses were diminished. This indicates an insurmountable mode of action, which is also in agreement with previous data (Mathiesen, et al., 2006). These results reveal unequivocally

that DMR measurement is competent to characterize and discriminate between these different antagonistic properties.

2.1.6 Functional DMR response reflects receptor surface expression

When different agonistic efficacies at the level of cAMP resulted in nearly similar DMR responses (**Fig. 14**), how would DMR responses reflect different receptor surface expression levels? In order to address this question, HEK293 cells were transiently transfected with different amounts of a CRTH2 expression plasmid or an empty vector as a control. Additionally, stable CRTH2-HEK cells and untransfected HEK293 cells were used. 48 h after transfection, DMR assays and ELISAs were performed in parallel. As expected, in ELISAs the stable CRTH2-HEK cells provided the strongest signals (**Fig. 16a**). The receptor surface expression of transiently transfected cells were graded according to the applied amounts of DNA. Non-transfected HEK cells as well as vector-transfected cells indicated the background level. The corresponding DMR responses were found consistent with the rank order of the surface expression (**Fig. 16b**). This demonstrates that surface expression levels are well reflected in DMR responses.

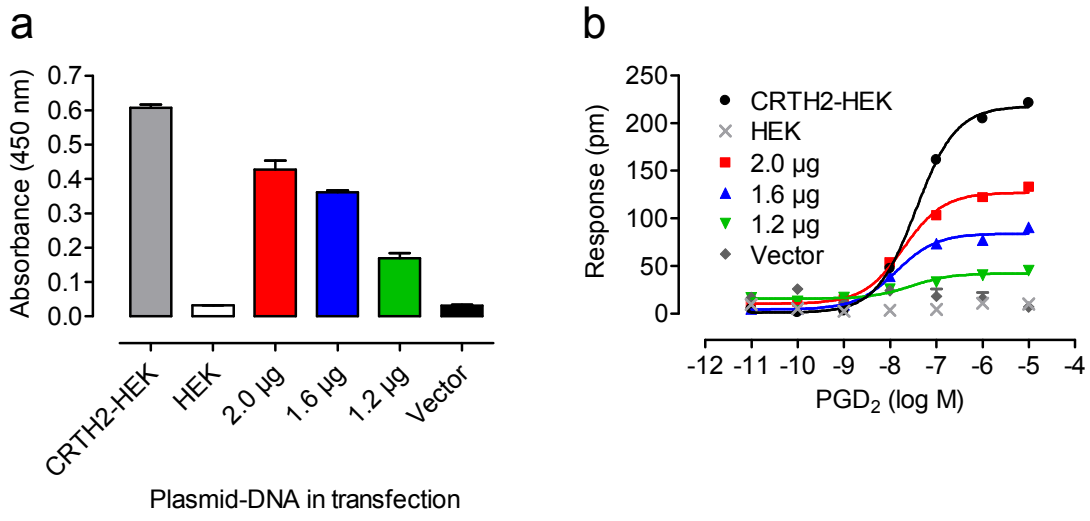

Figure 16: CRTH2 surface expression is consistent with the corresponding efficacy in DMR assays. (**a**) Detection of CRTH2 surface expression was performed by ELISA at CRTH2-HEK, HEK cells and HEK cells transiently transfected with the indicated amounts of CRTH2 expression vector or empty pcDNA3.1+ vector. (**b**) Concentration effect curves obtained from DMR assays which were performed in parallel. Shown are representative data (mean and SEM) of at least three independent experiments, each performed in triplicates.

2.1.7 DMR technology enables signaling analysis in human primary cells

Receptor behavior can nicely be studied in overexpression systems, utilizing immortalized cell lines. However, the artificial character may imply less physiological relevance. The possibility of DMR technology to study receptor signaling label-free and in living cells seems to be particularly advantageous for examinations in primary cells. Thus, immortalized human keratinocytes (HaCaT) and primary human keratinocytes were chosen to investigate whether DMR technology is sufficiently sensitive to detect GPCR-mediated signaling in a native environment.

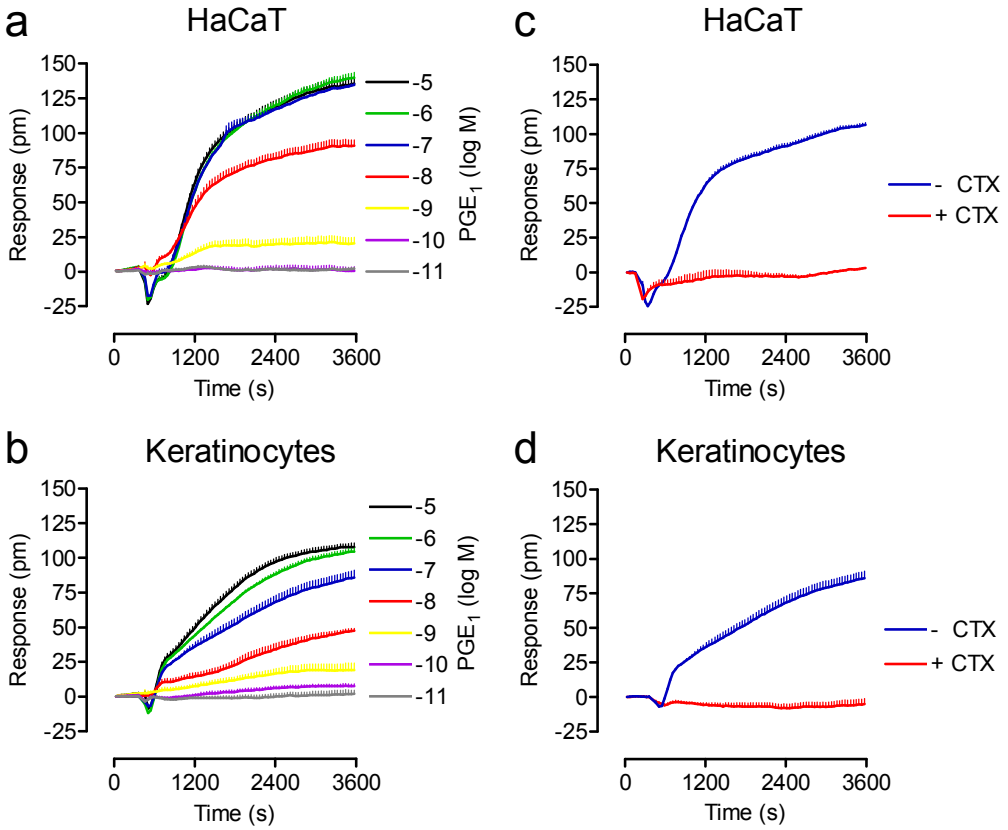

Figure 17: PGE_1 induce $G\alpha_s$-linked signaling in immortalized (HaCaT) and primary human keratinocytes is captured by DMR measurements. Cells were challenged with the indicated concentrations of PGE_1 and wavelength shift was monitored over time. (**a**) Representative data (+ SEM) of at least four independent experiments. (**b**) Representative data (+ SEM) of cells from one human donor. Cells from five additional donors yielded comparable signatures (data not shown) (**c,d**) DMR signatures of 100 nM PGE_1 are masked when cells are pretreated with 250 ng/ml of cholera toxin (CTX). (**c**) Representative data (+ SEM) of at least four independent experiments. (**d**) One representative data set (+ SEM) from one out of six human cell samples.

Primary keratinocytes were obtained from six healthy patients who underwent skin surgery (see also 5.3.1). As stimulus, the cAMP elevating agent PGE1 was used, which is referred to as effective in topical treatment for cutaneous ulcerations (Zhang, et al., 1994) and known to affect cell growth and cytokine production of human keratinocytes (Murota, et al., 2008).

Challenged with PGE_1, HaCaTs and primary human keratinocytes responded with concentration-dependent optical traces (**Fig.17a,b**) comparable to those already observed in PGE_1-treated HEK293 cells (**Fig. 5**). Pathway determination in HaCaTs and primary human keratinocytes was performed by pretreatment with CTX, and the resulting inhibition of PGE_1-mediated signaling in both cell lines verified the assumed $G\alpha_s$ origin (**Fig. 17c,d**). As already observed previously in the case of HEK cells (chapter 2.1.2, **Fig. 7**), PGE_1-stimulated signaling was mediated by the $G\alpha_s$-coupled E-prostanoid receptors EP2 and EP4, because the responses were inhibited by a combination of the EP2 and EP4 receptor antagonists AH6809 and L161,982 respectively (**Fig. 18a,b**), but the signatures were hardly decreased by one of the antagonists alone (**Fig. 18c,d**).

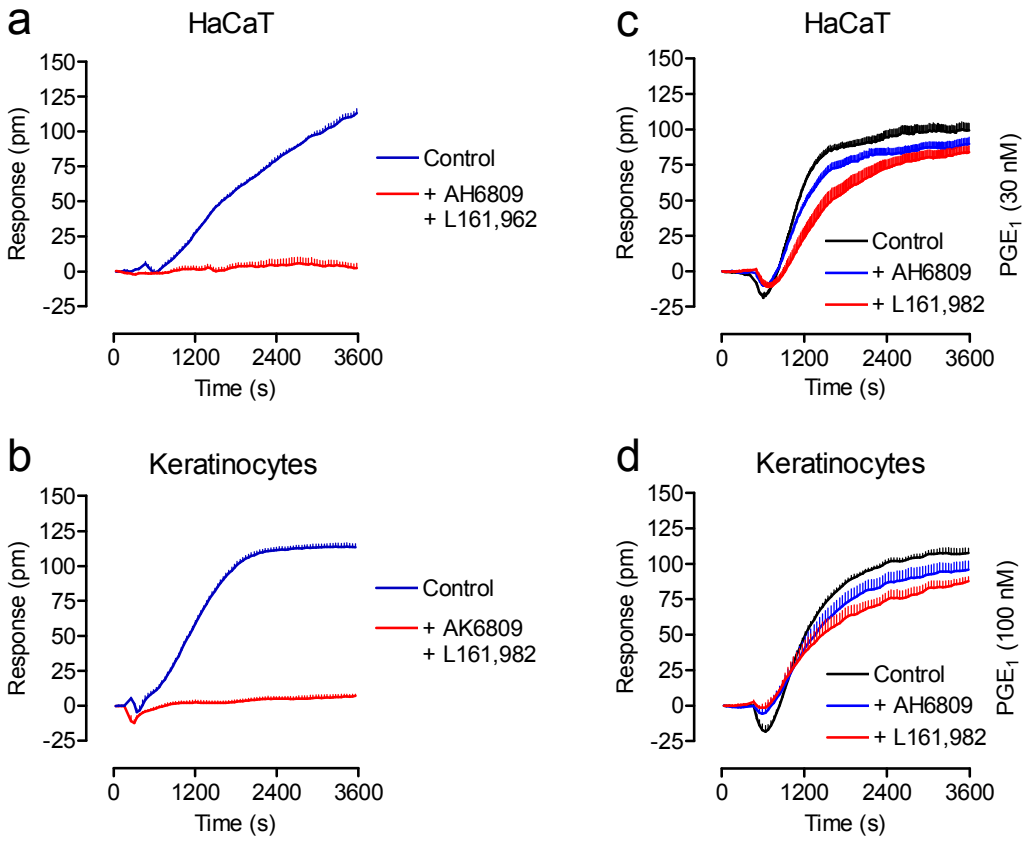

Figure 18: PGE_1 signaling is mediated by the $G\alpha_s$ coupled EP2 and EP4 receptors.
Depicted are DMR traces in immortalized (HaCaT) and primary human keratinocytes, challenged with the indicated concentrations of PGE_1.(**a,b**) PGE_1-induced DMR was inhibited by pretreatment with a combination of the EP2 and EP4 receptor antagonists AH6809 and L161,982 respectively. Optical traces resulted from addition of 30 nM PGE_1 (**a**) or 100 nM PGE_1 (**b**) in the absence and presence of a combination of 10 µM AH6809 and 3 µM L161,982. All data are representative data (+ SEM) of at least four independent experiments. (**c,d**) Signatures of PGE_1 were hardly inhibited by one of the antagonists alone. Shown are representative data (+ SEM) of three independent experiments, each performed in triplicates.

In both cell lines cAMP assays were performed in parallel to DMR assays, revealing that cAMP formation occurred (**Fig. 19**). Concentration effect curves from HaCaT were found slightly left-ward shifted in DMR assays. For primary keratinocytes potencies in the cAMP assays were similar compared to those obtained from DMR assays. However, the detection of cAMP increase in primary keratinocytes was challenging, which was displayed by the small assay window and the large error bars (**Fig. 19b**). In case of the primary cells used in these assays, it can be concluded that DMR measurements are superior with respect to the quality of the signal window and seem highly superior to detect PGE_1-induced signaling in both cell lines.

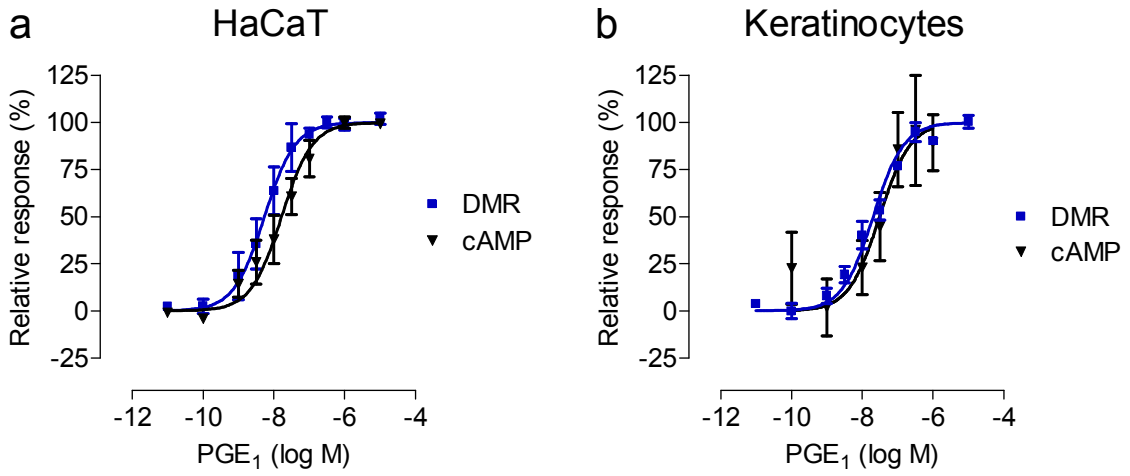

Figure 19: PGE_1-dependent cAMP increases are virtually superimposable to DMR signals.
DMR assays were compared with traditional endpoint second messenger cAMP assays. DMR data were generated by determination of the area under the curve (AUC) between 0 and 3600 s. Calculated molar pEC_{50} values are: (**a**) Immortalized keratinocytes (HaCaT): DMR: 8.27 ± 0.09, cAMP: 7.78 ± 0.09, and (**b**) primary keratinocytes: DMR: 7.70 ± 0.06, cAMP: 7,60 ± 0.12. All data are means ± SEM of at least four independent experiments, each performed in triplicates.

2.2 Utilizing DMR technology for eicosanoid screening at CRTH2

CRTH2, described as the second PGD_2 receptor and therefore also referred to as DP2 receptor (chapter 1.7.1.1), is not exclusively activated by PGD_2, but characterized by its responsiveness to a rather broad spectrum of endogenous ligands, which belong to the 2-series of prostanoids (Kostenis and Ulven, 2006, Schuligoi, et al., 2009).

For this reason, it was of interest to determine whether CRTH2 ligands may differ regarding their induced signaling behavior at CRTH2 and if there are additional, still unknown ligands.

Most of the 2-series prostanoids had been tested at CRTH2, whereas the 1-series had not yet been examined. Due to the close structural relationship of the 1-series and 2-series of prostanoids (chapter 1.6) and the non-selectivity of CRTH2 towards some members of the 2-series, the 1-series prostanoids may not generally be excluded as ligands for CRTH2. Examination of 1-series prostanoids at the pro-inflammatory CRTH2 receptor appears also obligatory, given the nutrition recommendations with regard to diets enriched with ω-3 fatty acids and γ-linolenic acid, resulting in increased levels of dihomo-γ-linolenic acid (DHGLA), the biosynthetic precursor of all 1-series prostanoids (Chilton, et al., 2008).

2.2.1 DMR measurements of 2-series prostanoids at CRTH2

In order to address the issues mentioned above, ligand screening was performed using the known CRTH2 ligands of the 2-series of prostanoids and in addition the main representatives of the 1-series, including arachidonic acid (AA) and prostaglandin H_2 (PGH_2), the precursors of the 2-series as well as DHGLA and prostaglandin H_1 (PGH_1), which represent the precursors of the 1-series of prostaglandins (PGs) (chapter 1.6, **Fig. 1**).

The screening approach was realized utilizing the DMR assay technology (**Fig. 20-24**), which was previously validated for functional GPCR analysis (chapter 2.1). Two of the prostanoid derivates, PGD_2 and DK-PGD_2, have been examined already during the validation process (chapter 2.1.1 and 2.1.5). The used eicosanoid compounds, structural formulas and the corresponding molar pEC_{50} values are listed in **table 1**.

In DMR measurements, various concentrations of these substances were applied to both CRTH2-HEK and HEK cells. Resulting DMR traces of prostaglandins with D- and F-rings are depicted in **figure 20**. The data of prostaglandins with J-rings and the one known thromboxane, being active at CRTH2, are presented in **figure 21**.

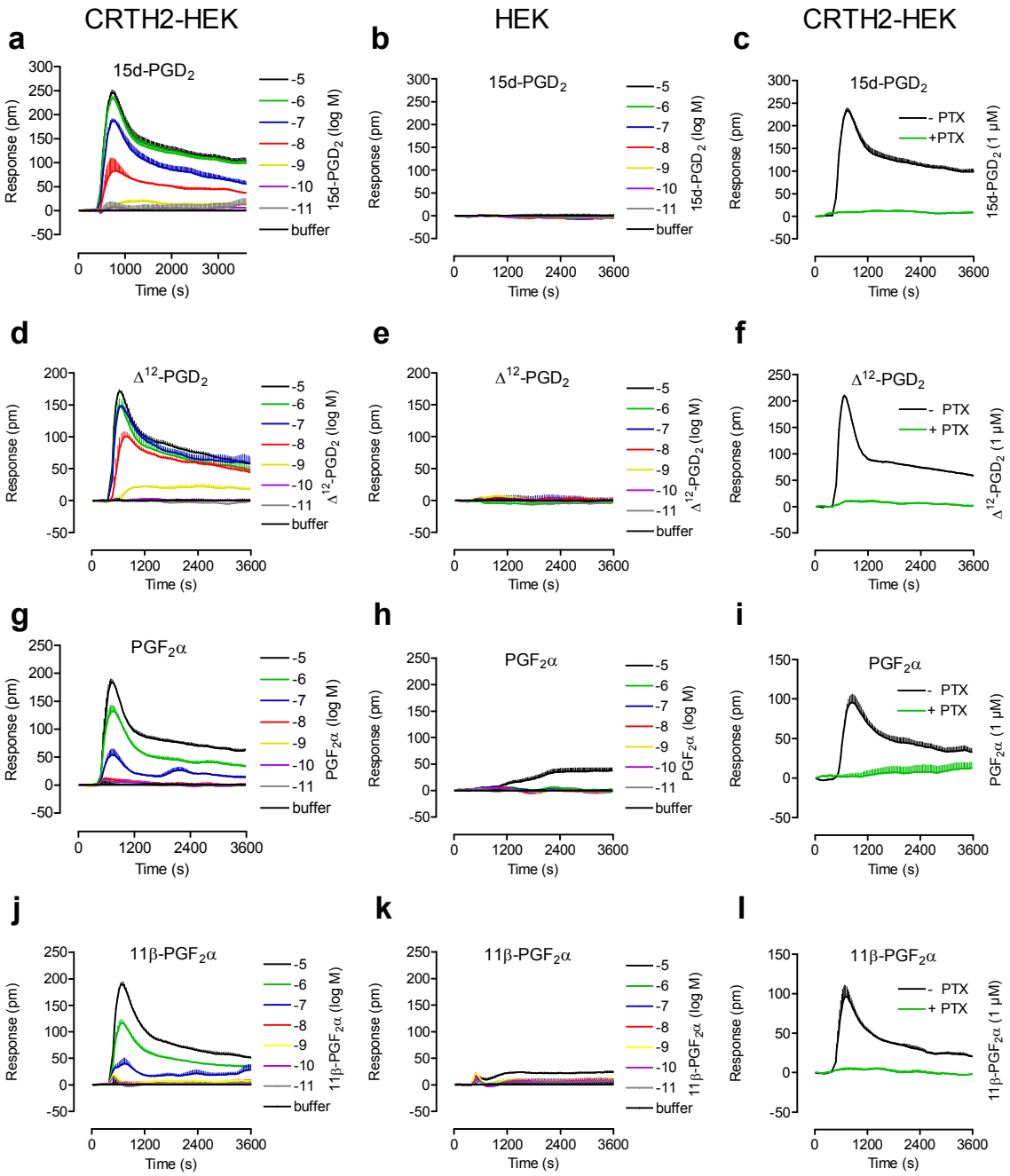

Figure 20: 2-series prostanoids induce $G\alpha_i$-dependent responses in CRTH2-HEK.
(**a-l**) DMR measurements were performed in HEK293 cells stably expressing CRTH2 (CRTH2-HEK) (left and right panels) and native HEK293 cells (HEK) (middle panels). (Left and middle panels) CRTH2-HEK and HEK cells were challenged with various concentrations of (**a,b**) 15-deoxy-$\Delta^{12,14}$-prostaglandin D_2 (15d-PGD_2), (**d,e**) Δ^{12}-prostaglandin D_2 (Δ^{12}-PGD_2), (**g,h**) prostaglandin $F_2\alpha$ ($PGF_2\alpha$), and (**j,k**) 11β-prostaglandin $F_2\alpha$ (11β-$PGF_2\alpha$), and wavelength shift was monitored over time. (Right panels) Pathway determination in CRTH2-HEK cells was performed by pretreatment with 50 ng/ml of pertussis toxin (PTX) and subsequent DMR measurement of the indicated compounds and concentrations. For control, PTX-untreated cells were employed. Shown are representative data (mean + SEM) of three to four independent experiments, each performed in triplicates.

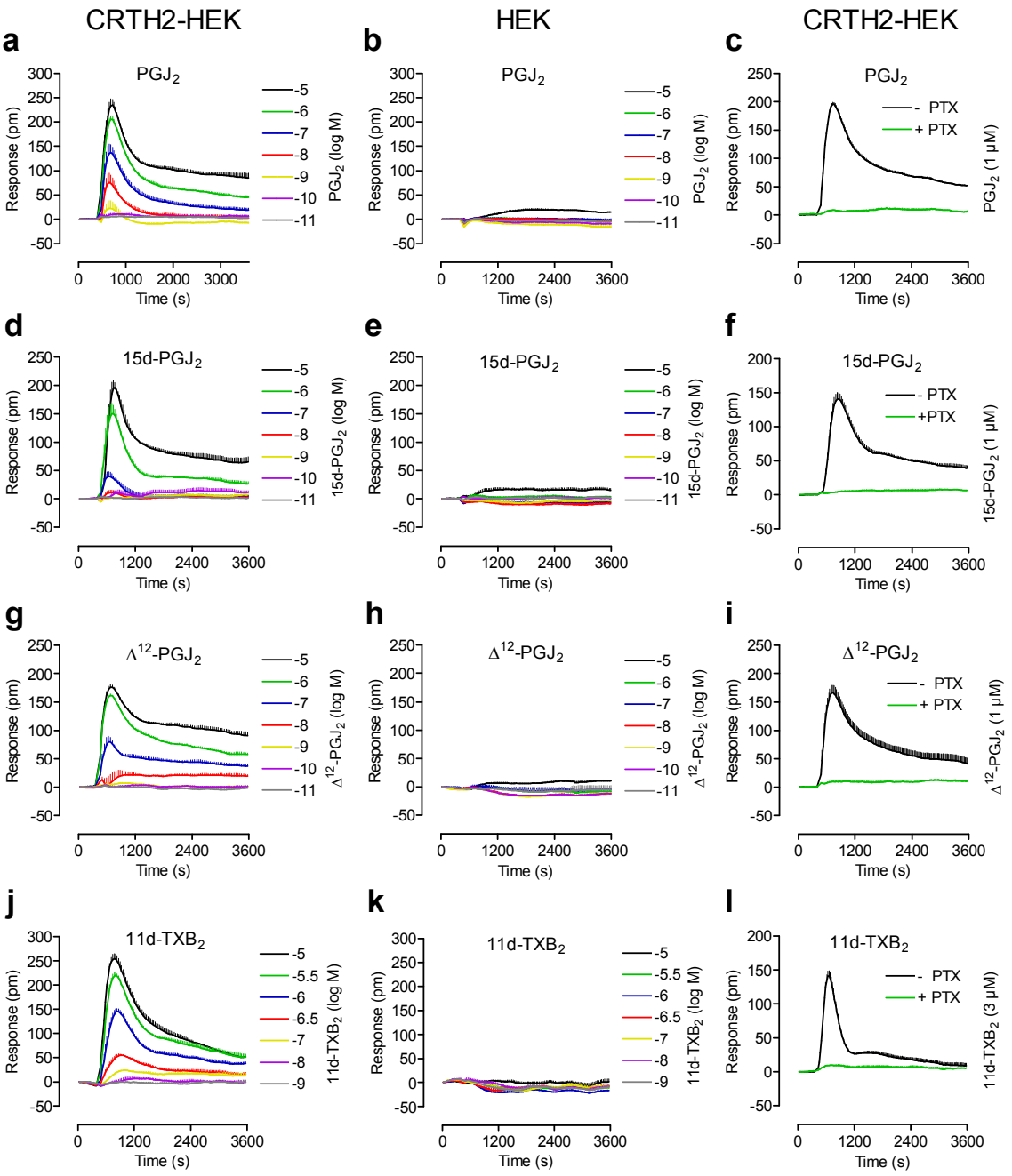

Figure 21: 2-series prostanoids induce Gα_i-dependent responses in CRTH2-HEK.
(**a-l**) DMR measurements were performed in HEK293 cells stably expressing CRTH2 (CRTH2-HEK) (left and right panels) and native HEK293 cells (HEK) (middle panels). (Left and middle panels) CRTH2-HEK and HEK cells were challenged with various concentrations of (**a,b**) prostaglandin J_2 (PGJ_2), (**d,e**) 15-deoxy-$\Delta^{12,14}$-prostaglandin J_2 (15d-PGJ_2), (**g,h**) Δ^{12}-prostaglandin J_2 (Δ^{12}-PGJ_2) and (**j,k**) 11-dehydro-thromboxane B_2 (11d-TXB_2), and wavelength shift was monitored over time. (Right panels) Pathway determination in CRTH2-HEK cells was performed by pretreatment with 50 ng/ml of pertussis toxin (PTX) and subsequent DMR measurement of the indicated compounds and concentrations. For control, PTX-untreated cells were employed. Shown are representative data (mean + SEM) of three to four independent experiments, each performed in triplicates.

The known CRTH2 agonists 15-deoxy-$\Delta^{12,14}$-prostaglandin D_2 (15d-PGD_2), Δ^{12}-prostaglandin D_2 (Δ^{12}-PGD_2), prostaglandin $F_2\alpha$ ($PGF_2\alpha$), 11β-prostaglandin $F_2\alpha$ (11β-$PGF_2\alpha$), prostaglandin J_2 (PGJ_2), 15-deoxy-$\Delta^{12,14}$-prostaglandin J_2 (15d-PGJ_2), Δ^{12}-prostaglandin J_2 (Δ^{12}-PGJ_2) and 11-dehydro-thromboxane B_2 (11d-TXB_2) triggered robust concentration-dependent signatures and the traces were found to be of similar shape as compared to those obtained with DK-PGD_2 and PGD_2 (compare left panels of **Fig. 20** and **Fig. 21** with chapter, 2.1.1, **Fig. 3a** and chapter, 2.1.5.1, **Fig. 14a**). The detected responses were CRTH2-dependent, since compound application in HEK cells generally did not induce any response, except of the occasional appearance of weak signals at the highest compound concentration of 10 µM. Only the addition of 10 µM $PGF_2\alpha$ led to a small but reproducible signal in HEK cells and might result from activation of targets endogenously expressed in HEK cells. The typical shape of agonist induced signatures at CRTH2-HEK cells led to the assumption that in all cases $G\alpha_i$ coupling occurs, as previously demonstrated for DK-PGD_2 and PGD_2 (chapter 2.1.1, **Fig. 4** and chapter 2.1.5.1, **Fig. 14c**). To prove this, CRTH2-HEK cells were pretreated with 50 ng/ml of PTX as depicted in the right panels of **figure 20** and **figure 21**. In all cases the agonist induced signals were fully abrogated by pretreatment with PTX.

Summarized, the investigated known CRTH2 ligands were all active at CRTH2 in DMR assays, but no other signaling events, which may occur additionally to, or instead of, the known $G\alpha_i$ pathway, could be detected.

2.2.2 DMR measurements of 1-series prostanoids at CRTH2

The results of DMR measurements utilizing the 1-series of prostanoids prostaglandin D_1 (PGD_1), prostaglandin A_1 (PGA_1), prostaglandin E_1 (PGE_1) and 6-keto-prostaglandin $F_1\alpha$ ($PGF_1\alpha$) are presented in **figure 22**. It was found that PGD_1 activates CRTH2 (**Fig. 22a,b**) and the resulting signature was completely sensitive towards PTX (**Fig. 22c**). PGD_1 has not been reported as CRTH2 agonist to date, but since this prostanoid had not yet been found in vivo, the resulting ligand-receptor pair may lack physiological relevance. PGA_1 and PGE_1 induced concentration-dependent signatures in both CRTH-HEK and HEK cells (**Fig. 22d,e** and **Fig. 22g,h**). The captured traces of each compound looked very similar at both CRTH2-HEK and HEK cells, by presenting a comparable maximum response and shape, which is obviously different from the observed CRTH2 dependent $G\alpha_i$ signaling events.

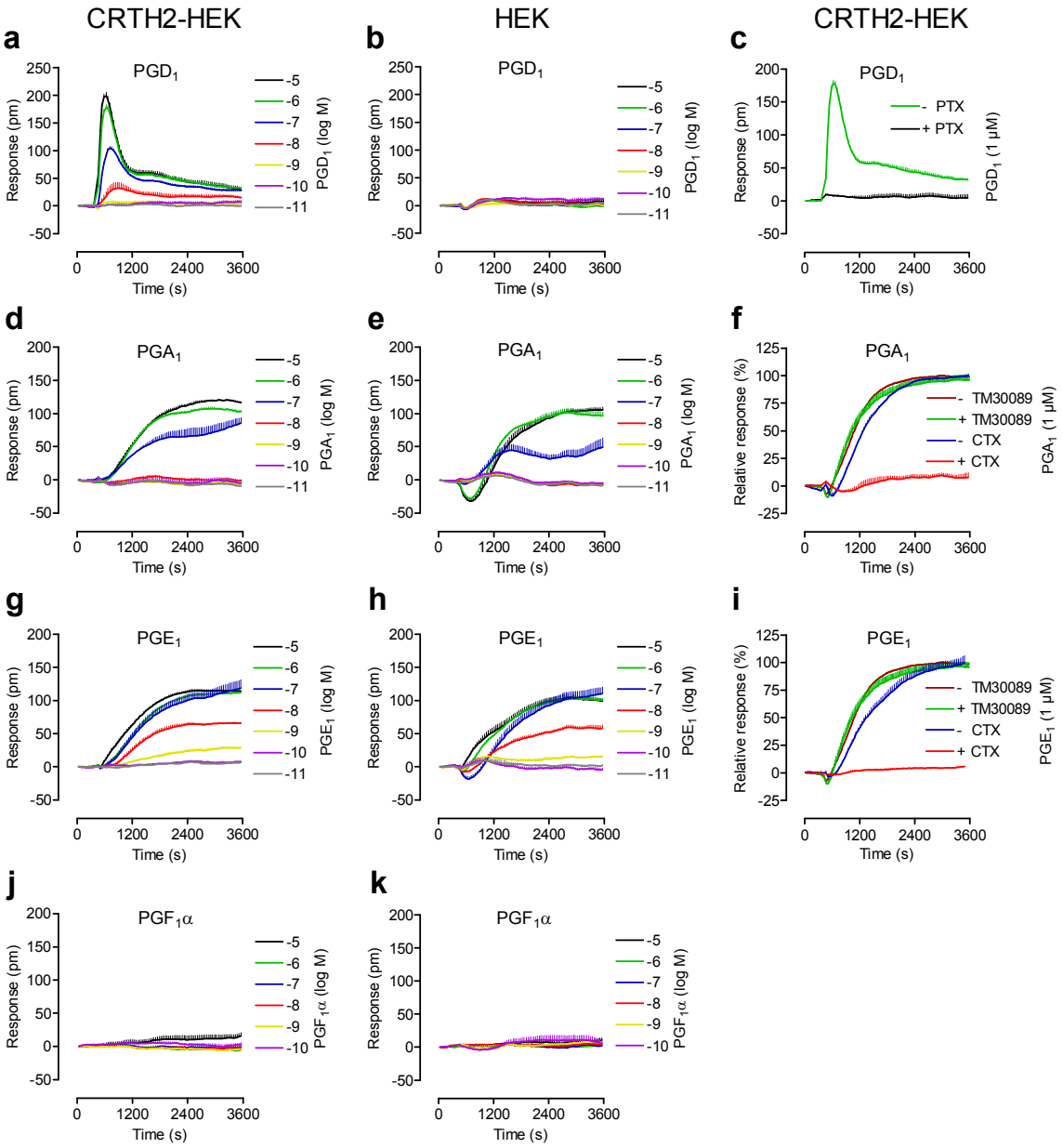

Figure 22: The 1-series prostanoid PGD_1 induces $G\alpha_i$-dependent responses in CRTH2-HEK. (**a-k**) DMR measurements were performed in HEK293 cells stably expressing CRTH2 (CRTH2-HEK) (left and right panels) and native HEK293 cells (HEK) (middle panels). (Left and middle panels) CRTH2-HEK and HEK cells were challenged with various concentrations of (**a,b**) prostaglandin-D_1 (PGD_1), (**d,e**) prostaglandin A_1 (PGA_1), (**g,h**) prostaglandin E_1 (PGE_1) and (**j,k**) 6-keto-prostaglandin $F_1\alpha$ ($PGF_1\alpha$), and wavelength shift was monitored over time. Pathway determination in CRTH2-HEK cells was performed by pretreatment with or without (**c**) 50 ng/ml of pertussis toxin (PTX) or (**f,i**) with or without 250 ng/ml of CTX. Shown are representative data (mean + SEM) of three to four independent experiments, each performed in triplicates.

For PGE_1 it was shown that in HEK cells endogenous EP2 and EP4 receptors were activated (chapter 2.1.2, **Fig. 7**). However, in CRTH-HEK cells the signal looks comparable and there were no indications for signaling in addition to that observed in HEK cells. The same was true for PGA_1-induced signaling: no additional signaling events could be observed in CRTH2-

HEK cells, however the origin of the endogenous response was unknown, These data suggest that CRTH2 was not activated by PGA_1 or PGE_1. To verify this assumption, CRTH2-HEK cells were treated with 10 µM of the CRTH2 specific antagonist TM30089, before PGA_1 or PGE_1 were applied. In both cases the detected signals were not affected, verifying that PGA_1 and PGE_1 are not active at CRTH2.

The signal induced by PGE_1 has already been shown to be $G\alpha_s$-dependent (chapter 2.1.2, **Fig. 6**). The PGA_1-induced traces, due to similarities of shape, may be linked to the same pathway. This was proven by pretreatment of CRTH2-HEK cells with CTX. After PGA_1 addition, the signal totally disappeared in comparison to cells not CTX-treated. These data confirmed that the PGA_1-induced signaling was mediated by $G\alpha_s$ proteins, too.

In contrast to the other tested 1-series prostaglandins, in both cell lines no DMR response was induced by $PGF_1\alpha$.

2.2.3 Both PGH_2 and PGH_1 are active at CRTH2

To provide a comprehensive overview, also the biosynthetic precursor of the 2- and 1-series of prostanoids PGH_2 and PGH_1, respectively, in addition to arachidonic acid (AA) and dihomo-γ-linolenic (DHGLA), were applied at both CRTH2-HEK and HEK cells (**Fig. 23a-k**). DMR measurements revealed that neither AA, nor DHGLA induced any response in both cell lines (**Fig. 23a-c**).

PGH_2 and PGH_1 were described as labile substances when solved in aqueous solutions (Hamberg, et al., 1974b, Hamberg and Fredholm, 1976, Samuelsson, et al., 1978). For this reason the assay procedure was modified in so far, as PGH_2 and PGH_1 dilutions were not incubated for 1 h at 28°C as practiced for the cell containing biosensor microplates (chapter 5.4.1), but were freshly prepared and loaded immediately before being added to the assay. When PGH_2 and PGH_1 were applied, in contrast to what was expected, concentration-dependent signatures were detected (**Fig. 23d-i**), and obviously the traces derived from CRTH2-HEK cells were different with regard to their size and shape compared to those obtained from HEK cells. In comparison to HEK cells, CRTH2-HEK cells responded considerably stronger. The first part of the traces up to about 1200 s was reminiscent to the known $G\alpha_i$ signals, characterized by a strong increase of signal strength, followed by a steep decrease after the maximum.

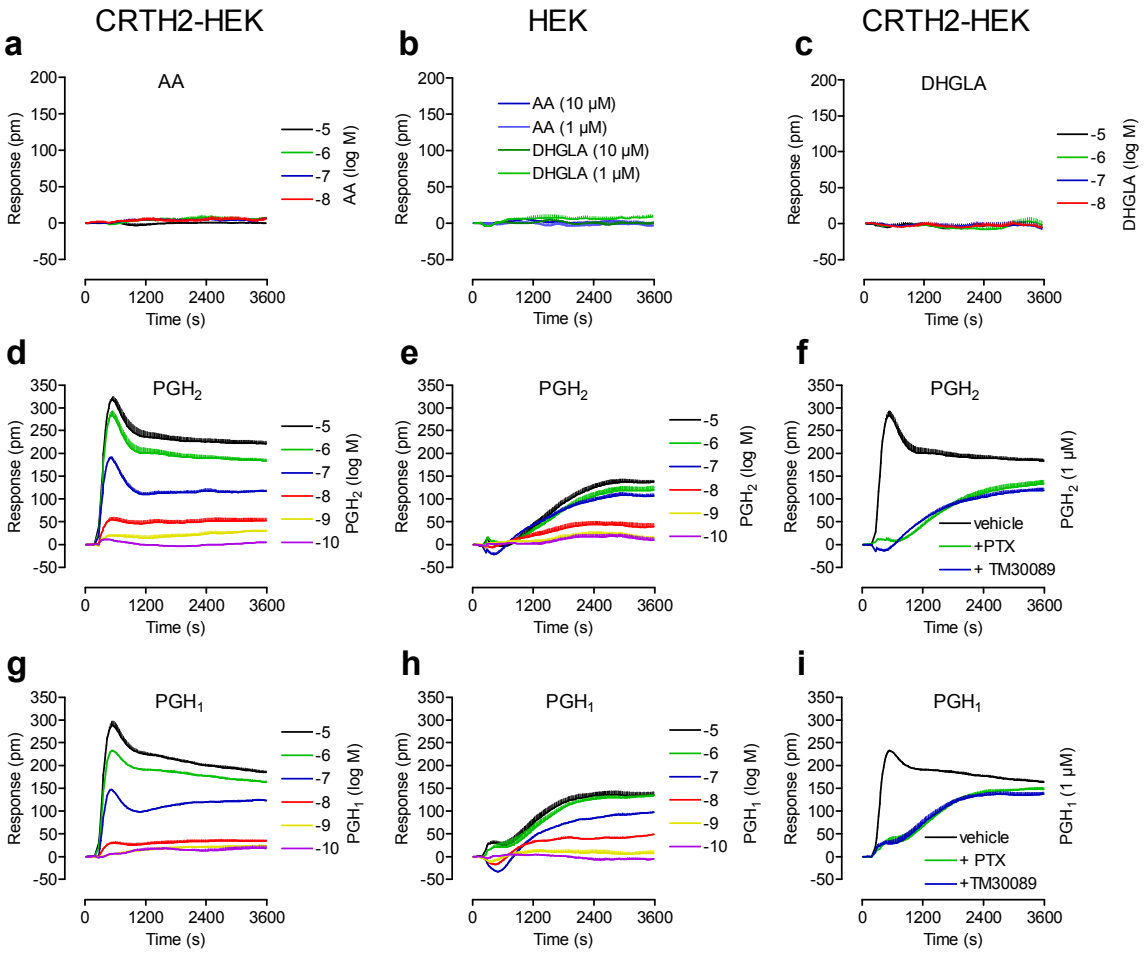

Figure 23: PGH_1 and PGH_2 are active at CRTH2.
(**a-i**) DMR measurements were performed in HEK293 cells stably expressing CRTH2 (CRTH2-HEK) (left and right panels) and native HEK293 cells (HEK) (middle panels). (Left and middle panels) CRTH2-HEK and HEK cells were challenged with various concentrations of (**a,b**) arachidonic acid (AA), (**b,c**) dihomo-γ-linolenic acid (DHGLA), (**d,e**) prostaglandin H_2 (PGH_2) and (**g,h**) prostaglandin H_2 (PGH_2), and wavelength shift was monitored over time. (**f,i**) Pathway determination in CRTH2-HEK cells was performed by pretreatment with or without 50 ng/ml of pertussis toxin (PTX). CRTH2-dependent responses were identified by pretreatment with or without of the specific CRTH2 antagonist TM30089 in a concentration of 10 µM. Shown are representative data (mean + SEM) of three to six independent experiments, each performed in triplicates.

However, in contrary to the known $G\alpha_i$ shape, observed for PGD_2 and other typical CRTH2 agonists, the decrease was not very prominent and the signal remained stable over time at a rather high plateau.

Of particular interest was the great difference between the signals obtained from CRTH2-HEK and HEK cells. Assuming that DMR responses are additive as observed for the $G\alpha_q$ and $G\alpha_i$ events mediated by FFA1 (chapter 2.1.3, **Fig. 9**), it is conceivable that CRTH2-dependent signaling was included in the overall response detected in CRTH2-HEK cells. At that time both, PGH_1 and PGH_2 had not been known as agonists for CRTH2.

To address the previous assumption, PGH_1 and PGH_2-induced signaling in CRTH2-HEK cells was examined by the use of TM30089 (the CRTH2 specific antagonist), resulting in a partial inhibition (**Fig. 23f,i**). Of note, the remaining trace was shaped like the signals obtained from HEK cells. These data suggest that CRTH2 was activated by the addition of PGH_2 and PGH_1 and that there was an additional CRTH2-independent response, found in both cell lines. PTX pretreatment of CRTH2-HEK cells led to the same partial inhibition (**Fig. 23f,i**) as observed with TM30089, implying that a part of the PGH_1 and PGH_2-induced responses in CRTH2-HEK cells are CRTH2-dependent and $G\alpha_i$-triggered. The origin of the background response remains to be elucidated, but it is reasonable to assume that activation of endogenous receptors accounts for these responses.

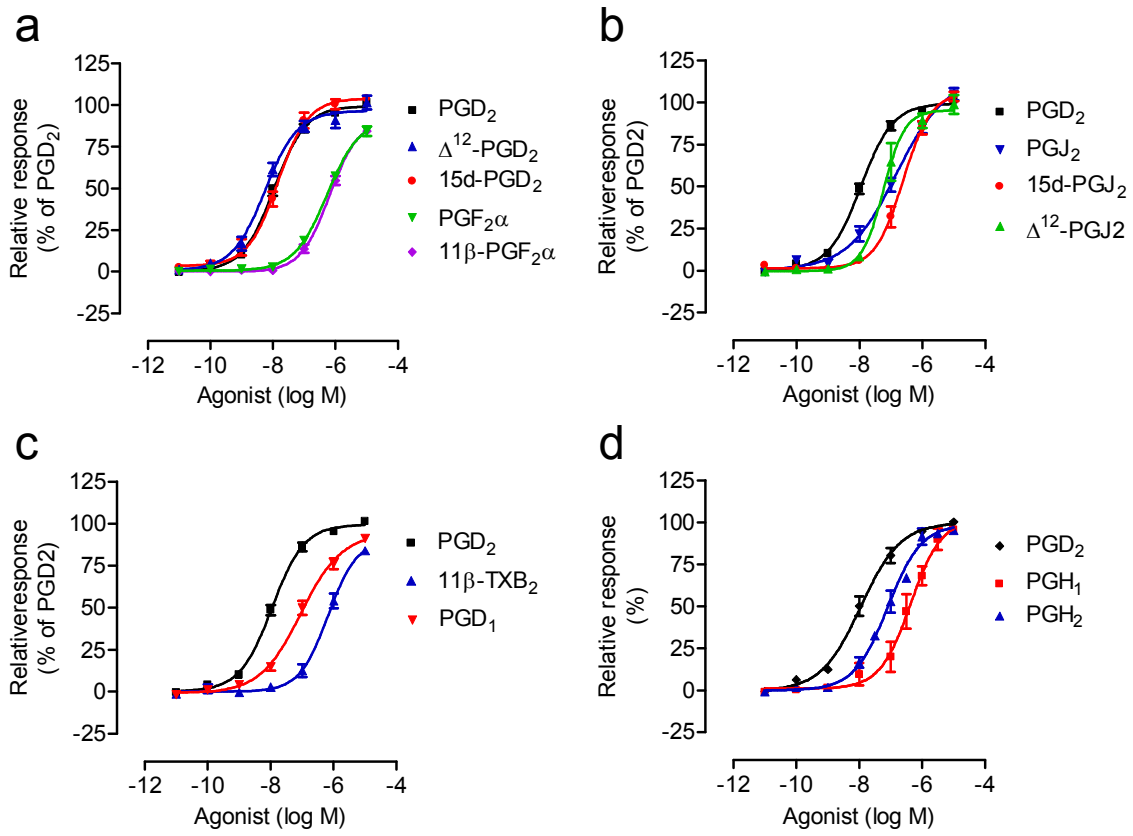

Fig. 24: DMR-derived concentration effect curves of prostanoids with activity at CRTH2.
(**a-d**) Concentration effect curves of DMR data were generated by the maximum response between 300 and 1200 s. The prostaglandin D_2-derived curve and data points are depicted in each panel for comparison. Shown are data of (**a**) 15-deoxy-$\Delta^{12,14}$-prostaglandin D_2 (15d-PGD_2), Δ^{12}-prostaglandin D_2 (Δ^{12}-PGD_2), prostaglandin $F_2\alpha$ ($PGF_2\alpha$) and 11β-prostaglandin $F_2\alpha$ (11β-$PGF_2\alpha$), (**b**) prostaglandin J_2 (PGJ_2), 15-deoxy-$\Delta^{12,14}$-prostaglandin J_2 (15d-PGJ_2), Δ^{12}-prostaglandin J_2 (Δ^{12}-PGJ_2), (**c**) 11-dehydro-thromboxane B_2 (11d-TXB_2) and prostaglandin-D_1 (PGD_1), (**d**) prostaglandin H_2 (PGH_2) and prostaglandin H_1 (PGH_1). (**a-c**) Data are normalized to the maximum response of PGD_2. (**d**) Data are normalized to the maximum response of each compound. (**a-d**) Depicted are mean values ± SEM of at least three independent experiments, each performed in triplicates. Calculated molar pEC_{50} values are depicted in **table 1**.

The background response was always nearly the same with regard to its shape and size in both CRTH2-HEK and HEK cells, which was observed in at least five parallel but independent experiments. To acquire the CRTH2-dependent responses, the signatures obtained from HEK cells were subtracted from those obtained from CRTH2-HEK cells. Then the maximum response between 300 and 1200 s was determined and utilized for the calculation of concentration effect curves. Concentration effect curves of all compounds active at CRTH2 are depicted in **figure 24** and calculated molar pEC50 values are listed in **table 1**.

In DMR assays, PGD_2, 15d-PGD_2, Δ^{12}-PGD_2 and DK-PGD_2 were detected as most potent compounds, whereas $PGF_2\alpha$, 11β-$PGF_2\alpha$ and 11d-TXB_2 were about 100-fold less potent. Potencies of PGJ_2, 15d-PGJ_2, Δ^{12}-PGJ_2 and PGD_1 are inbetween these values. Compared with the hitherto known CRTH2 agonists, PGH_1 was as least as potent as the F-ring PGs and PGH_2 was comparable to the J-ring PGs. The rank order of potencies is as follows: Δ^{12}-$PGD_2 \geq PGD_2$ = DK-$PGD_2 \geq$ 15d$PGD_2 > \Delta^{12}$-$PGJ_2 > PGH_2 = PGD_1 \geq PGJ_2 \geq$ 15d$PGJ_2 \geq PGH_1 \geq PGF_2$a = 11β-$TXB_2$ = 11β-PGF_2. Differences of potencies were considered as "equal" (=) if the difference of molar pEC_{50} values (Δ pEC_{50}) is < 0.1, as "greater than/equal" (≥) if ΔpEC_{50} is < 0.5 and as "greater than" (>) if ΔpEC_{50} is ≥ 0.5.

Table 1-a: DMR assay-derived potencies of eicosanoid compounds for CRTH2 stably expressed in HEK293 cells

Ligand	Structural formula	Molar pEC_{50}
Prostaglandin D_2 (PGD_2)	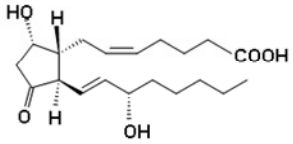	7,96 ± 0.04 (n=6)
13,14-Dihydro-15-keto-prostaglandin D_2 ($DK\text{-}PGD_2$)	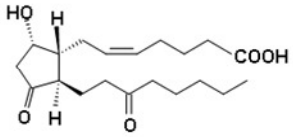	7,96 ± 0.05 (n=6)
15-Deoxy-$\Delta^{12,14}$-prostaglandin D_2 ($15d\text{-}PGD_2$)	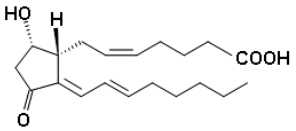	7,84 ± 0.09 (n=3)
Δ^{12}-Prostaglandin D_2 ($\Delta^{12}\text{-}PGD_2$)	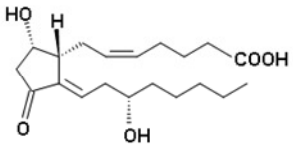	8.25 ± 0.09 (n=3)
Prostaglandin $F_2\alpha$ ($PGF_2\alpha$)	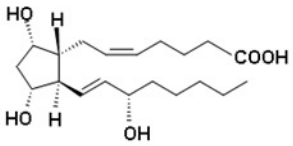	6.27 ± 0.06 (n=4)
11β-Prostaglandin $F_2\alpha$ ($11\beta\text{-}PGF_2\alpha$)	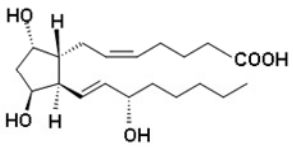	6.20 ± 0.05 (n=4)
Prostaglandin J_2 (PGJ_2)	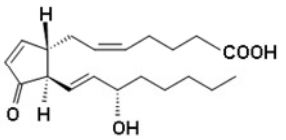	6.82 ± 0.14 (n=3)
15-Deoxy-$\Delta^{12,14}$-prostaglandin J_2 ($15d\text{-}PGJ_2$)	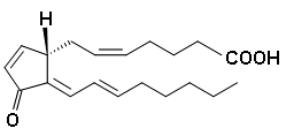	6.61 ± 0.07 (n=3)
Δ^{12}-Prostaglandin J_2 ($\Delta^{12}\text{-}PGJ_2$)	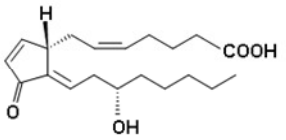	7.24 ± 0.03 (n=3)

Table 1-b: DMR assay-derived potencies of eicosanoid compounds for CRTH2 stably expressed inHEK293

Ligand	Structural formula	Molar pEC_{50}
11-Dehydro-Thromboxane B_2 ($11d\text{-}TXB_2$)	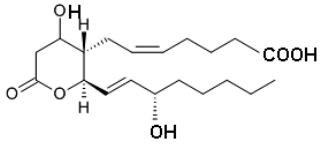	6.20 ± 0.08 (n=3)
Prostaglandin D_1 (PGD_1) Prostaglandin D_1 (PGD_1)	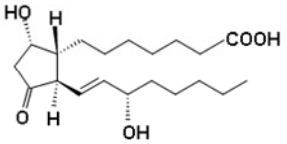	7.04 ± 0.09 (n=4)
Prostaglandin A_1 (PGA_1)	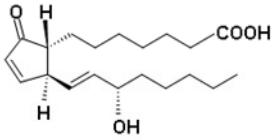	no response
Prostaglandin E_1 (PGE_1)	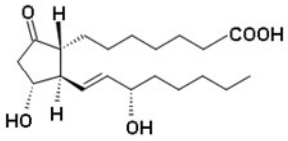	no response
6-keto-Prostaglandin $F_1\alpha$ ($PGF_1\alpha$)	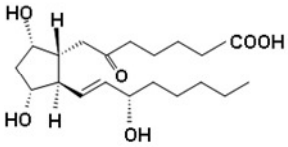	no response
Arachidonic acid (AA)	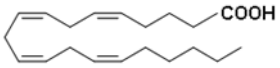	no response
Dihomo-γ-linolenic acid (DHGLA)	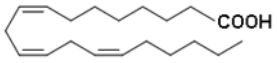	no response
Prostaglandin H_2 (PGH_2)	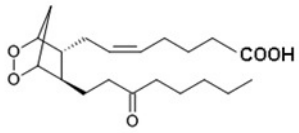	7.09 ± 0.08 (n=4)
Prostaglandin H_1 (PGH_1)	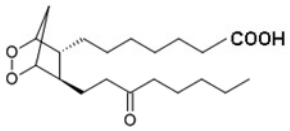	6.37 ± 0.10 (n=5)

2.2.4 $G\alpha_i$ and $G\alpha_s$ responses are simultaneously captured by DMR measurement

Both PGH_1 and PGH_2 were found to be not only active at CRTH2, but also inducing a background response, which was not CRTH2 or $G\alpha_i$-dependent (**Fig. 23f,i**). This remaining response, and also the response in HEK cells, was shaped like the known $G\alpha_s$-dependent signatures, suggesting that this pathway was activated by hitherto unknown targets. Since no interacting receptors were described for both derivatives, these targets were also of interest, and further investigations are mainly described in chapter 2.4.

In order to further explore the capability of DMR technology, it was of interest whether the captured background signal was CTX sensitive and in particular, whether the mixed response obtained from CRTH2-HEK cells could be dissected into their individual components. To examine this, CRTH2-HEK and HEK cells were pretreated with CTX, TM30089, and a combination of both (**Fig. 25a,b**). As expected, TM30089 displayed no effect at the signals derived from HEK cells (**Fig. 25b**), when challenged with PGH_1. But pretreatment with CTX, and the combination of CTX and TM30089 totally erased the traces, indicating that $G\alpha_s$ coupling events occur. In CRTH2-HEK cells pretreatment with TM30089 led to the known $G\alpha_s$-like signature (**Fig. 25a**), while the use of CTX alone led to a $G\alpha_i$ like trace, whereas the signals were fully abrogated by the use of a combination of TM30089 and CTX.

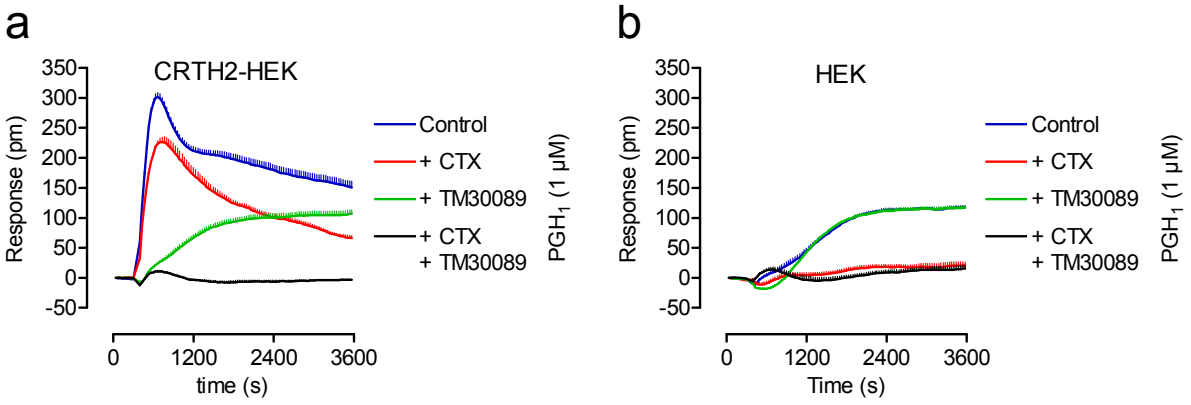

Fig. 25: The PGH_1-induced background signal in CRTH2-HEK cells is $G\alpha_s$-mediated.
DMR measurements were performed in (**a**) HEK293 cells stably expressing CRTH2 (CRTH2-HEK) and (**b**) native HEK293 cells (HEK). (**a,b**) Pathway determination and dissection was performed by pretreatment of CRTH2-HEK and HEK cells with 250 ng/ml of CTX, 10 µM TM30089, or a combination of both. Shown are representative data (mean + SEM) of three to four independent experiments, each performed in triplicates.

These data demonstrate that the background signal in CRTH2-HEK cells has a $G\alpha_s$ origin. Therefore the results described in this chapter suggest that PGH_1 and PGH_2 are agonists at

CRTH2 and also activators of still unknown endogenous $G\alpha_s$-linked targets in HEK293 cells. In addition, it is obvious and remarkable, that DMR technology is capable to simultaneously capture $G\alpha_i$ and $G\alpha_s$ coupling events, which are contrary at the cAMP level and would thus neutralize each other in a cAMP accumulation assay.

Activation of CRTH2 by both PGH_1 and PGH_2 was corroborated by further investigations, which are presented in chapter 2.3.

Continued examinations of PGH_1 and PGH_2-induced $G\alpha_s$ responses in HEK cells are described in chapter 2.4.

2.3. Activation of CRTH2 by PGH_1 and PGH_2

The precursors of the 1- and the 2-series of prostanoids, PGH_1 and PGH_2, respectively, were found to be active at CRTH2, as described in chapter 2.2. These findings came from DMR measurements in HEK293 cells stably expressing CRTH2. Herein, the activation of CRTH2 by PGH_1 and PGH_2 was corroborated in additional independent assays and extended to primary human cells.

Since CRTH2 activation by PGH_2 is meanwhile known und published (Schuligoi, et al., 2009), this chapter focuses on PGH_1.

2.3.1 Stability of PGH_1 and PGH_2

Both, PGH_1 and PGH_2 are described to be instable substances. PGH_2 can be converted enzymatically to PGD_2 by PGD synthases (Kanaoka, et al., 1997), whereas spontaneous decomposition to PGE_2 takes place when PGH_2 is dissolved in aqueous solutions (Hamberg, et al., 1974b, Hamberg and Fredholm, 1976, Samuelsson, et al., 1978). PGH_1 is less well examined and described in literature, but considering that the modifications mentioned for PGH_2 are related to the molecular ring structure, which is equal for both derivatives, it can be assumed that the risk of decomposition is also true for PGH_1.

Given the reported instability of the PGH derivatives, the possibility that the compounds might degrade during DMR assays was examined. Two experimental sets were performed in parallel using the same biosensor microplate: for one set both PGH derivatives were diluted immediately before they were applied to the cells, for the other set the compounds were diluted and stored for 90 minutes at 28°C (the DMR assay temperature) before being added to the assay. DMR measurements of both, PGH_1 and PGH_2, prepared under the different conditions, did not indicate decomposition of these derivatives (**Fig. 26**). The captured signatures were virtually superimposable, demonstrating that PGH_1 and PGH_2 were stable during the assay period and under the applied conditions.

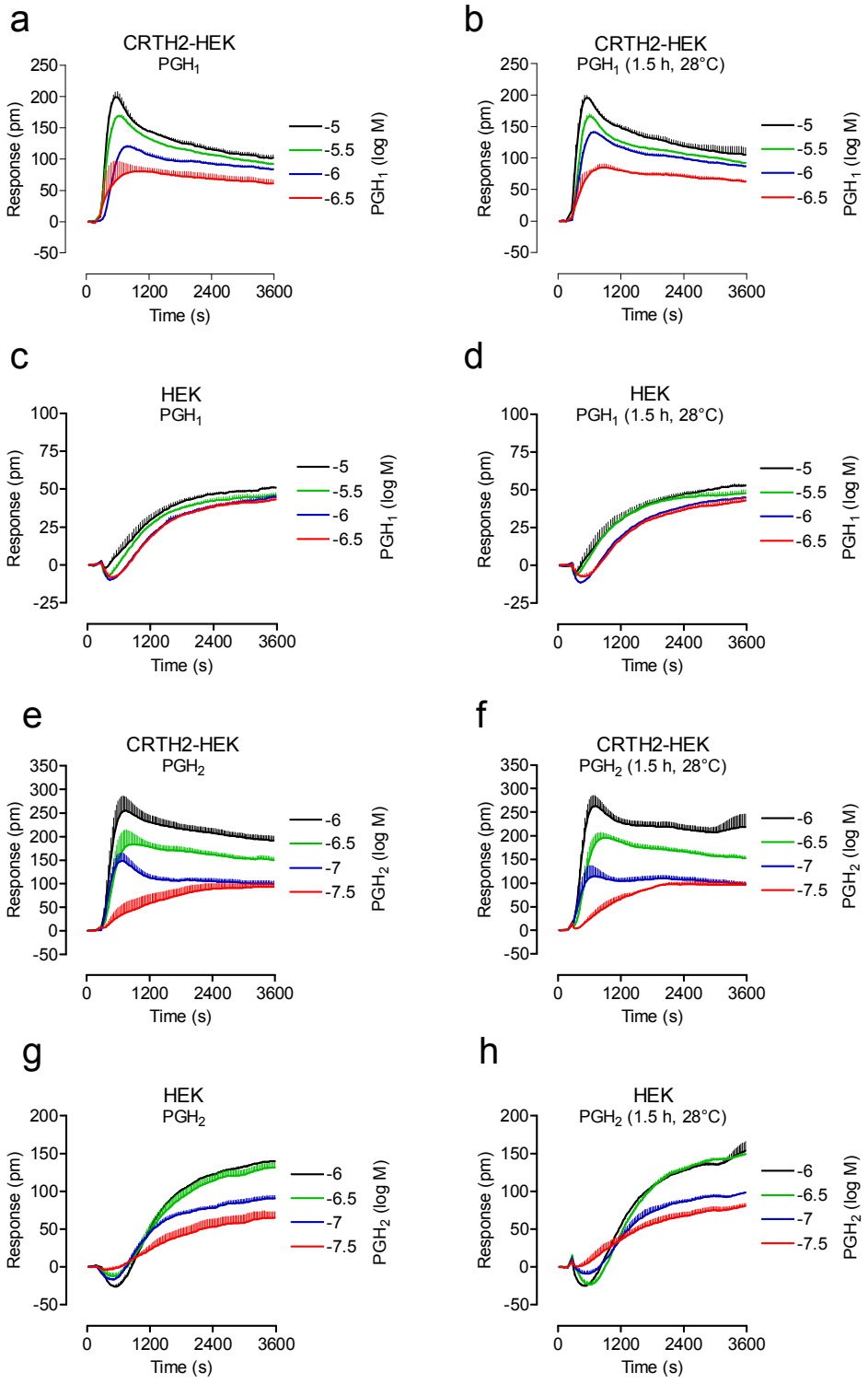

Figure 26: DMR data indicate that PGH derivatives do not decompose during an assay period. (**a-h**) DMR measurements in HEK293 cells stably expressing CRTH2 (CRTH2-HEK) and native HEK293 cells (HEK). CRTH2-HEK cells (**a,e**) and HEK cells (**c,g**) were challenged with the indicated compound concentrations, which were prepared and diluted in assay buffer immediately before use or (**b,d,f,h**) diluted and stored at 28°C for 90 minutes before addition. Optical traces obtained from the different pretreated compound samples are virtually superimposable. Shown are representative data (mean + SEM) of three independent experiments, each performed in triplicates.

To further confirm that PGH_1 and PGH_2 induce activation of CRTH2, calcium mobilization assays were performed. CRTH2-HEK cells were transiently transfected with cDNA coding for the promiscuous G protein Gq_i5 (chapter 5.2.1), which funnels GPCR response from $G\alpha_i$ to $G\alpha_q$. This enables the detection of $G\alpha_i$-coupled receptor activity via calcium release. Cells were challenged with the PGH derivatives as well as with PGD_2 for comparison and reference purposes and intracellular calcium efflux was detected by fluorescence measurement (**Fig. 27**). Detection of calcium release represents a very rapid readout for receptor activation. PGH_1 and PGH_2 were freshly diluted immediately before addition and both compounds induced robust calcium peaks, although the signals induced by PGH_1 displayed reduced efficacy compared to PGD_2 and PGH_2. The calcium response maxima were reached within 20 s after compound addition, ensuring that compound decomposition was minimized during this time frame.

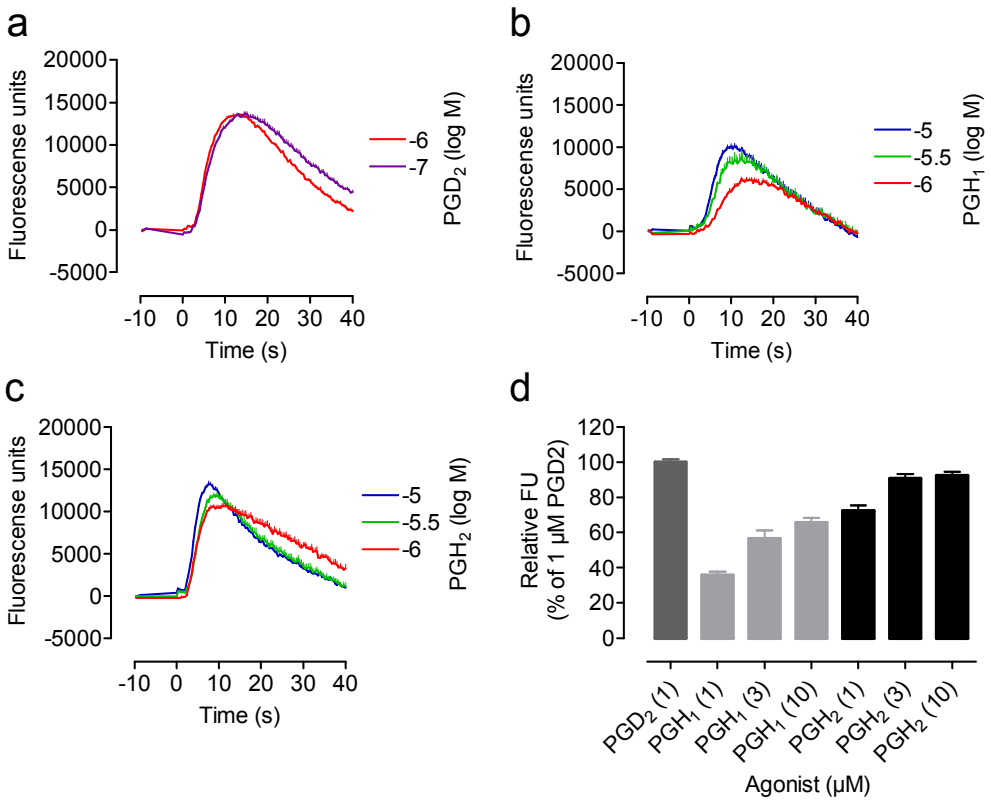

Figure 27: PGH_2 and PGH_1 stimulate calcium mobilization in CRTH2 transfectants.
(**a-d**) Measurement of calcium release in HEK293 cells stably expressing CRTH2 (CRTH2-HEK) and cotransfected with the promiscuous G protein Gq_i5, that funnels GPCR response from $G\alpha_i$ to $G\alpha_q$. Cells were challenged with the indicated agonist concentrations and calcium release was detected with a fluorescence-sensitive dye. Assays were performed in the presence and absence of the CRTH2 antagonist TM30089. The depicted traces were background corrected by subtraction of CRTH2-independent response. Shown are representative data (mean + SEM) of three independent experiments, each performed in triplicates. (**d**) Maximum responses were normalized to 1 µM PGD_2. Data are mean and SEM of three independent experiments, each performed in triplicates.

2.3.2 PGH_1 promotes internalization of CRTH2 in HEK cells

Most GPCRs are known to internalize after agonist activation and this is also true for CRTH2 after the ligation with its main agonist PGD_2 (Ferguson, 2001, Schröder, et al., 2009, Sorkin and von Zastrow, 2009b). To corroborate the activation of CRTH2 by PGH_1 in another independent assay, the ability of PGH_1 to internalize CRTH2 in CRTH2-HEK cells was investigated. This was realized by fluorescent staining of the receptor and detection of cellular distribution after compound addition using confocal microscopy as described in chapter 5.4.6 and **figure 28** (see legend). In non-stimulated cells, the cell membranes were predominantly stained (**Fig. 28a**), indicating that CRTH2 was mainly located in these regions. Upon stimulation with PGH_1 or PGD_2, CRTH2 staining appeared in intracellular vesicles in high density (**Fig. 28b,c**), indicating altered cellular receptor distribution. These data demonstrate that CRTH2 internalized subsequent to addition of PGH_1 or PGD_2, which was confirmed by using the selective CRTH2 antagonist TM30089 (**Fig. 28e,f**). In the presence of TM30089, PGH_1 and PGD_2-mediated internalization of CRTH2 was inhibited, whereas TM30089 showed no effect when applied alone (**Fig. 28d**). These results further corroborate the interaction of PGH_1 and CRTH2.

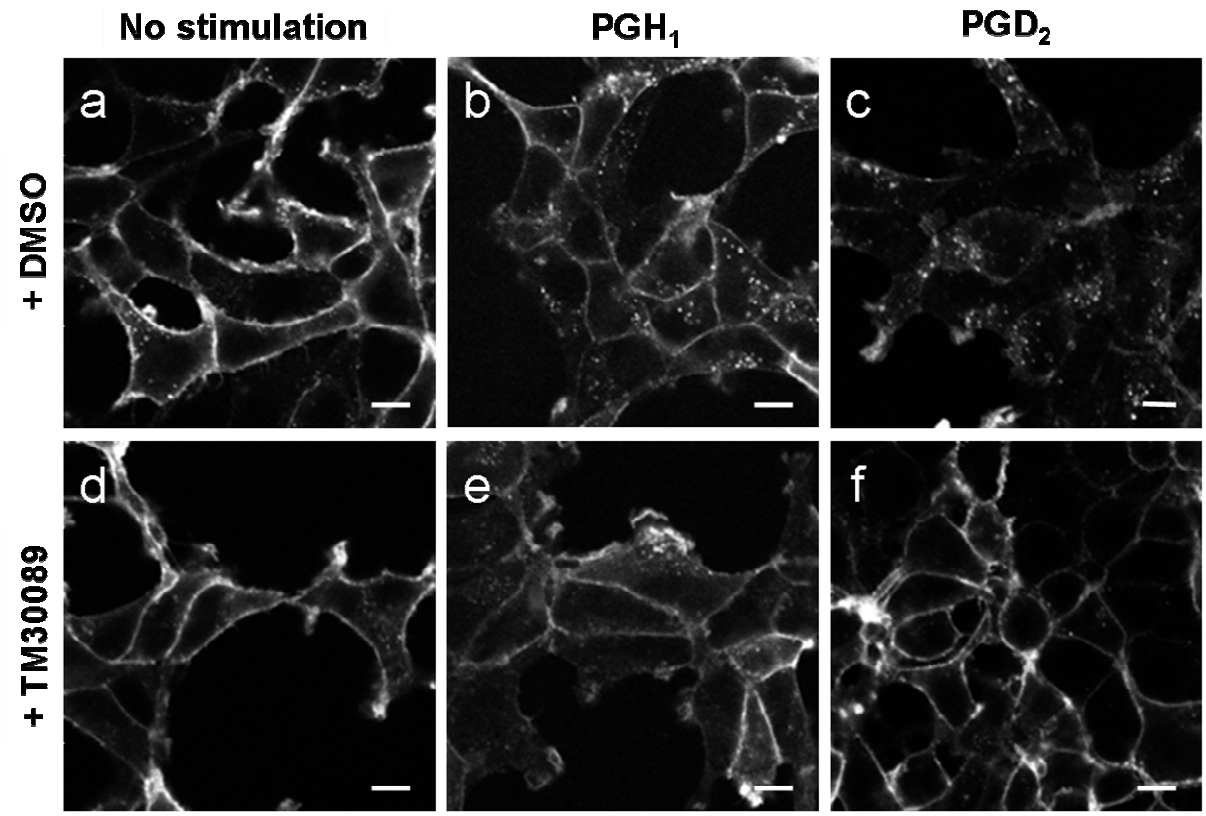

Figure 28: PGH_1 promotes internalization of CRTH2.
The utilized HEK293 cells stably expressing CRTH2 (CRTH2-HEK) had been engineered in order to express a CRTH2 molecule that possesses a FLAG epitope at its N-terminus (chapter 5.3.1). CRTH2-HEK cells were incubated with the anti-FLAG M1 antibody (Sigma, St. Lois, MO, US) recognizing the FLAG-tag of CRTH2. Cells were then treated with either solvent control (**a,d**), 1 µM PGH_1 (**b,e**) or 1 µM PGD_2 (**c,f**) in the absence (**a-c**) or presence (**d-f**) of the CRTH2 antagonist TM30089 (10 µM). All ligand stimulations were performed for 30 min at 37°C. Following stimulation, cells were fixed, permeabilized and immunostained with a fluorescent secondary antibody (Alexa-Fluor 488-conjugated goat anti mouse, Sigma, St. Lois, MO, US). This antibody binds to the anti FLAG antibody and is capable to pass through the permeabilized cell membrane, hence all CRTH2 molecules present at the cell surface in the first step are now stained and visible by microscopy. The cellular receptor localisation was imaged by confocal microscopy using a LSM 510 Meta laser scanning microscope (Zeiss, DE). For control, CRTH2-HEK and HEK cells were treated with both antibodies without stimulation and permeabilization. Under these conditions surface staining was observed for CRTH2-HEK but not for native HEK cells, indicating that the detection is CRTH2 specific (data not shown).
(**a-f**) Experiments were performed three times, and the shown images are representative for cell populations. Scale bars are 10 µm. Assays were performed by Dr. Lene Martini from the Ernest Gallo Clinic & Research Centre, University of California, San Fransisco, Emeryville, CA 94608, US.

2.3.3 PGH_1 and PGH_2 induce the activation of primary human lymphocytes

The discovery that PGH_1 and PGH_2 activate CRTH2 was made in a HEK293 cell-based overexpression system. Thus, the question arose whether PGH derivatives induce CRTH2-dependent bioactivity also in primary human cells, which are generally considered as being of higher physiological relevance. CRTH2 is predominantly expressed in lymphocytes such as eosinophils and T-helper type 2 (Th2) cells and mediates the activation of these cells in inflammation and allergic responses. This activation is characterized by detectable events like shape change, chemotaxis and migration. In addition intracellular calcium release represents a key event in ligand-induced activation of immune cells and is correlated with a variety of cellular processes in inflammation. Furthermore PGD_2 is known as potent inducer of calcium efflux in Th2 cells (Hirai, et al., 2001). Meanwhile, it has been shown that PGH_2 induces activation of CRTH2 resulting in shape change, migration and calcium release in eosinophils (Schuligoi, et al., 2009).

In the present study, it was examined whether both PGH_1 and PGH_2 are competent to induce shape change of eosinophils and moreover migration of and calcium release in Th2 cells.

2.3.3.1 PGH_1 and PGH_2 induce shape change in eosinophils via CRTH2

Shape change assays with primary human eosinophils were performed by flow cytometry (FCM) analysis as referred to in chapter 5.4.7 and **figure 29** (see legend). Alterations of cell shape induce differences in the scattering of applied light. The amount of light scatter is detected by FCM and a measure for shape change.

PGH_1 was found to induce shape change with similar efficacy as PGH_2, although both PGH derivatives displayed reduced efficacy and potency compared with PGD_2 (**Fig. 29**). The rank order of potencies matches well with the results obtained from DMR assays: $PGD_2 > PGH_2 > PGH_1$. The activation of eosinophils by PGH_1 and PGH_2 was inhibited by pretreatment with TM30089 before agonist addition, indicating that the effect was mediated by CRTH2.

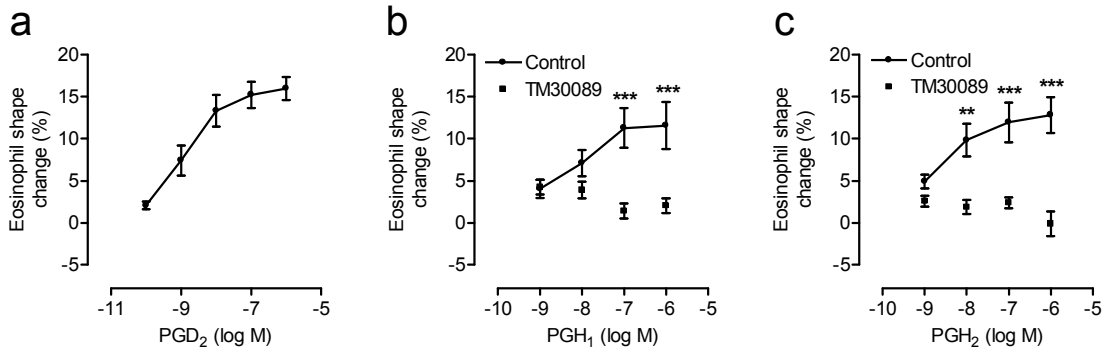

Figure 29: PGH_1 activates human eosinophils via CRTH2.
Human eosinophils were challenged with the indicated agonist concentrations and chemotactic activation was measured in shape change assays using the FACSArray (BD Biosiences, Oxford, UK). Shape change of eosinophils is inhibited in the presence of 1 µM of the CRTH2 specific antagonist TM30089. Results are presented as mean ± SEM of three experiments, each performed in triplicates with a separate donor used in each experiment. For statistical analysis, individual concentrations were compared by two-way ANOVA with Bonferroni's correction for multiple comparisons; ** $p < 0.01$, *** $p < 0.001$.Assays at primary human eosinophils were performed by Dr. Luzheng Xue and Dr. Roy Pettipher from Oxagen Ltd, 91 Milton Park, Abingdon Oxon, OX14 4RY, UK. Primary blood cells were purchased from the National Blood Service, Bristol, UK.

2.3.3.2 PGH_1 and PGH_2 induce intracellular calcium release and migration at Th2 cells

Activation of Th2 cells was investigated by calcium release assays and migration of Th2 cells towards the investigated compounds, as referred to in chapter 5.4.7 and **figure 30** (see legend).

In calcium release assays, primary Th2 cells were challenged with PGH_1, PGH_2 and PGD_2 and they respond with concentration-dependent signals (**Fig. 30a-c**). The PGH derivates were comparable to each other with regard to the induced potency and efficacy, but less effective compared to PGD_2. PGH_1 and PGH_2-induced calcium release was abolished by pretreatment with TM30089, indicating that the activation was CRTH2-mediated (**Fig. 30b,c**). The calcium responses peaked at ~50 sec after compound addition (data not shown) and provide further support that the PGH derivates by themselves and not degradation products were responsible for the observed CRTH2 activations.

Chemotactic migration of cells towards a chemoattractant substance can be detected by a cell culture two chamber system. One chamber contains the cells and the other chamber the test compound. Both chambers, filled with culture medium, are connected by a membrane, enabling the test compound to diffuse towards the connected cell-containing chamber, and in

turn enabling the cells to migrate in direction of a potential chemoattractant. Migrated cells remain at the membrane and can be counted.

The assays demonstrated that PGH_1 and PGH_2 were competent to induce migration of Th2 cells, but with reduced potency and efficacy as compared with PGD_2 (**Fig. 30d-f**). In the presence of TM30089, the PGH_1 and PGH_2-induced effect was totally erased, indicating that migration was mediated by activation of CRTH2.

These results demonstrate that both PGH_1 and PGH_2 were capable to induce CRTH2-dependent bioactivity in primary cells.

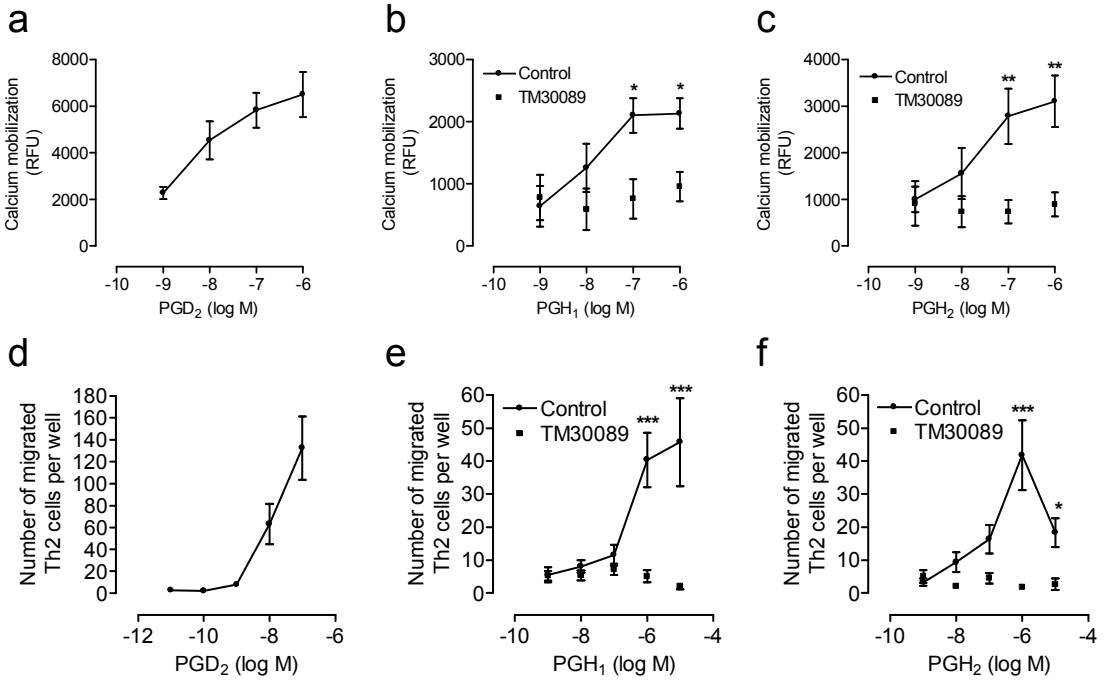

Figure 30: PGH_1 activates human Th2 cells via CRTH2.
Measurement of calcium mobilization (**a-c**) and cell migration (**d-f**) was performed at primary human T helper type 2 (Th2) cells utilizing the indicated concentrations of PGD_2, PGH_1, and PGH_2, respectively. Both calcium mobilization and cell migration were inhibited in the presence of 1 µM of the CRTH2 specific antagonist TM30089. Data are mean ± SEM of three experiments, each performed in duplicates and involving Th2 cells from a separate donor. Calcium mobilization was detected using the Calcium 5 assays kit and a FlexStation (both: Molecular Devices, CA, US). Migration assays were performed using 5-µm pore-sized 96-well ChemoTX plates (Neuro Probe, MD, US). Migrated cells were quantified by fluorescent activated cell sorting (FACS) using the FACSArray (BD Biosiences, Oxford, UK). For statistical analysis, individual concentrations were compared by two-way ANOVA with Bonferroni's correction for multiple comparisons; * $p < 0.05$, ** $p < 0.01$, *** $p < 0.001$. Assays with Th2 cells were performed by Dr. Luzheng Xue and Dr. Roy Pettipher from Oxagen Ltd, 91 Milton Park, Abingdon Oxon, OX14 4RY, UK. Primary blood cells were purchased from the National Blood Service, Bristol, UK.

2.4 The E-prostanoid receptors EP2 and EP4 are activated by PGH_2 and PGH_1

PGH_2 and PGH_1, the precursor of the 2- and 1-series of prostanoids, respectively, were found active at CRTH2 as described in chapter 2.2.3. However, an additional background signal was detected, which remained when CRTH2-HEK cells were treated with the CRTH2 antagonist TM30089, and a similar response was also detected in native HEK cells (chapter 2.2.3, **Fig. 23**). Herein investigations regarding the detected background responses unveiled EP2 and EP4 receptors as molecular targets of PGH_2 and PGH_1.

2.4.1 PGH_2 and PGH_1-induced responses in HEK cells are $G\alpha_s$ mediated

For PGH_1, the background response mentioned above was previously shown to be CTX sensitive (chapter 2.2.4, **Fig. 25**). This was also examined for PGH_2 as depicted in **figure 31**.

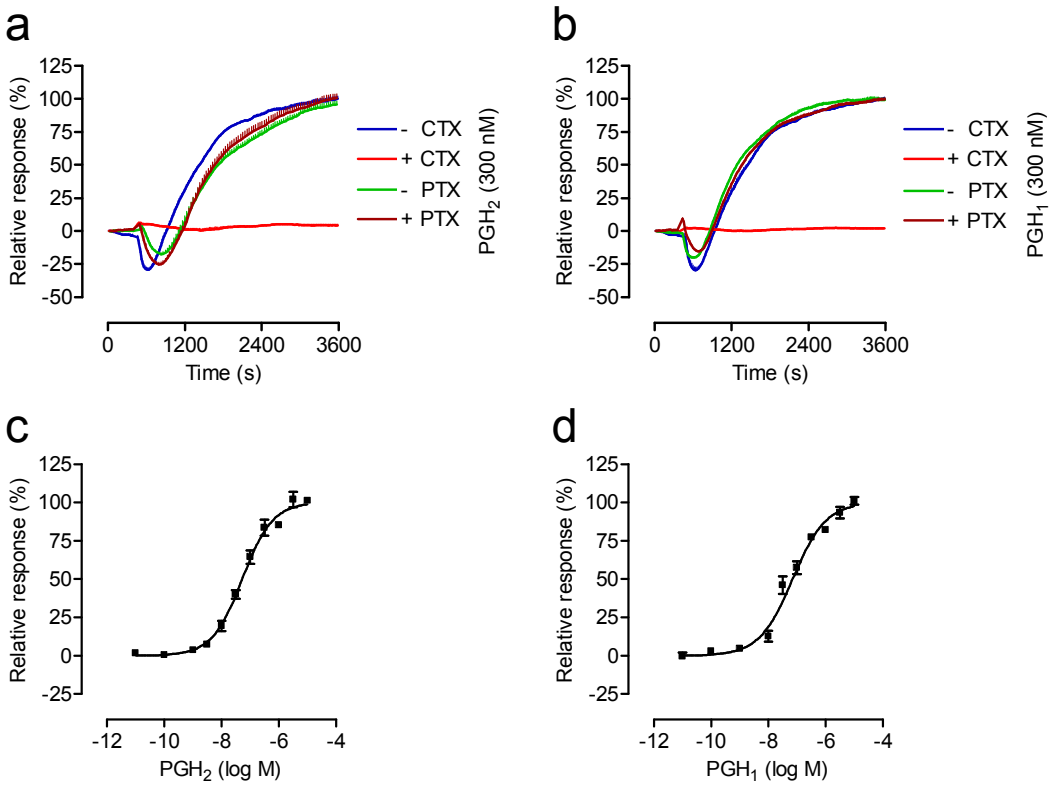

Figure 31: PGH2 and PGH1 cause Gs signaling in native HEK293 cells.
(**a,b**) Pathway determination was performed in native HEK293 cells (HEK) in the presence and absence of 250 ng/ml of cholera toxin (CTX) or 50 ng/ml of pertussis toxin (PTX). Cells were challenged with the indicated agonist concentrations and wave length shift was monitored over time. Shown are representative data (mean and SEM) of at least three independent experiments, each performed in triplicates. (**c,d**) DMR-derived concentration effect curves of PGH_2 and PGH_1 in HEK cells. Molar log EC_{50} values are 7.28 ± 0.06 for PGH_2 and 7,15 ± 0.07 for PGH_1. Shown are mean ± SEM of four independent experiments.

The DMR traces induced by both PGH_1 and PGH_2 were masked by pretreatment with CTX, whereas PTX pretreatment did not display any affect. This indicates a similar mode of action for both PGH derivatives. The observed sensitivities towards CTX demonstrate that the responses are triggered by endogenous $G\alpha_s$ coupled receptors.

Response traces of PGH_2 and PGH_1 in native HEK cells were found to be concentration-dependent (chapter 2.2.3, **Fig 23e,h**). Efficacies were determined by the area under the curve and resulting concentration effect curves exhibited similar potencies (**Fig. 31c,d**). Both derivatives always displayed similar maximum responses in parallel experiments (chapter 2.2.3, **Fig 23 e,h** and data not shown), hence concentration effect curves were normalized to the maximum response of each compound (**Fig. 31c,d**).

2.4.2 Identification of both EP2 and EP4 as molecular targets of PGH_2 and PGH_1

Considering that most prostanoid receptors are closely related and in some cases no exclusive ligand specificity exists, it was likely, that prostanoid receptors were the origin of the PGH_2 and PGH_1-induced responses. PGH_2 is described to activate the thromboxane receptor (TP) (Corey, et al., 1975, Saito, et al., 2003), which exists as two alternatively spliced variants. Both are predominantly $G\alpha_q$-coupled, but TPα additionaly couples to $G\alpha_s$ and TPβ to $G\alpha_i$. Prevailed coupling to $G\alpha_s$ is described for the D-prostanoid receptor 1 (DP1) and the E-prostanoid receptors EP2 and EP4 (Hata and Breyer, 2004). Since the DMR responses induced by the PGH derivates were found to be only $G\alpha_s$-dependent, DP1 and EP2/EP4 receptors were examined first.

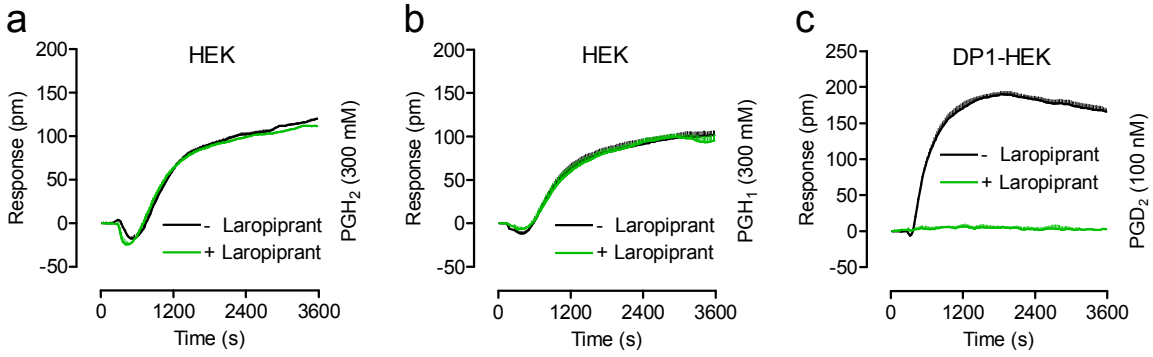

Figure 32: Signatures of PGH derivatives are unaffected by the DP1 antagonist laropiprant. (**a,b**) DMR traces derived from native HEK 293 cells challenged with the indicated agonists were not affected by pretreatment with laropiprant (10 µM). (**c**) PGD_2 induced signaling in HEK293 cells stably expressing DP1 (DP1-HEK) was fully abrogated by 10 µM laropiprant. Shown are representative data (mean and SEM) of three independent experiments, each performed in triplicates.

Due to the fact that PGD_2 did not induce signaling in native HEK cells, except for responses at the highest agonist concentrations, DP1 was unlikely to represent the endogenous PGH-sensitive receptor. Nevertheless, the selective DP1 antagonist laropiprant was tested for inhibition of PGH_2 and PGH_1-induced responses. As anticipated, the signatures obtained from HEK cells challenged with the PGH derivates were not affected by pretreatment with laropiprant (**Fig. 32a,b**). For control purposes, PGD_2 was applied to HEK cells stably expressing DP1 (DP1-HEK) in the absence and presence of laropiprant, verifying that the antagonist inhibits the DP1-derived response (**Fig. 32c**).

As described in chapter 2.1.2, in HEK cells the endogenously expressed E-prostanoid receptors EP2 and EP4 were activated by PGE_1, leading to $G\alpha_s$ signaling. Thus, the EP2 and EP4 receptor antagonist AH6809 and L161,982, respectively, were tested with regard to the responses derived from application of the PGH derivatives (**Fig. 33**).

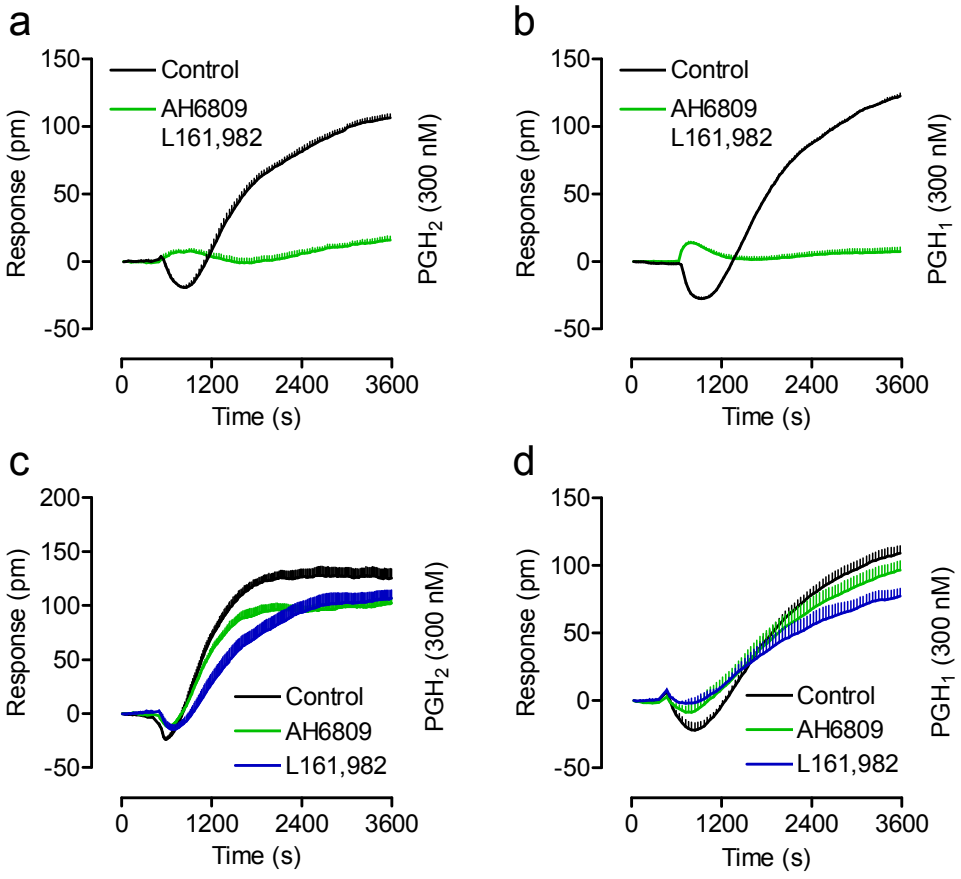

Figure 33: PGH derivatives signal via endogenous EP2 and EP4 receptors in HEK cells.
(**a,b**) The DMR responses of PGH_1 and PGH_2 in native HEK 293 cells were fully abrogated by pretreatment with a combination of AH6809 (10 µM) and L161,982 (10 µM). (**c,d**) Pretreatment with only one of the compounds (10 µM) did hardly affect the response. Shown are representative data (mean and SEM) of four (**a,b**) or three (**c,d**) independent experiments, each performed in triplicates.

DMR responses of both, PGH_2 and PGH_1, were completely inhibited in the presence of a combination of both antagonists (**Fig. 33a,b**). However, treatment with the individual compounds alone did hardly diminish the responses (**Fig. 33c,d**). These data demonstrate that PGH_2 and PGH_1 activate both EP2 and EP4 receptors in HEK cells.

2.4.3 Detection of EP2 and EP4 activation in primary human keratinocytes

For PGE_1, the activation of EP2 and EP4 receptors in HaCaT and primary human keratinocytes was demonstrated (chapter 2.1.7, **Fig. 18**). This was likewise tested for the PGH derivatives.

PGH_1 and PGH_2 were applied at HaCaT and primary keratinocytes and cells responded with robust and concentration-dependent DMR traces (**Fig. 34**). The signatures were markedly similar to those detected in the same cell lines after application of PGE_1 (chapter 2.1.7, **Fig. 17**). In HaCaT cells the molar pEC_{50} values of the resulting concentration effect curves are 7.60 (± 0.23) for PGH_2 and 7.36 (± 0.05) for PGH_1, and hence similar between the PGH derivatives (**Fig. 34 d,c**) but less potent compared to PGE_1 (8,27 ± 0.09). Similar results were found for primary keratinocytes. Concentration effect curves are depicted in **figure 34g,h**. The resulting molar pEC_{50} values are 6.61 (± 0,13) for PGH_2 and 6,73 (± 0.10) for PGH_1, and thus were comparable to each other, but again lower as compared with PGE_1 (7.77 ± 0.06). Efficacies of both compounds were similar in all experiments at the respective cell lines (**Fig. 34** and data not shown).

The PGH_2 and PGH_1-induced signatures at both, HaCaT and primary keratinocytes, were sensitive to treatment with CTX but PTX-insensitive (**Fig. 35a-d**), indicating that the cellular targets were $G\alpha_s$-linked. As depicted in **figure 35e-h**, the application of a combination of the EP2 and EP4 receptor antagonists AH6809 and L161,982 respectively, led to a full response inhibition.

These results demonstrate that EP2 and EP4 receptors are the cellular targets of PGH_2 and PGH_1 in HaCaT and primary keratinocytes.

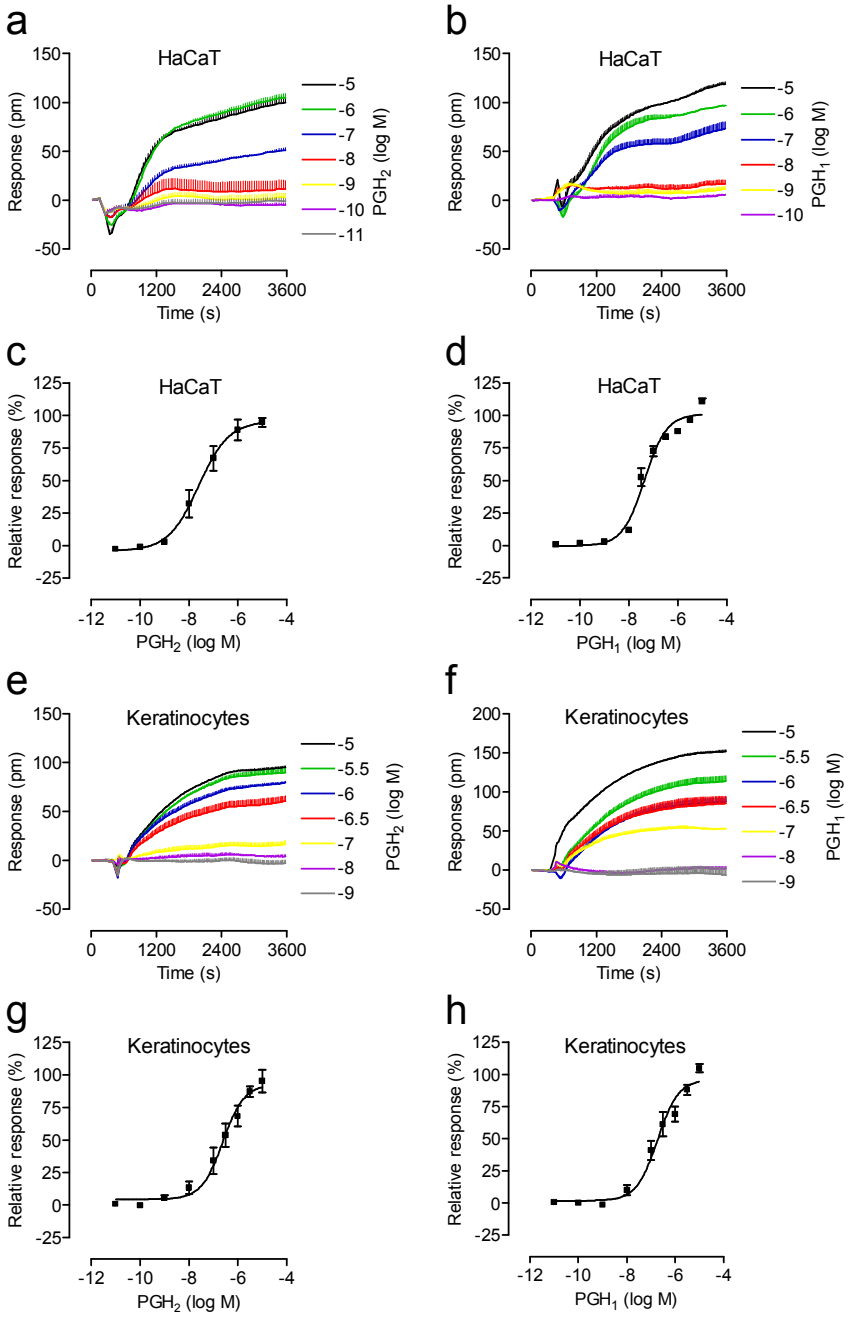

Figure 34: PGH derivatives induce DMR responses in HaCaT and primary keratinocytes.
DMR measurements in the presence of the indicated compounds were performed in immortalized (HaCaT) (**a-d**) and primary keratinocytes (**e-h**). (**a,b,e,f**) Shown are representative data (mean and SEM) of three independent experiments, each performed in triplicates. (**c,d,g,h**) Concentration effect curves were generated by the area under the curve (AUC). Depicted are mean ± SEM of three experiments, each performed in triplicates. Calculated molar pEC_{50} values are for HaCaT: PGH_2: 7.60 ± 0.23, PGH_1: 7.36 ± 0.05 and for primary keratinocytes: PGH_2: 6.61 ± 0.13, PGH_1: 6.73 ± 0.10.

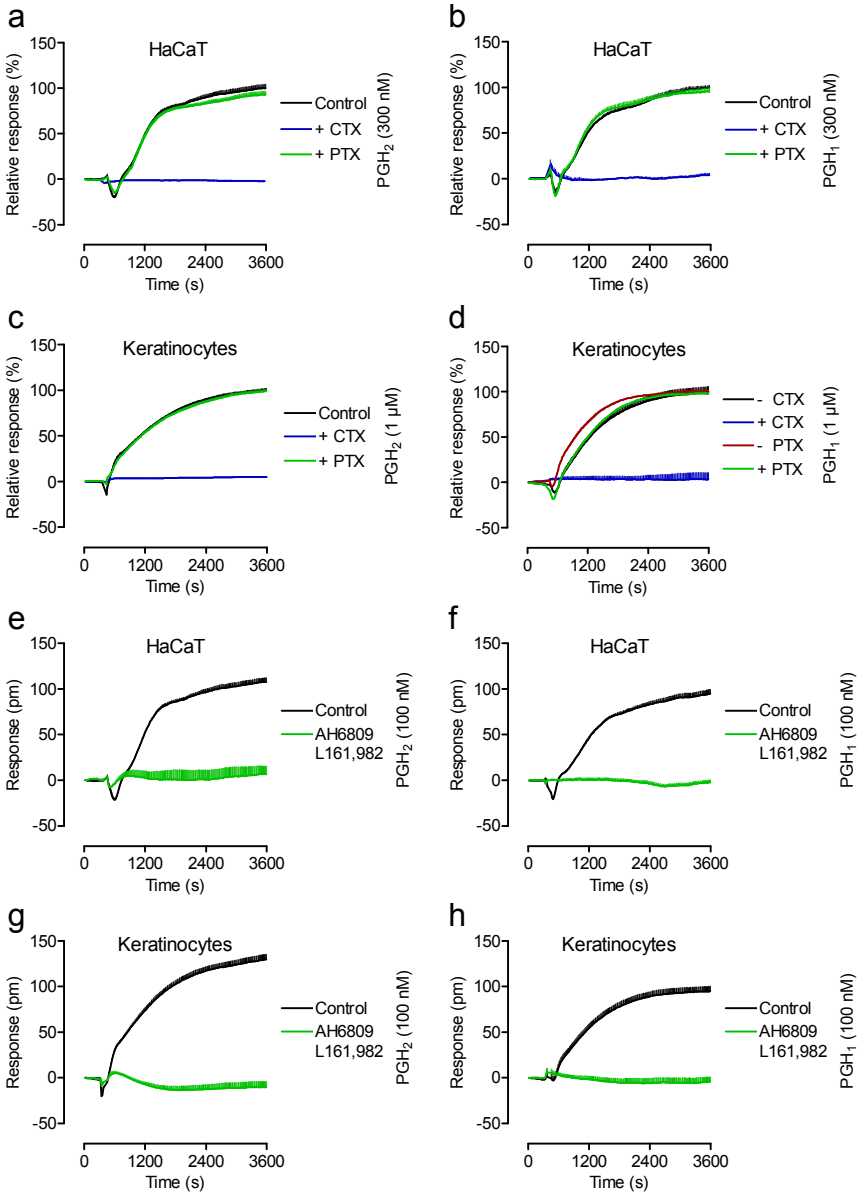

Figure 35: PGH derivatives activate the Gα_s-coupled EP2 and EP4 receptors in HaCaT and primary keratinocytes.
(**a-d**) DMR responses resulting from PGH_1 and PGH_2 application in immortalized (HaCaT) and primary keratinocytes were sensitive to pretreatment with cholera toxin (CTX) (250 ng/ml), but pertussis toxin (PTX) (50ng/ml) insensitive. (**e-h**) Signaling of both PGH derivatives was fully abrogated by pretreatment with a combination of AH6809 (10 µM) and L161,982 (10 µM). Shown are representative data (mean and SEM) of at least three independent experiments, each performed in triplicates.

3. Discussion

3.1 DMR technology captures signaling along all four major G protein pathways

The presented results demonstrate for the first time that a label-free detection system is competent to record activation of GPCRs associated with all four major G protein coupling classes (Schröder, et al., 2010). This is at present beyond reach for most other technology platforms. Detection of specific signaling events was established regarding the examles of CRTH2, EP2 and EP4, FFA1 and GPR55 for $G\alpha_i$, $G\alpha_s$, $G\alpha_q$/$G\alpha_i$ and $G\alpha_{12/13}$ coupling events, respectively. Origins of the captured DMR traces were defined using pharmacological tools including pathway inhibitors as PTX and YM, activators as CTX, forskolin and ALF, as well as receptor antagonists. Additionally, the detection of $G\alpha_{12/13}$ signaling was substantiated utilizing a dominant negative form of the $G\alpha_{13}$ protein ($G\alpha_{13}$dn). In this way heterotrimeric G proteins were defined as post receptor trigger for the complex DMR signatures. Moreover it was demonstrated that DMR technology simultaneously detects mixed signaling events, which could be deconvoluted into individual response components.

Generally DMR measurements appear highly suitable for detection of GPCR signaling events (Lee, et al., 2008, Dodgson, et al., 2009, Peters, et al., 2009, Rocheville and Jerman, 2009). However, previous validation had been done in a more empirical way to enable high-throughput drug screening approaches or pharmacological ligand profiling, but no in-depth analytical study had been published, that truly defined DMR recordings and compared them with second messenger assays, which are state of the art in current receptor research.

3.1.1 Detection of $G\alpha_{12/13}$ signaling

One of the most remarkable results was the demonstration that $G\alpha_{12/13}$ signaling is captured by DMR recordings. The current study for the first time provides evidence that $G\alpha_{12/13}$ signaling can be detected by label-free DMR technology using GPR55 as a model. GPR55 is the only receptor reported to date with exclusive bias towards the $G\alpha_{12/13}$ pathway (Ryberg, et al., 2007, Henstridge, et al., 2009, Ross, R. A., 2009). However, for this pathway no second messengers are known and therefore no direct assays are available (chapter 1.3). The possibility to detect GPR55-dependent signaling via DMR measurements was shown

previously (Henstridge, et al., 2010), suggesting that $G\alpha_{12/13}$ signaling might indeed be captured. Importantly, however, this study has not proven $G\alpha_{12/13}$ involvement and hence a G protein-independent signaling event might have led to the observed optical response. The absence of inhibitory effects of PTX and YM treatment or masking by the use of CTX indicated that signaling occurs independent of $G\alpha_i$, $G\alpha_s$ or $G\alpha_q$ proteins (chapter 2.1.4, **Fig. 11**). This was assured by the lack of IP1 formation and unresponsiveness in stimulatory and inhibitory cAMP assays (chapter 2.1.4, **Fig. 12**). The full abrogation of signaling by pretreatment with the pan-G protein activator AlF points to the fact that G protein-dependent signaling was detected nevertheless. Evidence for $G\alpha_{12/13}$ signaling was provided by cotransfection of GPR55-AD-HEK cells with a dominant negative $G\alpha_{13}$ protein, which significantly diminished receptor response, whereas receptor surface expression was not affected. Generally, dominant negative G proteins do not fully erase a receptor response since their effectiveness may depend on the individual expression levels of the competing G proteins as well on their binding affinity towards the receptor, which do not have to be so prevalent that no wild type G protein may bind at all (Barren and Artemyev, 2007). In addition, transfection efficiency is rarely equal to hundred percent, and hence uptake of dominant negative inhibitors by all cells in culture is unlikely.

Detection of signaling along the $G\alpha_{12/13}$ pathway may be of great relevance in drug discovery and GPCR research including deorphanisation strategies. Receptors considered to be non-signaling might exclusively signal through $G\alpha_{12/13}$. Furthermore unexpected mixed signaling might be discovered more easily.

3.1.2 $G\alpha_i$ signaling

Label-free DMR measurement was shown to be highly suitable for detection of $G\alpha_i$ signaling events. DK-PGD_2-induced DMR signatures in CRTH2-HEK cells could be defined as $G\alpha_i$-dependent because pretreatment with PTX was able to abrogate them, while the traces were unaffected by YM or CTX (chapter 2.1.1, **Fig. 3 and Fig. 4**). The concentration effect curve of DK-PGD_2 and the corresponding molar pEC_{50} value generated by DMR were in good agreement with the data derived from cAMP second messenger assays. However, the assay window in cAMP assays was very small. Because of its inhibitory character and the fact that cAMP generation has to be induced by pre-stimulation with forskolin, detection of $G\alpha_i$ signaling by second messenger assays is always more challenging compared for instance with $G\alpha_s$ signaling. In addition, CRTH2 is known for its weak signaling compared to other $G\alpha_i$-coupled receptors (Schröder, et al., 2009) and the fact that DK-PGD_2 is described as a

partial agonist (Hirai, et al., 2001, Kostenis and Ulven, 2006) may foster the weak responses in cAMP assays.

Comparison of PGD_2, the main and full CRTH2 agonist, with the specific but partial agonist DK-PGD_2 shows that both compounds not only display similar potencies but also induce comparable efficacies in DMR measurement. This is in contrast to data derived from cAMP accumulation assays, where PGD_2 induces an obviously higher efficacy (chapter 2.1.5.1, **Fig. 14**). The similarity of both agonist efficacies in DMR assays may be caused by the holistic read out, where also far downstream signaling events contribute to the captured overall response. It is suggested that at the level of the DMR readout signaling efficacies will be equalized due to enhancement during the signaling cascade amplification. In this context the high receptor expression level in the CRTH2-HEK over-expressing system may also contribute to the effect that downstream responses of compounds, known as full or partial agonists, may converge resulting in similar efficacies. For the experimental setup used herein, DMR technology appears to be limited in differentiating these pharmacological agonist properties. However, different pharmacological antagonist properties were accurately captured by this method, as demonstrated for TM30642 and TM30089, referred to as surmountable and insurmountable antagonists of CRTH2, respectively (chapter 2.1.5.2, **Fig. 15**) (Mathiesen, et al., 2006). High sensitivity of DMR assays towards $G\alpha_i$ signaling was also observed for the FFA1 receptor. Hence, $G\alpha_i$-coupling events represented a considerable portion of the mixed $G\alpha_q/G\alpha_i$ DMR response, whereas for cAMP assays, this was hardly detectable (response was less than 6% of forskolin induced cAMP inhibition (chapter 2.1.3, **Fig. 9**). Finally, gene dosing experiments revealed not only that DMR-derived efficacies correlate with receptor expression levels, but also that DMR technology enables the detection of $G\alpha_i$ signaling under decreased expression conditions (chapter 2.1.6, **Fig. 16**).

These data point to the fact that DMR technology provides high sensitivity towards $G\alpha_i$ signaling and thus access to concealed signaling events which may be barely detectable by conventional methods, whereas their obvious impact upon DMR alludes cellular relevance.

3.1.3 $G\alpha_s$ signaling

PGE_1-induced DMR responses by native HEK cells were defined as $G\alpha_s$-dependent due to their sensitivity towards CTX and forskolin, but not to PTX and YM. The fact that CTX totally erases PGE_1-dependent signaling but did not affect the CRTH2 mediated $G\alpha_i$ traces reveals also the suitability of CTX for pathway discrimination in this assay system. Nevertheless, since CTX acts by pre-activation and not by inhibition, results generated by the

usage of CTX, and pathway pre-activation in general, should be considered carefully, since activation of any pathway may have horizontal effects on other components of signaling cascades. For example, this was observed for the $G\alpha_q$-coupled muscarinic M3 receptor, that extended its signaling repertoire in the presence of enhanced cAMP levels to the $G\alpha_i$ pathway (Schröder, et al., 2010).

By the use of a combination of the respective antagonists EP2 and EP4 receptors could be defined as cellular targets of PGE_1. In contrast to recently reported BRET-based studies with transiently transfected HEK293E cells, where for EP4 also interaction with $G\alpha_i$ proteins was detected (Leduc, et al., 2009), in DMR assays and for the used conditions herein, no indication for $G\alpha_i$ signaling events were observed. Interestingly, one of the EP2/EP4 antagonists alone was hardly effective to decrease PGE_1-induced responses. This might be caused by the holistic DMR readout including far downstream signaling events. At this level the individual receptor efficacies seem to converge close to a maximum response, which can not be exceeded, indicating a high sensitivity also towards $G\alpha_s$ signaling events. This is in accordance with results from Jiang and colleagues (2010), where high sensitivty of DMR measurements towards PGE_2-activated EP2 receptors was observed in stable EP2 transfectants of rat C6 glioma cells (C6G-EP2) and human colon tumor cells (HCT-EP2).

3.1.4 $G\alpha_q$ and mixed signaling events

The ability of DMR technology to detect $G\alpha_q$ specific signaling was verified by the example of FFA1-mediated signaling (chapter 2.1.3). It was demonstrated, that FFA1-derived DMR traces were sensitive towards YM, although not totally blocked. Parallel second messenger assays revealed IP1 formation, which was fully erased by YM. Notably, the DMR response remaining after YM treatment was PTX sensitive, and $G\alpha_i$ signaling was verified in parallel cAMP assays. Thus, an additional pathway could be determined for FFA1, which was previously solely described as $G\alpha_{q/11}$ coupled (Briscoe, et al., 2003, Itoh, et al., 2003, Stoddart, et al., 2007).

These results demonstrate the capability of DMR technology to simultaneously detect signaling of more than one G protein coupling event, reflecting the experimental power of an all-encompassing response in combination with appropriate pharmacological tools.

This was also shown for the mixed $G\alpha_i/G\alpha_s$ response obtained from CRTH2-HEK cells when challenged with PGH_2 and PGH_1 (chapter 2.2.3, **Fig. 22** and chapter 2.2.4, **Fig. 25**), where different receptors mediated the individual signals. However, DMR technology provides the possibility of simultaneous detection of cellular responses which are contrary at the second messenger level. Thus, detection by cAMP accumulation assays could be expected to fail:

because of the adversary nature of signaling, simultaneous stimulation and inhibition of cAMP is expected to neutralize each other, which is also obvious from bell-shaped dose response profiles of mixed $G\alpha_i/G\alpha_s$-sensitive receptor as observed for the muscarinic M2 receptor stably in expressed in CHO cells, when challenged with acethylcholine (Schröder et al., 2010, supplementary material).

Given the increasing number of receptors and associated ligands found to exhibit ligand-dependent biased signaling and the growing perception and importance of pluridimensional efficacy in the field of GPCR research (Galandrin and Bouvier, 2006, Galandrin, et al., 2007, Kenakin, T., 2010), the capability of DMR technology to simultaneously detect different signaling events seems particularly valuable to seize and unravel these features.

3.1.5 DMR detection in primary human keratinocytes

Label-free DMR recording of native signaling has already been reported before (Rocheville and Jerman, 2009). However, in these studies immortalized cell lines were analyzed. Here, for the first time, label-free DMR measurement of GPCR-mediated signaling in primary human cells was demonstrated (Schröder, et al., 2010).

Activation and inhibition of PGE_1-dependent signaling was detected in immortalized keratinozytes (HaCaT) and in primary human keratinocytes, cell lines known to be endowed with PGE_1-responsive receptors (Zhang, et al., 1994, Murota, et al., 2008). The strategy of pathway determination by the use of toxins could successfully be adopted and unveiled the captured traces to be $G\alpha_s$-dependent. Further analysis using receptor antagonists determined both EP2 and EP4 as molecular targets of PGE_1 (chapter 2.1.7). High sensitivity of DMR measurements towards GPCR signaling events was once more demonstrated with regard to the quality of the assay window by comparison of DMR responses from primary keratinocytes with second messenger assays (chapter 2.1.7, **Fig. 19**). The possibility to investigate GPCR signaling in living cells in a label-free manner seems to be particularly advantageous for primary cells, which are difficult to analyze with biochemical methods as well as difficult to transfect with labeled components of the GPCR signaling cascade for optical studies (Fang, 2007, Fang and Ferrie, 2007, Rocheville and Jerman, 2009).

DMR technology opens the opportunity to analyze drug candidates in primary human cells, i.e. the cell type in which therapeutics are intended to mediate their effect. The presented results provide compelling evidence that DMR is a technology platform ideally suited to examine GPCR signaling in the receptor's native environment and therefore promises to perform studies about the mechanism of action in physiologically relevant cells.

3.1.6 General aspects of functional GPCR detection by DMR technology

DMR traces derived from GPCR-mediated signaling events often exhibit a characteristic shape which can be quite different between individual signaling routes, as observed particularly evident for the recordings of $G\alpha_s$ vs. $G\alpha_i$-dependent events in HEK293 cells (chapter 2.1.2 **Fig. 3** vs. chapter 2.1.3, **Fig. 5**). Thus, it may be tempting to deduce signaling specificity of receptors simply by visual inspection of the captured response profile and comparison with historical data.

Such predictions may be correct in some instances, particularly if the cellular background is known, but generally the shape of DMR traces does not allow direct extrapolation of the signaling origin. This is illustrated in **figure 37**, considering the response traces of $G\alpha_{12/13}$-mediated signaling (**Fig. 37a** and chapter 2.1.4) and the mixed $G\alpha_q/G\alpha_i$ signature derived from FFA1 activation (**Fig. 37c** and chapter 2.1.3), which display strong analogies at least for some concentrations. Additionally, mixed $G\alpha_s$ and $G\alpha_i$ signatures as observed for CRTH2-HEK cells challenged with the H-prostaglandins may provide similar shapes (**Fig. 37e** and chapter 2.2.3). Only in the presence of pharmacological tools can such signaling origins be uncovered, as depicted in **figure 37b,d,f**.

In this context, it is important to mention that DMR response profiles might be cell type-dependent. In Chinese hamster ovary (CHO) cells, $G\alpha_s$ signaling was observed as downward-(negative) directed response, whereas $G\alpha_i$ traces derived from CHO cells are reflected by positive responses (Antony, et al., 2009, Kebig, et al., 2009, Schröder, et al., 2010). It is therefore even conceivable that simultaneous stimulation of pathways with opposing nature of DMR responses may lead to “Zero-signatures” that neutralize each other and therefore mask one or both signaling events. Nevertheless, the use of pathway blockers would uncover of such hidden pathway activations (Antony, et al., 2009, Kebig, et al., 2009). This may exemplify that pathway deconvolution by means of appropriate pharmacological tools or other methods is highly recommended and indispensable for mechanistic investigations.

The strategy to deconvolute cumulative responses by pathway affecting substances as presented herein, demonstrates that G protein-dependent signaling was found to be mainly responsible for the DMR traces triggered by the receptors and ligands of this study. In fact, no serious indices were found for sensing G protein-independent signaling events as might have been anticipated for CRTH2, a receptor known to recruit β-arrestin2 in a G protein-independent manner (Mathiesen, et al., 2005).

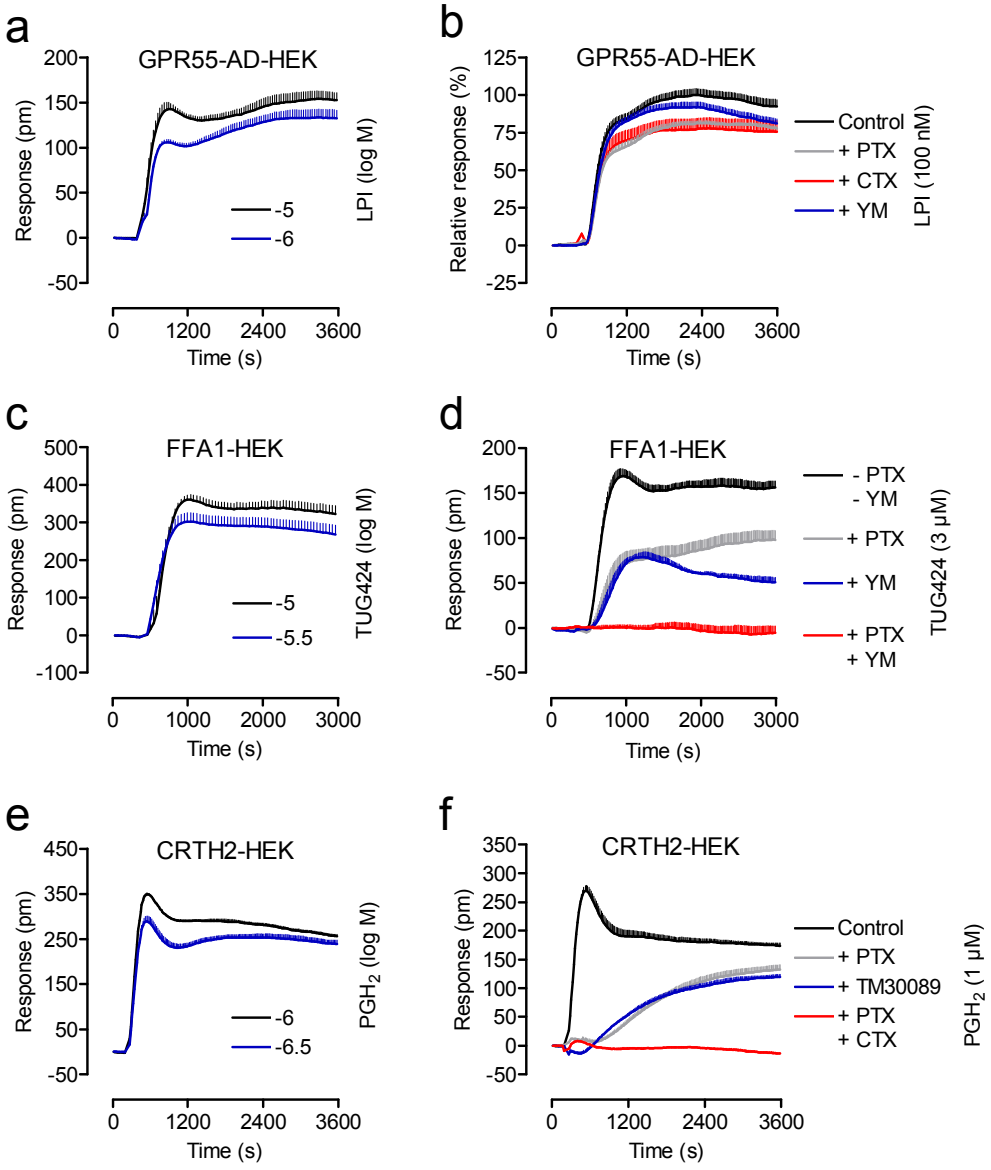

Figure 37: Similar response shapes derived from different signaling origins. Although DMR traces visually resemble each other, the use of pharmcological tools indicates different signaling events. DMR responses obtained from AD-HEK293 cells stably expressing GPR55 (GPR55-AD-HEK) (**a,b**), HEK293 cells stably expressing the FFA1 receptor (FFA1-HEK) (**c,d**) and HEK293 cells stably expressing CRTH2 (CRTH2-HEK) (**c,d**) challenged with the indicated agonists. Cells were pretreated with 100 ng/ml of cholera toxin (CTX) (**b**), 5 ng/ml of pertussis toxin (PTX) (**b,d**), 300 nM YM254890 (YM) (**b,d**) or with a buffer control. CRTH2-HEK were pretreated with 10 µM TM30089, 50 ng/ml of PTX or 250 ng/ml CTX (**f**). Shown are representative data (mean + SEM) of at least three independent experiments, each performed in triplicates.

DMR-derived traces may contain an unimaginable wealth of intracellular players (chapter 1.2) and study is focused on the responsibility of G proteins as upstream triggers, but of course it cannot solve the multifarious downstream consequences. Due to the used toxins and other pathway affecting substances herein, especially the different Gα proteins or their heteromeric complexes were found responsible for DMR responses. Thus it would be exciting

to uncover whether Gβγ subunit-mediated events do also contribute to the detected overall responses, which might be accomplished by specific Gβγ inhibitors such as M119 or related small molecules (Bonacci, et al., 2006). In addition, details of DMR signatures could be elucidated by the use of inhibitors or siRNA regarding the signaling of downstream effectors including phospolipases, protein kinases and exchange factors. In this context it may be of interest to note that cytochalasin D, a potent inhibitor of actin polymerization, was reported to obviously diminish signal strength of GPCR dependent-DMR traces (Peters, et al., 2009). This suggests that changes in cytoskeleton assembly, as a far downstream event, contribute to the complex DMR responses.

Second messenger data presented herein were found to be in accordance with DMR responses and detected potencies in both assays were in good agreement whereas the sensitivity of DMR was equal or even superior to the traditional biochemical assays. DMR technology and second messenger assays base on completely different readouts. DMR captures an overall cellular response as single functional optical output that includes far downstream cellular events, which may also be enhanced by signaling cascade amplification. This is in contrast to the classical determination of second messenger generation, which represents a less downstream event and only a part of the overall response. Thus agonist potencies determined in both assays may, but do not necessarily have to converge.

Summarized, DMR technology provides a pathway-unbiased yet pathway-sensitive approach towards receptor activation of all four main GPCR coupling classes and provides a continuous and highly sensitive kinetic measurement of signaling activity in a manner, which is unachievable by traditional second messenger assays. Due to its holistic readout of cell function, DMR detection promises access to the plasticity of receptor-mediated signaling behavior, even in primary cells, and can be suggested to advance clinical predictability of drug candidates at early research stages. Also expectable are improving effects towards systems biology and systems pharmacology promoting therapeutics with novel mechanisms.

3.2 Prostanoid screening at CRTH2

The most remarkable result from the prostanoid screening approach was the identification of the biosynthetic precursor of the 2- and 1-series of prostanoids PGH_2 and PGH_1, respectively, as functional agonists of CRTH2, whereas AA and DHGLA did not display any effect. In addition, PGH_2 and PGH_1 were shown to also induce CRTH2-independent $G\alpha_s$-linked signaling, which was identified to be mediated by endogenous EP2 and EP4 receptors.

The DMR screen of the prostanoid derivatives demonstrates that all used 2-series of prostanoids, known to activate CRTH2, induced concentration-dependent DMR responses and pathway determination studies revealed that the tested derivatives did not elicit qualitatively different G protein activation profiles. Differential activation of G protein-independent signaling appears to be undetectable by DMR measurements since treatment with PTX virtually abolished the response, although CRTH2 is known to signal also G protein-independently via β-arrestin2 (Mathiesen, et al., 2005). To address this issue, further investigations using BRET approaches appear necessary, to enable the detection of ligand-induced interaction of CRTH2 and β-arrestin2.

Some slight differences in ligand induced DMR responses may occur in the later phase of the recorded responses. After reaching the maximum response at about 1000 s, for some derivatives as Δ^{12}-PGD_2 and 11d-TXB_2, the signal decline appeared to be distinctively different (chapter 2.2.1 **Fig. 20** and **Fig. 21**). This may be a hint towards different post-activation behavior of receptors, as for instance ligand-induced internalization or persistent receptor activation after internalization as recently described for the S1P agonist fingolimod (Müllershausen, et al., 2009). To unravel such phenomena, internalization assays based on microscopic techniques would be required.

DMR studies with the 1-series of prostanoids demonstrate for the first time, that PGD_1 but not PGA_1, PGE_1 or $PGF_1\alpha$ are functional agonists of CRTH2. PGD_1 also induced PTX-sensitive DMR responses, but since this derivative had not yet been found *in vivo*, physiological relevance of this result is unclear. The results concerning the 1-series prostanoids are nevertheless of interest, since CRTH2 is described to be activated by 2-series PGs containing D-, J-, and F-rings, but not A- or E-rings (Sawyer, et al., 2002). Interestingly, only PGD_1, but not PGA_1, PGE_1 and in particular not $PGF_1\alpha$ were found to activate CRTH2. Since $PGF_2\alpha$ and $PGF_1\alpha$ share identical rings, these data suggest that CRTH2 activation is not exclusively determined by the ring systems, but also by the side chain (chapter 2.2.3, **Tab. 1**).

3.3 PGH_2 and PGH_1 induce activation of EP2 and EP4 receptors

DMR measurements indicate that both PGH_2 and PGH_1 prostaglandins were not only active at CRTH2 but additional "background" responses could be identified as PGH_2 and PGH_1-dependent $G\alpha_s$ signaling of EP2 and EP4 receptors endogenously expressed in HEK293 cells (chapter 2.2 and 2.4). The activation of both receptors was also detected in immortalized and primary human keratinocytes, when challenged with PGH_2 and PGH_1. Compared to PGE_1 in

all investigated cell lines no differences in signaling quality was detectable. It would be of interest to explore whether EP1 and EP3 receptors are also targets for PGH_2 and PGH_1, and if so whether PGH-induced signaling events are comparable to those elicited by PGE_1 or PGE_2. As discussed below (chapter 3.4), EP receptor activation by H-prostaglandins may also be relevant in the context of CRTH2-dependent activation of eosinophils.

With regard to primary keratinocytes multiple effects of E prostanoids and their receptors are reported including involvement of EP2 receptors in growth regulation (Konger, et al., 2002), protection of UV-induced skin carcinogenesis in EP2 knockout mice (Brouxhon, et al., 2006) as well as inflammatory skin diseases (Murota, et al., 2008).

There is strong evidence that PGE_2 facilitates cancer diseases by tumor initiation, progression, and metastasis through multiple biological effects, including increased proliferation and angiogenesis, decreased apoptosis, and modified immunosuppression. These effects are mediated via multiple signaling pathway including EP receptors (Radmark and Samuelsson, 2010). PGE_2 generation is mediated by enzymatic conversion of PGH_2 by three types of PGE synthases (PGES), the microsomal PGES1 (mPGES1), the microsomal PGES2 (mPGES2) and the cytosolic PGES (cPGES). Accordingly, a currently investigated strategy to combat cancer but also diseases associated with inflammation and pain is pursued by the development of (subtype specific) PGES inhibitors (Hara, et al., 2010, Radmark and Samuelsson, 2010). In this context it might be of interest that EP receptor activation may also be achieved independent of PGES by the H-prostaglandins.

3.4 PGH_2 and PGH_1 induce activation of CRTH2

It was shown that both PGH_2 and PGH_1 were active at CRTH2 stably expressed in HEK293 cells. This was first found in DMR assays, but also calcium release could be detected, and for PGH_1 induction of CRTH2 internalization was shown (chapter 2.2 and 2.3).

Activation of CRTH2 by PGH_2 was not only demonstrated in the presented study. Schuligoi, et al. (2009) reported that PGH_2 is competent to induce CRTH2-mediated migration of primary human eosinophils, and in HEK293 cells stably expressing CRTH2 or DP1, activation of both receptors could be detected by calcium response via cotransfected promiscuous G proteins.

Eosinophils are described as important effectors in allergic diseases. Upon their activation by chemoattractants like PGD_2 and eotaxin, shape change takes place, and they migrate towards the side of inflammation. Subsequently they release chemoattractants by themselves that in

turn causes further influx of inflammatory cells into the tissue (Hata and Breyer, 2004, Luster and Tager, 2004, Kostenis and Ulven, 2006, Sturm, et al., 2008).

The current study provides evidence that PGH_2 and PGH_1-induced activation of CRTH2 is detectable in the receptor's native environment, since both compounds were capable to stimulate chemotactic activation of human eosinophils (shape change) as well as migration and calcium release of human Th2 cells, effects which were sensitive to inhibition by a CRTH2 specific antagonist. Compared to PGD_2 both H-prostaglandins acted as full agonists in DMR assays using CRTH2-HEK cells, but in eosinophils and Th2 cells they behave as partial agonists. Nonetheless, these data suggest that eosinophils and Th2 cells, both involved in the promotion of inflammation, can be activated in the absence of endogenous PGD_2 generation.

Interestingly, H-prostaglandins were not only found to be active at CRTH2 but also stimulation of EP2 and EP4 receptors was detected. Recently, activation of EP2 receptors by PGE_2 and Butaprost, a synthetic EP2 agonist, was reported to partially inhibit eosinophil trafficking to sites of inflammation in response to known chemoattractants such as eotaxin, C5a and PGD_2 (Sturm, et al., 2008). Since PGD_2 is known to activate eosinophil shape change and trafficking via CRTH2, and PGH_2 was found to activate both CRTH2 and EP2 receptors, these data may explain the partial agonism of the H-prostaglandins at eosinophils observed herein. H-prostaglandins might induce eosinophil shape change and trafficking via CRTH2 but simultanously reduce this effect via EP2 receptor activation, and thus may also protect against exaggerated effects. Since inflammatory reactions are regulated by a host of opposing factors apart from those considered herein, contrary stimuli are not generally unexpected. For example, CRTH2 and DP1, both expressed in eosinophils, basophils and Th2 cells and both activated by PGD_2, are also hypothesized to counteract each other in inflammatory diseases (Kostenis and Ulven, 2006, Pettipher, 2008). The data presented herein provide compelling evidence that H-prostaglandins are efficacious activators of CRTH2 and EP2/4. However, the above considerations also indicate the difficulty to predict which effects may be exerted by H-prostaglandins *in vivo*. Clearly, it would be of interest to investigate the PGH_2 and PGH_1-induced reactions in eosinophils with regard to involvement of EP receptors, for instance by the use of selective EP antagonists.

Regarding the potential bioactivity of the PGH derivatives *in vivo* two major points have to be considered: (i) physiological availability of untransformed H-prostaglandins and (ii) their chemical stability.

(i) In most cells that express cyclooxygenases, PGH_2 and PGH_1 are rapidly converted to downstream prostanoids by also expressed prostanoid synthases (chapter 1.6 **Fig. 1**). Thus, at first glance, only little PGH_2 or PGH_1 is expected to be released untransformed. However, in several studies release of larger amounts of genuine H-prostaglandins has been described for certain cells and tissues such as endothelial cells, platelets, mesangial cells and lung tissue (Hamberg, et al., 1974a, Svensson, et al., 1975, Soler, et al., 2001, Folco and Murphy, 2006). In these cells, upon mechanical or chemical stimuli such as acetylcholine and endothelin-1, overproduction of H-prostaglandins was detected outranging the catalytical capacity of the downstream synthases, resulting in release of the untransformed precursor (Kato, et al., 1990, Asano, et al., 1994, Camacho, et al., 1998, Saito, et al., 2003).

(ii) Due to spontaneous isomerization to PGE derivatives the half-life of PGH metabolites in phosphate buffered aqueous media has been described to be 5-10 min (Hamberg, et al., 1974a, Hamberg and Fredholm, 1976, Samuelsson, et al., 1978). More rapid conversion of PGH_2 to PGD_2 takes place in the presence of serum albumin (Hamberg and Fredholm, 1976) and by the lipocalin-type prostaglandin D synthase (L-PGDS) and hematopoietic PGDS (H-PGDS) (Kanaoka, et al., 1997, Urade and Hayaishi, 2000, Kanaoka and Urade, 2003). Nevertheless, resulting effects from release of genuine H-prostaglandins were described as induction of platelet aggregation and vasoconstriction mediated by the thromboxane receptor (TP) for which PGH_2 is a potent agonist (Corey, et al., 1975, Saito, et al., 2003).

With regard to the presented data, particularly in calcium assays for both HEK-CRTH2 and primary Th2-cells, responses upon receptor activation appeared within seconds and also DMR responses occurred immediately after compound application. Taken together, this indicates a potential physiological relevance for CRTH2 activation by both metabolites.

CRTH2 is not only stimulated by PGD_2 but also by several of its conversion products including DK-PGD_2, 15d-PGD_2, Δ^{12}-PGD_2, 11β-$PGF_2\alpha$, PGJ_2, 15d-PGJ_2 and Δ^{12}-J_2 as depicted in **figure 37**. All these PGD_2-derived ligands are initially formed by conversion of PGH_2 by L-PGDS and H-PGDS. Accordingly, inhibition of PGDS is being considered as an therapeutic strategy to treat inflammatory disorders (Inoue, et al., 2004, Aritake, et al., 2006, Hohwy, et al., 2008, Irikura, et al., 2009). However, more recently additional PGH_2-derived prostanoids were identified, which were active at CRTH2, whereas their formation occurs independently of PGDS. These are $PGF_2\alpha$ (Sandig, et al., 2006), the thromboxane A_2 metabolite 11d-TXB_2 (Böhm, et al., 2004), PGH_2 (Schuligoi, et al., 2009) and PGH_1 as presented herein (**Fig. 37**).

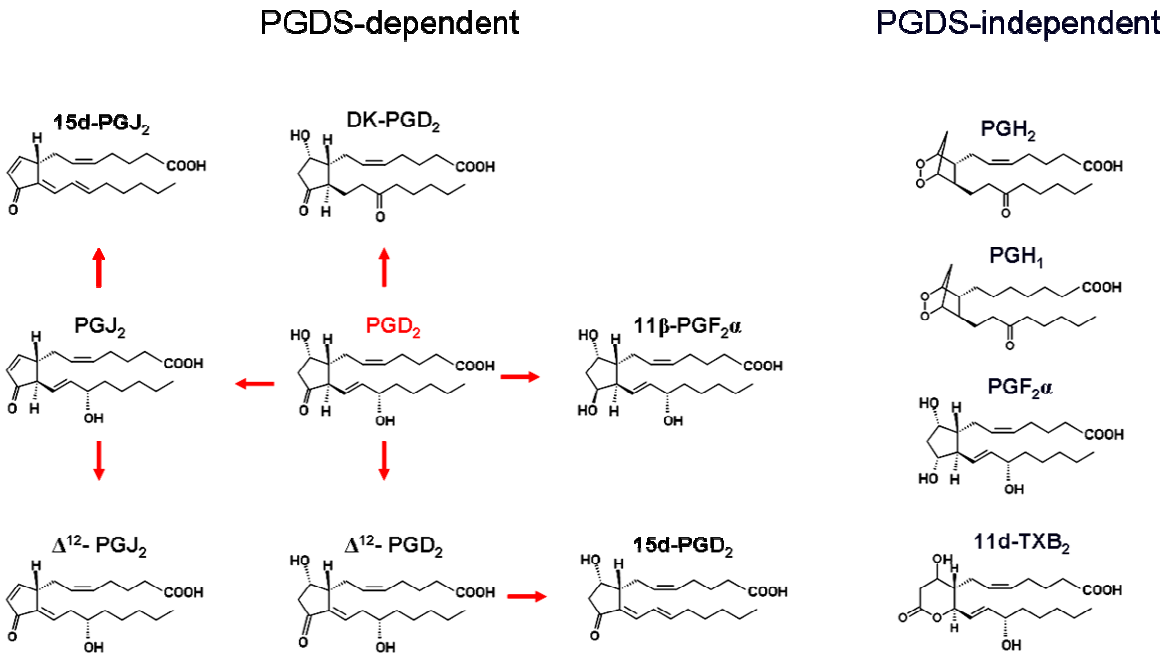

Figure 37: PGDS-dependent and -independent CRTH2 agonists
(Left and middle structures) Prostaglandin D_2 (PGD_2), the product of prostaglandin D synthase-(PGDS) dependent conversion of PGH_2 is enzymatically metabolized or spontaneously converted to many other products, some of which are active at CRTH2. (Right structures) CRTH2 activating prostanoids generated independently of PGDS.

The identification of PGH_2 and also PGH_1 as active ligands at CRTH2 has strong implications for strategies to combat inflammation and allergic responses, because there are two additional lipid mediators which are competent to activate CRTH2 independent of PGDS. These results raise the option that effective suppression of inflammation might be better supported by pharmacological inhibition of CRTH2 rather than abrogation of PGDS activity.

CRTH2 activation by PGH_1 is remarkable, because it is viewed as precursor for PGs with predominantly anti-inflammatory properties. Although the 2-series of PGs is the most well characterized and biologically abundant (arachidonic acid is the preferred substrate for COX-1 and COX-2 enzymes), anti-inflammatory effects of 1-series PGs, in particular PGA_1 and PGE_1 have been repeatedly demonstrated *in vivo* and *in vitro* in diverse cell types and animal models. PGA_1, for example, has been shown to limit inflammatory responses in activated monocytes/macrophages via induction of anti-inflammatory cytokine IL-10 expression (Kim, et al., 2008) and to suppress NFkappaB activation which in turn is essential for COX-2 gene expression (Mandal, et al., 2005). PGE_1, appears to possess anti-inflammatory properties which favorably affect a variety of inflammatory conditions, as adjuvant arthritis and inflammatory skin diseases (Zurier and Quagliata, 1971, Murota, et al., 2008) among others.

In this context it is noteworthy that PGH_1, the precursor for these two anti-inflammatory PGs, is an activator of the pro-inflammatory receptor CRTH2. The results presented herein not only have identified PGH_1 as novel CRTH2 ligand; they also, at least in part, provide a proof of principle that PGH_1 may be competent to promote allergic inflammation via stimulation of CRTH2. This appears noteworthy when fatty acid composition of cell membrane phospholipids and hence potential eicosanoid formation are intended to be altered applying diets enriched in ω-3 fatty acids and γ-linolenic acid resulting in increased levels of DHGLA to in turn enhance the production of apparently anti-inflammatory eicosanoids (Chilton, et al., 2008). Notably, increased DHGLA levels were also correlated with negative effects as reported by Kompauer, et al. (2008) where the DGHLA content in serum phospholipids has been found to negatively influence lung function parameters in asthmatic subjects, and also a positive association between DHGLA plasma levels and the occurrence of asthma was found in young adults (Woods et al., 2004). The precise mechanisms for these observations have not been elucidated, but since CRTH2 is known for its pathological function in inflammatory airway diseases, it is tempting to speculate that CRTH2 activation by PGH_1 may also contribute to these clinical phenotypes. To further estimate the *in vivo* relevance of the findings presented herein and since PGH_1 production and release is much less examined as compared with PGH_2, a first step could be to explore whether enhanced PGH_1 generation and release from endothelial cells upon DHGLA application are detectable

Taken together, PGH_1 and PGH_2 were found as efficacious activator of the pro-inflammatory CRTH2. Given that both prostanoids are released untransformed in substantial amounts, for instance from endothelial cells or lung tissues, it is suggested that H-prostaglandins via CRTH2 stimulation could be involved in recruitment of immune cells to sites of allergic reactions, resulting in enhancement of allergic asthma and other inflammatory diseases. This may occur independent of PGDS-mediated PGD_2 generation.

4. Summary

The presented study deals with the validation of the recently developed label-free dynamic mass redistribution (DMR) assay technology (Corning® Epic® system) as a cell based G protein-coupled receptor (GPCR) functional assay as well as the subsequent utilization of DMR assays for an eicosanoid ligand screen at the pro-inflammatory D-prostanoid receptor DP2 also referred to as chemo attractant receptor homologous molecule expressed on T-helper type2 (Th2) cells (CRTH2).

DMR technology represents an assay platform that allows non-invasive and real-time recording of integrated cellular responses in living cells upon GPCR activation. The cumulative response of the whole cell is captured by detection of refractive index alterations by an optical biosensor, resulting in distinct "signatures" which in turn reflect receptor activity. Since previous applications of DMR technology were based on a more empirical validation to provide feasibility for drug screening approaches, the first objective of this thesis was to investigate the applicability of DMR technology for GPCR basic research. This was realized using CRTH2 (DP2), the E-prostanoid receptors (EP) EP2/EP4, the free fatty acid receptor 1 (FFA1) and GPR55 as representatives for $G\alpha_{i/0}$, $G\alpha_s$, $G\alpha_{q/11}$/($G\alpha_{i/0}$) and $G\alpha_{12/13}$-linked signaling events, respectively. The cellular mechanisms underlying the integrated cellular DMR responses could be precisely assigned by the use of pharmacological tools including pathway inhibitors as pertussis toxin (PTX) and YM254890 (YM) and activators as cholera toxin (CTX) and aluminum fluoride (AlF_4^-). Detection of receptor activation in parallel second messenger assays was in good agreement with DMR-derived results, whereas sensitivity of DMR was at least equal or even superior. Not accessible by conventional second messenger assays, the detection of $G\alpha_{12/13}$ mediated signaling by DMR technology was of particular interest and substantiated utilizing a dominant negative form of the $G\alpha_{13}$ protein ($G\alpha_{13}$dn, Q226L,D294N). Herein, for the first time, evidence was provided that $G\alpha_{12/13}$ signaling can be detected by label-free DMR technology. These results demonstrate that the holistic nature of DMR reflects GPCR functionality along all four major G protein signaling pathways and defines heterotrimeric G proteins as post-receptor trigger for the complex DMR responses.

The holistic DMR readout enabled simultaneous detection of mixed signaling events, which could be dissected into individual response components. One example is the identification of additional $G\alpha_i$ signaling for the FFA1 receptor, previously solely described as $G\alpha_{q/11}$-coupled.

Sensitivity of DMR technology was further examined at endogenously expressed receptors in primary human cells. The strategy to define signaling events with pharmacological tools could successfully be adopted and PGE_1-induced responses in both immortalized and primary human keratinocytes were defined as $G\alpha_s$-linked signaling via EP2 and EP4 receptors.

This demonstrates that DMR technology represents a universal, pathway-unbiased yet pathway-sensitive approach towards investigations of G protein-mediated effects and that the cumulative readout provides access to complex GPCR signaling behavior. It is suggested that DMR is an enabling technology for both GPCR basic research and drug discovery.

CRTH2, involved in inflammation and allergic diseases, is activated by several endogenous eicosanoid ligands. Thus, it was of interest to determine whether these ligands may differ regarding their induced signaling behavior and if additional, still unknown ligands, might exist. The successful definition of DMR-reflected G protein-mediated signaling events allowed the utilization of DMR technology for a ligand screening approach at CRTH2 stably expressed in HEK293 cells. The screening was designed with 2-series prostanoids known to activate CRTH2, as well as with the main representatives of the 1-series of PGs, including the corresponding biosynthetic precursors.

The most remarkable result obtained from the screening approach was the identification of PGH_2 and PGH_1, the precursor of the 2- and 1-series of prostanoids, respectively, as functional agonists of CRTH2. For all tested compounds with bioactivity at CRTH2, no differences in signal quality were detectable with regard to G protein-mediated events. Additionally, PGH_2 and PGH_1 were shown to activate endogenous EP2 and EP4 receptors in HEK293 cells as well as in primary human keratinocytes.

The PGH_2 and PGH_1-induced stimulation of CRTH2 was verified in calcium release assays and was also detectable in the receptor's native environment. In cooperation with the Oxagen Ltd, UK, it was shown, that both compounds stimulate chemotactic activation of primary human eosinophils as well as migration and calcium release in primary human Th2 cells, effects which were sensitive to inhibition by a CRTH2 specific antagonist. Identification of PGH_1 and PGH_2 as activators of the pro-inflammatory CRTH2 is at least a proof of principle for potential physiological relevance. Thus, it is conceivable that H-prostaglandins could be involved in recruitment of immune cells to sites of allergic reactions, resulting in enhancement of allergic asthma and other inflammatory diseases, via stimulation of CRTH2. This might occur independent of endogenous PGD_2 generation and during potential blockage of PGDS.

PGH_1 is the cyclo oxygenase (COX) product from dihomo-γ-linolenic acid (DHGLA) and the precursor for the 1-series prostanoids which are often viewed as "anti-inflammatory". This is reflected in recommendations for diets enriched with ω-3 fatty acids and γ-linolenic acid, resulting in increased levels of DHGLA and subsequent "anti-inflammatory" metabolites, among other effects. Thus, it is remarkable that PGH_1 was found active at the pro-inflammatory CRTH2. Since increased DGHLA levels were also reported to be in correlation with inflammatory asthma it is tempting to speculate that PGH_1 may contribute to the clinical phenotype.

5. Material and methods

5.1 Material

5.1.1 General chemicals, reagents and ready-mixed solutions

Agar	Fluka, Hamburg, DE, #05040
Agarose, ultra pure	Invitrogen®, Darmstadt, DE, #15510-27
Aluminium chloride	ZVE, Bonn, DE, #125098
Ampicillin sodium salt	Roth, Karlsruhe, DE, #K029.1
Blasticidin	InvivoGen, Toulouse, FR, #ant-bl-1
Bromphenol blue	Fluka, Hamburg, DE, #32712
Bovine serum albumin (BSA), fatty acid free	Sigma, Taufkirchen, DE, #A6003
Calcium chloride, dihydrate	Sigma, Taufkirchen, DE, #C3306
Dimethyl sulfoxide (DMSO)	Riedel-de Haen, Seelze, DE, #60153
Distilled water, ultra pure	Invitrogen®, Darmstadt, DE, #10977
Dry milk, blotting grade	BioRad®, CA, US, #170-6404
Dulbecco´s modified Eagle medium (DMEM)	Invitrogen®, Darmstadt, DE, #41965
Doxycycline hyclate	Sigma, Taufkirchen, DE, #D9891
Ethylenediaminetetraacetic acid disodium salt, dihydrate (EDTA)	Roth, Karlsruhe, DE, #8040.3
Ethanol	KMF Optichem, Lohmar, DE, #08-205
Fetal calf/bovine serum (FCS)	Sigma, Taufkirchen, DE, #-0804
Genenticin (G418)	Gibco, Paisley, UK, #11811
D-(+)-Glucose	Sigma, Taufkirchen, Hamburg, DE, #G7021
Glycerol	Sigma, Taufkirchen, DE, #G2025
3-Isobutyl-1-methylxanthine (IBMX)	Sigma, Taufkirchen, DE, #15879
Isopropanol	Merck, Darmstadt, DE, #107022
Hanks balanced salt solution (HBSS)	Invitrogen®, Darmstadt, DE, #14025
Hydrochloric acid	Applichem, Darmstadt, DE, #A1437
4-(2-Hydroxyethyl)-1-piperazineethane-sulfonic acid (HEPES)	Applichem, Darmstadt, DE, #A3268
Hygromycin B	InvivoGen, Toulouse, FR, #ant-bl-1
Keratinocyte growth medium II	Promocell, Heidelberg, DE, #C-20011
Lithium chloride solution	Sigma, Hamburg, DE, #L7026
Magnesium chloride, hexahydrate	Fluka, Hamburg, DE, #63068
Magnesium sulphate, heptahydrate	Applichem, Darmstadt, DE, #A1037

Methanol	VWR, Langenfeld, DE, #20847.307
3-(N-Morpholino)propanesulfonic acid (MOPS)	Sigma, Taufkirchen, DE, #M-1254
Paraformaldehyde	Fluka, Hamburg, DE, #76240
Penicillin/streptomycin solution	Invitrogen®, Darmstadt, DE, #15140
Poly-D-lysin	Sigma, Taufkirchen, DE, #P-6407
Potassium acetate	Merck, Darmstadt, DE, #1.04820
Potassium chloride	Fluka, Hamburg, DE, #60128
Potassium carbonate	Fluka, Hamburg, DE, #60110
Potassium dihydrogen phosphate	ZVE, D-53121 Bonn, #1.04873
Dipotassium hydrogen phosphate	Merck, Darmstadt, DE, #105104
Potassium hydroxide	Merck, Darmstadt, DE, #1.05033
RPMI-1640 Medium	Invitrogen®, Darmstadt, DE, #21875
Rubidium chloride	Merck, Darmstadt, DE, #107615
Sodium acetate	Applichem, Darmstadt, DE, #4555
Sodium chloride	Fluka, Hamburg, DE, #71376
Sodium fluoride	ZVE, Bonn, DE, #125310
Sodium dihydrogen phosphate	Roth, Karlsruhe, DE, #T878.2
Disodium hydrogen phosphate	Roth, Karlsruhe, DE, #T876.2
Sodium hydrogen carbonate	Merck, Darmstadt, DE, #1.06323.2500
Sodium hydroxide	Merck, Darmstadt, DE, #1.06482.1000
Sulfuric acid	Merck, Darmstadt, DE, #1007311000
3, 3', 5, 5'-Tetramethylbenzidine (TMB) Liquid substrate system	Sigma, Taufkirchen, DE, # T8665
Tris(hydroxymethyl)-aminomethane (TRIS)	Roth, D-76231 Karlsruhe, #5426
Tryptone	Roth, D-76231 Karlsruhe, #8952.1
Yeast extract	Roth, Karlsruhe, DE, #2363
Zeocin	Invitrogen®, Darmstadt, DE, #R25001

5.1.2 Compounds and reagents for functional assays

AH6809	Cayman, MI, US, #14050
Arachidonic acid (AA)	Cayman, MI, US, #90010.1
AH6809	Cayman, MI, US, #14050
Cholera toxin (CTX)	Sigma, Taufkirchen, DE, #C8052
Carbachol (Cch)	Merck, Darmstadt, DE, #212385
Dihomo-γ-linoleic acid (DHGLA)	Cayman, MI, US, #90230

Forskolin (Fsk)	Tocris, Bristol, UK, #1099
L161,982	Cayman, MI, US, #10011565
Laropiprant	Chemie Tek, IN, US, #CT-LR001
Lysophosphatidyl inositol (LPI)	Sigma, Taufkirchen, DE, #L7835
Pertussis toxin (PTX)	Sigma, Taufkirchen, DE, #2980
Prostaglandin A_1 (PGA_1)	Cayman, MI, US, #10010
Prostaglandin D_1 (PGD_1)	Cayman, MI, US, #12000
Prostaglandin D_2 (PGD_2)	Cayman, MI, US, #12010
Δ^{12}-Prostaglandin D_2 (Δ^{12}-PGD_2)	Cayman, MI, US, #12650
15-Deoxy-$\Delta^{12,14}$-prostaglandin D_2 (15d-PGD_2)	Cayman, MI, US, #12700
13,14-Dihydro-15-keto-prostaglandin D_2 (DK-PGD_2)	Cayman, MI, US, #12610
Prostaglandin E_1 (PGE_1)	Cayman, MI, US, #13010
Prostaglandin $F_2\alpha$ ($PGF_2\alpha$)	Cayman, MI, US, #16020
11β-Prostaglandin $F_2\alpha$ (11β-$PGF_2\alpha$)	Cayman, MI, US, #16520
6-keto-Prostaglandin $F_1\alpha$ (6k-$PGF_1\alpha$)	Cayman, MI, US, #15210
11β-Prostaglandin $F_2\alpha$ (11β-$PGF_2\alpha$)	Cayman, MI, US, #16520
Prostaglandin H_1 (PGH_1)	Cayman, MI, US, #17015
Prostaglandin H_2 (PGH_2)	Cayman, MI, US, #17020
Prostaglandin J_2 (PGJ_2)	Cayman, MI, US, #18500
Δ^{12}-Prostaglandin J_2 (Δ^{12}-PGJ_2)	Cayman, MI, US, #18550
15-Deoxy-$\Delta^{12,14}$-Prostaglandin J_2 (15d-PGJ_2)	Cayman, MI, US, #18570
11-Dehydro-Thromboxane B_2 (11d-TXB_2)	Cayman, MI, US, #19500
TM30089	Kindly provided by Dr. Trond Ulven, University of Southern Denmark, DK
TM30642	Kindly provided by Dr. Trond Ulven, University of Southern Denmark, DK
TUG424	Kindly provided by Dr. Trond Ulven, University of Southern Denmark, DK
YM254890	Kindly provided by Prof. Dr. Graeme Milligan, University of Glasgow, UK

5.1.3 Devices

Autoclave	Varioclav 500 E, H+P Labortechnik, Oberschleissheim, DE
Balance	TE64, Sartorius, Göttingen, DE
Balance (analytical)	TE6101, Sartorius, Göttingen, DE
Centrifuge	5810, Eppendorf, Hamburg, DE
Centrifuge	6K10, Sigma, Osterode, DE
Centrifuge	MiniSpin, Eppendorf, Hamburg, DE
Counting chamber	Neubauer, Brand, Wertheim, DE
DMR assay system	Epic®, Corning®, NY, US
DNA-Gel documentation system	Devision D-Box, Decon Science Tec, Vilbert Lourmant, Cedex, FR
Dry block heater	QBT2, Grant Instruments, Cambridge, UK
Electrophoresis chambers	Mini-Subcell® GT, BioRad®, CA, US
	Wide Mini-Subcell® GT, BioRad®, CA, US
ELISA reader	Sunrise, Tecan, Männedorf, CH
Freezer, - 80°C	Herafreeze, Heraeus, Hanau, DE
Freezer, liquid-N2	MVE-Tec 3000, GermanCryo, Jüchen, DE
Electroporation device	Gene Pulser Xcell, BioRad®, CA, US
Incubator/shaker (bacteria)	HT-INFORS, Buch+Holm, CH
Microscope (cell culture)	CKX31, Olympus, Hamburg, DE
Microwave	Microwave 800, Severin, Sundern, DE
Multimode reader	Mithras LB940, Berthold Technologies, Bad Wildbad, DE
Ca^{++} flux reader	NovoStar®, BMG LabTech, Offenburg, DE
Pipettes	Eppendorf, Hamburg, DE
Pipettes, multi-channel	Alpha, Genex, Torquay, UK
Power Supply	Power Pac HC, BioRad®, CA, US
pH-meter	SevenEasy, Mettler Toledo, Giessen, DE
Sterile bench	HeraSafe, Thermo Fisher, Schwerte, DE
Spectro-photometer	Smart Spec Plus, BioRad®, CA, US
Vortexer	Reaxtop, Heidolph, Schwabach, DE
Water purification system	Milli Q® Water system, Millipore, MA, US

5.1.4 Software

Office Excel® 2003	Microsoft Corporation, Unterschleißheim, DE
Office PowerPoint® 2003	Microsoft Corporation, Unterschleißheim, DE
Office Word® 2003	Microsoft Corporation, Unterschleißheim, DE
Prism® 4.02	GraphPad Software Inc, CA, US
DeVision® G v1.0	Decon Science Tec GmbH, Hohengandern, DE
Assay Development Mode Epic® V1.22.2	Corning® Incorporated, NY, US
Microplate Analyzer v1.5 modified for Excel 2002	Corning® Incorporated, NY, US
NOVOstar® 1.20-0	BMG Labtech, Offenburg, DE
EndNote® 9.0.0 (Bld 1425)	Thomson, PA, US
Mikrowin® 4,41 (at Mithras)	Mikrotek Laborsysteme Gmbh, Overath, DE
X Fluor4 V4.51 (at Tecan)	Tecan, Männedorf, CH
SymyxDraw 3.2 (chemical structures)	Symyx, San Diego, CA, US

5.1.5 Consumables

5.1.5.1 General material

Cell culture vessels:	
- Plates: 6, 24, 48 and 96 well	Corning®, NY, US, #3506, 3512, 3548, 3596
- Flasks: 25, 75 and 175 cm^2	Corning®, NY, US, #430168, 430720, 431079
- Dishes: 6, 10 and 150 cm^2	Corning®, NY, US, #430161, 430167, 430599
Gene Pulser cuvette, 0.4cm,	BioRad®, CA, US, #1652088
Petri dishes (for bacteria)	Greiner, Frickenhausen, DE, #632102
Eppendorf reaction tubes	Eppendorf, Hamburg, DE
Pipet tips	Sarstedt, Nümbrecht, DE
Tips + trays 384 (for Epic®)	CyBio, Jena, DE, #3800-25-513-N
Tubes 15 and 50 ml	Corning®, NY, US

5.1.5.2 Microplates for functional assays

DMR measurement, Epic®:	
384 well, Epic®, fibronectin-coated, biosensor cell assay microplate	Corning®, NY, US, #5042
384 well, Epic®, source plate	Corning®, NY, US, #3657
ELISA:	
96 well, flat bottom costar plate, clear	Corning®, NY, US, #9017
HTRF® cAMP and IP-One assay:	
384 well, LIA-plate, white, TC, F-form Greiner bio one 4550	Greiner, Frickenhausen, DE, #632102
Calcium mobilization assay:	
96 well, flat bottom, costar cell plate	Corning®, NY, US, #3599
96 well, v-bottom, costar plate	Corning®, NY, US, #3357
96 well, round bottom, costar plate	Corning®, NY, US, #3795

5.1.5.3 Kits

Calcium 4 assay kit FLIPR	Molecular Devices, CA, USA, #8142
cAMP Dynamic 2 HTRF® assay kit	Cisbio Bioassays, Gif-sur-Yvette, FR, #62AM4PEC
IP-One HTRF® assay kit	Cisbio Bioassays, Gif-sur-Yvette, FR, #62P1APEB
HitHunter™ cAMP-HS+ kit	DiscoveRx Corporation, Fremont, US, #90-0090S
QIAprep® Plasmid Mini kit	QIAGEN GmbH, Hilden, DE, #27106
QIAprep® Plasmid Maxi kit	QIAGEN GmbH, Hilden, DE, #12145

5.1.6 Restriction endonucleases

*Eco*RI	New England BioLabs®, MA, US, #R0101S
*Bam*HI	New England BioLabs®, MA, US, #R0136S
*Hind*III	New England BioLabs®, MA, US, #R0104S
*Kpn*I	New England BioLabs®, MA, US, #R0142S
*Xba*I	New England BioLabs®, MA, US, #R0145S
*Xho*I	New England BioLabs®, MA, US, #R0146S

5.1.7 Antibodies

Anti-CRTH2 (BM16) (monoclonal from rat)	Santa Cruz, Heidelberg, DE, #sc-21798
Anti-HA (monoclonal from mouse)	Roche, Grenzach-Wyhlen, DE, #11583816001
Anti-rat (from goat) (horseradish peroxidase coupled)	Santa Cruz, Heidelberg, DE, #sc-2006
Anti-mouse (from goat) (horseradish peroxidase coupled)	Sigma, Taufkirchen, DE, #A4416

5.1.8 Buffers and solutions

Phosphate buffered saline (PBS)

PBS consists of 150 mM NaCl, 2.5 mM KCl, 7.5 mM Na_2HPO_4 and 1.5 mM KH_2PO_4 solved in deionized water. The pH value was adjusted to 7.2 by addition of hydrochloric acid. Subsequently the solution was autoclaved.

EDTA solution (0.5 M)

93.5 g of Ethylenediaminetetraacetic acid (EDTA) disodium salt were solved in 400 ml deionized water and the pH was adjusted to 8.0 with NaOH. Then the solution was filled up to 500 ml.

Super optimal broth (SOB)

SOB medium consists of 2% Bactotryptone, 0.5% (w/v) yeast extract, 10 mM NaCl and 2.5 mM KCl solved in deionized water. The pH was adjusted to 7.4 and the medium was sterilized by autoclaving. Afterwards the following solutions were added: 10 ml of 10 mM $MgCl_2$ and 10 ml of 10 mM $MgSO_4$, each autoclaved separately.

Competent bacteria buffer 1 (CB buffer 1)

CB buffer 1 consists of 30 mM $C_2H_3O_2K$, 50 mM $MnCl_2$, 100 mM $CaCl_2$ and 15 % (v/v) glycerol solved in deionized water. The pH was adjusted to 5.8 and finally the solution was filter-sterilized (0.2 µm).

Competent bacteria buffer 2 (CB buffer 2)

CB buffer 2 consists of 10 mM RbCl, 75 mM $CaCl_2$, 10 mM MOPS and 15 % (w/v) glycerol solved in deionized water. The pH was adjusted to 6.8, and finally the solution was filter-sterilized (0.2 µm).

Luria Bertani (LB) medium

10 g of Bactotryptone (1% w/v), 5 g of yeast extract (0.5% w/v) and 5 g of NaCl (0.5% w/v) were solved in 900 ml of deionized water. The pH was adjusted to 7.5 with NaOH, and finally the solution was filled up to 1,000 ml. The medium was autoclaved and stored at 4°C. If necessary, antibiotics were added before usage.

Luria Bertani (LB) 1.5% agar

For 20 LB agar plates (10 cm dishes) 400 ml medium were prepared: 4 g of Bactotryptone (1% w/v), 2 g of yeast extract (0.5% w/v) and 2 g of NaCl (0.5% w/v) were solved in 350 ml deionized water and pH value was adjusted to 7.5 with NaOH. 6 g Agar (1.5% w/v) were added and the volume was filled up to 400 ml. The medium was autoclaved and cooled down to approximately 60°C. If necessary, antibiotics were added and the solution was casted into the plates at approximately 20 ml/plate and cooled down to room temperature. Finally plates were stored bottom up at 4°C.

Tris acetate EDTA (TAE) buffer for agarose gel electrophoresis (50x)

242 g of Tris(hydroxymethyl)-aminomethane (Tris) base was solved in 700 ml of deionized water. 57.1 ml of glacial acetic acid and 100 ml of a 0.5 M EDTA solution were added and the volume was filled up to 1000 ml with deionized water. Final concentrations (50x) were 2 M TRIS and 1 mM EDTA.

DNA loading dye (6x)

DNA loading dye consists of bromphenol blue (0,25% w/v) solved in equivalent amounts of glycerol and deionized water.

Tris EDTA (TE) buffer

TE buffer consists of 10 mM Tris and 1 mM EDTA solved in deionized water. The pH value was adjusted to 8.0 with HCl. Finally the solution was filter-sterilized (0.2 µm) or autoclaved.

Tris HCl solution (0.5 M, 10x)

61 g of Tris were solved in deionized water, the pH was adjusted to 7.5 with HCl and the solution was filled up to a final volume of 1000 ml.

Solutions for calcium phosphate transfection

$CaCl_2$ aqueous solution (2 M)

14.7 g of $CaCl_2$ were solved in 50 ml of deionised water (2 M) and the solution was filter-sterilized (0.2 µm).

Hepes bufferd saline (HBS) (2x)

HBS consists of 50 mM HEPES, 280 mM NaCl and 1.5 mM Na_2HPO_4 solved in deionized water. The pH value was adjusted to 7.1, and the solution was filter-sterilized (0.2 µm).

Solutions for transfection by the electroporation method

Electroporation buffer (EB) (5x)

EB buffer contains 250 mM K_2HPO_4, 100 mM CH_3COOK and 100 M KOH solved in deionized water. The pH was adjusted to 7.4 with acetic acid, and the solution was filter-sterilized (0.2 µm).

$MgSO_4$ solution (1 M)

12.3 g of $MgSO_4$ heptahydrate were solved in 50 ml of deionized water and the solution was filter-sterilized (0.2 µm).

Solutions for ELISA

Blocking buffer (3% dry milk)

Tris base was solved at a concentration of 50 mM in deionized water. The pH was adjusted to 7.4 with HCl and 3% dry milk (w/v) was added.

Paraformaldehyde (PFA) fixative solution (4%)

8 g of paraformaldehyde were stirred in 100ml of deionized water at 60°C and NaOH (1 M) was added drop wise until PFA was solved. Phosphate buffer (0.2 M, pH 7.4) was added to a total volume of 200 ml.

HEPES solution (1 M)

119.1 g of HEPES were solved in deionized water, and the pH was adjusted to 7.2 and the solution was filter-sterilized (0.2 µm).

DMR assay buffer (Epic® assay)

Hank's balanced salt solution (HBSS) was supplemented with 10 ml of a HEPES solution (1 M) to a final concentration of 20 mM HEPES in HBSS (pH 7.2).

Krebs HEPES buffer (KHP) for Ca^{2+} assay

The KHB buffer consists of an aqueous solution of 118.6 mM NaCl, 4.7 mM KCl, 1.3 mM $MgSO_4$, 1.2 mM $CaCl_2$, 1.2 mM KH_2PO_4, 4.2 mM $NaHCO_3$, 11.7 mM D-glucose and 10 mM HEPES. The pH was adjusted to 7.4 by addition of NaOH. The buffer was prepared in a 5-fold concentration without $CaCl_2$ and $MgSO_4$ and stored at -20°C. For usage the buffer was diluted, and $CaCl_2$ and $MgSO_4$ were added.

Aluminium fluorid solution (AlF_4^-)

A 1.2 mM AlF_4^- solution was generated by mixing equal amounts of 2.4 mM $AlCl_3$ and 80 mM NaF, each solved in DMR assay buffer (20 mM HEPES in HBSS).

5.2 Molecular biology

5.2.1 Vectors

pcDNA3.1+

Purchased from Invitrogen®, Darmstadt, DE, #V790-20

CRTH2 cDNA in pcDNA3.1+

cDNA of CRTH2 (Gen-bank accession-number NM_004778) had been inserted into pcDNA3.1+ by *Hind*III and *Eco*RI restriction sides. The plasmid originated from an internal source: research group of Prof. Dr. Evi Kostenis, Institute of Pharmaceutical Biology, University of Bonn, Germany.

$G\alpha_{13}$dn cDNA in pcDNA3.1+

cDNA of the dominant negative mutant of $G\alpha_{13}$ ($G\alpha_{13}$dn, Q226L/D294N) had been inserted into pcDNA3.1+ by *Kpn*I and *Xba*I. The plasmid was purchased from UMR cDNA Resource Center, MO, US, #GNA13000X0

Gαq$_i$5 cDNA in pcDNA3.1+

cDNA of the promiscous G protein that funnels GPCR response from Gα$_i$ to Gα$_q$, (Conklin, et al., 1993, Kostenis, et al., 2005a) had been inserted in pcDNA3.1+ by *Bam*HI and *Xba*I restriction sides. The plasmid originated from an internal source: research group of Prof. Dr. Evi Kostenis, Institute of Pharmaceutical Biology, University of Bonn, Germany.

5.2.2 Bacterial strains

XL1blue (Stratagene, CA, US), *Escherichia coli*, genotype: *recA1 endA1 gyrA96 thi-1 hsdR17 supE44 relA1 lac* [F´ *proAB lacI*qZΔ*M15* Tn*10* (Tetr)]

DH5α (Invitrogen®, Karlsruhe, DE), *E. coli*, genotype: F- φ80*lac*ZΔM15 Δ(*lac*ZYA-*arg*F)U169 *rec*A1 *end*A1 *hsd*R17(r_k^-, m_k^+) *pho*A *sup*E44 *thi*-1 *gyr*A96 *rel*A1 λ^-

5.2.3 Cultivation techniques for bacterial cells

Cultivation of bacteria

5 ml of LB-medium were inoculated by a single bacterial colony or a cryo-culture and cultivated (if required with antibiotics) over night (200 rpm, 37°C).

Freezing of bacteria

Bacteria were grown as described before and settled by centrifugation (3000 g, 5 min). The supernatant was removed and the cells were resuspended in LB-medium containing 15% glycerol. Subsequently the bacterial suspension was stored at -80°C.

Thawing of bacteria

Bacteria were thawn by picking with a sterile pipette tip into the frozen glycerol stock and applying the used pipette tip into an already prepared liquid LB-medium (if required with antibiotics). The culture was then incubated over night (200 rpm, 37°C).

5.2.4 Generation of competent bacteria

E. coli XL-blue cells were plated onto a LB agar plate (without antibiotics) and incubated overnight at 37°C. The next day 5 ml of SOB medium were inoculated by a single colony and cultivated for 16 h (37°C, 200 rpm). 1 ml of this culture was used to inoculate 100 ml of SOB broth. Bacteria were cultivated at 37°C and 200 rpm until an optical density (OD 600 nm) of 0.5 was reached, followed by centrifugation in pre-cooled tubes for 10 min (3000 g, 4°C). The following working steps were performed using pre-cooled tips and tubes. The pellet was resuspended in 2 x 12.5 ml of ice-cold CB buffer 1 and centrifuged again for 10 min (3000 g, 4°C). After the pellet was resuspended in 8 ml of CB buffer 2, the suspension was portioned in aliquots of 100 µl/tube, frozen in liquid nitrogen and stored at -80°C until usage.

5.2.5 Tranformation

Competent cells (100 µl) were thawed on ice, and 20-50 ng of plasmid DNA were added. After being incubated for 20 min on ice, tubes containing cells and DNA were put in a water bath (42°C) for 90 s and subsequently cooled on ice. Cells were mixed with 900 µl LB-medium and incubated for 1 h at 37°C. An appropriate volume was plated onto LB-agar plates supplemented with ampicillin (100 µg/ml) and incubated at 37°C over night.

5.2.6 Plasmid DNA isolation (mini/maxi preparation)

For mini preparations, 1.5 ml of an overnight culture were centrifuged, and DNA was isolated using the QIAprep® Mini-Kit (QIAGen) according to the manufacturer's instructions.
For maxi preparations 200-300 ml of an overnight culture were centrifuged, and DNA was isolated using the QIAprep® Maxi-Kit (QIAGen) according to the manufacturer's instructions.

5.2.7 Photometric measurement of nucleic acid concentration

DNA concentrations in aqueous solution were determined by measurement of the photometric absorbtion at 260 nm and 280 nm (Smart Spec Plus, BioRad®), the absorbtion maxima for nucleic acids and proteins, respectively. An absorption value of 1 at 260 nm corresponds to a concentration of 50 µg/ml double strand DNA (dsDNA). The ratio of 260nm/280nm indicates the purity and should be ~ 1.8 (or higher).

5.2.8 Restriction analysis

Plasmid digest was performed for diagnostic purpose. Single and double digestions with restriction endonucleases were performed as recommended by the manufacturer (New England BioLabs®). Approximately 250 ng plasmid DNA were mixed with 0.5 µl of each restriction enzyme, 2 µl buffer (10 x), BSA (if required) and purified water (UltraPure, Invitrogen®) at a total volume of 20 µl, followed by 1 h incubation at 37°C.

5.2.9 Agarose gel electrophoreris

Gel electrophoresis was performed with 1 % agarose in TAE buffer (1-fold) and was used to resolve the DNA fragments of the diagnostic digest. For DNA staining, ethidium bromide (0.5 µg/ml) was added to gel. A 1 kb molecular weight marker and the DNA samples, mixed with 4 µl loading dye (6x) (5.1.8), were load onto the gel. The gel was run at 80 to 120 V in an electrophoresis chamber (Subcell® GT, BioRad®) for about 1 hour. Subsequently, the DNA was visualized using UV illumination and a digital imaging system (Devision D-Box, Decon Science Tec).

5.3 Cell culture

5.3.1 Cell lines

HEK293 (HEK)

The used HEK293 cell line was from an internal source: research group of Prof. Dr. Evi Kostenis, Institute of Pharmaceutical Biology, University of Bonn, Germany.

HEK293 cells stably expressing CRTH2 (CRTH2-HEK)

The HEK293 cell line stably expressing CRTH2 was from an internal source: research group of Prof. Dr. Evi Kostenis, Institute of Pharmaceutical Biology, University of Bonn, Germany. Cells were generated as described priviously (Schröder, et al., 2009). Cells include cDNA of CRTH2 (gene bank accession-number NM_004778) fused to a FLAG-tag at the N-terminus, inserted into the genome via pcDNA3.1+. Cells were selected by resistance towards geneticin (G418).

HEK293 cells stably expressing DP1 (DP1-HEK)

The HEK293 cell line stably expressing the D-prostanoid 1 receptor (DP1) (Schuligoi, et al., 2009) was kindly provided by Dr. Maria Waldhoer (University of Graz, Austria). Cells include the cDNA of DP1 (gene bank accession-number NM_000953), inserted into the genome via pcDNA3.1+Zeo (UMR cDNA center, #PTGDR00000). Cells were selected by resistance towards zeocin.

HEK293 -Flp-InTM T-RExTM cells stably expressing FFA1 (FFA1-HEK)

HEK293-Flp-InTM T-RExTM expressing FFA1 (FFA1-HEK) cells were from an internal source: research group of Prof. Dr. Evi Kostenis, Institute of Pharmaceutical Biology, University of Bonn, Germany. The cDNA of FFA1 (also referred to as FFAR1 or GPR40) corresponds to the gene bank accession-number NM_005303. Cells were selected by resistance towards blasticidin and hygromycin B. To induce receptor expression on demand, cells were treated with 1 µg/ml of doxycyline for 16 hours. For control purpose, cells were grown without doxycycline.

Adherent HEK293 cells (AD-HEK)

The AD-HEK293 cell line is a derivative of the commonly used HEK293 cell line, providing improved cell adherence and plaque formation properties (Stratagene, #240085). The AD-HEK cell line was kindly provided by Prof. Dr. Andy Irving (University of Dundee, UK).

AD-HEK cells stably expressing GPR55 (GPR55-AD-HEK)

AD-HEK cells stably expressing GPR55 (Henstridge, et al., 2009) were kindly provided by Prof. Dr. Andy Irving (University of Dundee, UK).

Immortalized human keratinocytes (human adult low calcium temperature = HaCaT)

The HaCaT cell line (Boukamp, et al., 1988) was kindly provided by Dr. Evelyn Gaffal (University of Bonn, Germany).

Human keratinocytes

Primary human keratinocytes were obtained from skin samples of healthy patients which underwent skin surgery. All patients had written an informed consent before excision. The study was approved by ethic committee of the University of Bonn (concession-no. 090/04). Cells were kindly provided by Dr. Jörg Wenzel (University of Bonn, Germany).

5.3.2 Culture media

Medium for HEK293 cells

HEK 293 cells were cultivated in Dulbecco's Modified Eagle's Medium (DMEM, Invitrogen®) supplemented with 10% (v/v) fetal calf serum (FCS), 100 U/ml penicillin and 100 µg/ml streptomycin.

Medium for CRTH2-HEK

CRTH2-HEK cells were cultivated in DMEM supplemented with 10% (v/v) FCS, 100 U/ml of penicillin, 100 µg/ml of streptomycin and 500 µg/ml of geneticin 418 (G418).

Medium for DP1-HEK

DP1-HEK cells were cultivated in DMEM supplemented with 10% (v/v) FCS, 100 U/ml of penicillin, 100 µg/ml of streptomycin and 200 µg/ml of zeocin.

Medium for FFA1-HEK

FFA1-HEK cells were cultivated in DMEM supplemented with 10% (v/v) FCS, 100 U/ml of penicillin, 100 µg/ml of streptomycin, 100 µg/ml of hygromycin B and 15 µg/ml of blasticidin.

Medium for GPR55-HEK

CRTH2-HEK cells were cultivated in DMEM supplemented with 10% (v/v) FCS, 100 U/ml of penicillin, 100 µg/ml of streptomycin and 500 µg/ml of G418.

Medium for HaCaT

HaCaT were cultivated in Roswell Park Memorial Institute 1640 medium (RPMI-1640, Invitrogen®) supplemented with 10 % (v/v) of FCS, 100 U/ml of penicillin and 100 µg/ml of streptomycin.

Medium for keratinocytes

Primary human keratinocytes were cultivated in keratinocyte growth medium 2 (KGM2, Pomocell) supplemented with 100 U/ml of penicillin and 100 µg/ml of streptomycin.

5.3.3 Cell culture techniques for mammalian cells

Cultivation of cells

All cell lines used in this study were adherent and cultivated at 37°C, 5% CO2 and a humidity of 95%, referred to as standard conditions. Size and shape of culture vessels were chosen according to the desired application (flasks: T25 cm2, T75 cm2 or T175 cm2; dishes: 6 cm, 10 cm, or 15 cm; multiplates: 6 well - 96 well; assay plates: 96 and 384 well). Medium was changed as required. Cells were sub-cultured when grown up to 80-90% confluence: the medium was removed and cells were washed once with PBS. Hereafter trypsin/EDTA solution was added and cells were incubated at 37°C until cells were detached. The reaction was stopped by addition of culture medium containing FCS. Subsequently cells were splitted in the required ratio and transferred into a new culture vessel.

Counting of cells

Cells were counted by using an improved counting chamber (Neubauer). 10 µl of cell suspension were applied between the counting surface and a cover slip. The numbers of cells counted at one main square was determined, and finally the cell number was calculated by the following term: cells per ml = (counted cells/main square) x 10,000.

Freezing of cells

Cells were harvested and counted as described before. After centrifugation (3 min, 120 g) medium was removed and cells were resuspended in freezing medium consisting of 90% culture medium without antibiotics and 10% DMSO or 90 % FCS and 10% DMSO. The cell suspension was transferred into cryo-tubes at about 3 million cells/tube. The cryo-tubes were put into a special freezing container placed at -80°C over night. On the next day the tubes were transferred into a liquid nitrogen tank (MVE-Tec 3000, GermanCryo) for long time storage.

Thawing of cells

A cryo-tube with cells was removed out of the liquid nitrogen tank and thawed at 37°C in a water bath. Cells were then transferred into a previously prepared tube with fresh medium and centrifuged (3 min, 120 g). The supernatant was aspirated and cells were resuspended in the required culture medium and cultivated under standard conditions.

5.3.4 Transfection by co-precipitation of calcium phosphate and DNA

24 h before transfection HEK293 cells were plated at a density of 4 million cells per dish (10 cm2) to reach 50-60 % confluence over night. At the next day, medium was aspirated, replaced by 10 ml of fresh medium and cells were incubated again for 2-4 h. 20 µg of plasmid DNA were mixed with 60 µl of CaCl2 (2 M) and TE-buffer to reach a total volume of 500 µl and incubated for 30 min at room temperature, leading to co-precipitation of calcium phosphate and DNA. (For some indicated approaches plasmid DNA was mixed in a ratio of 1:10 with pcDNA3.1+ (the empty vector), since this had improved the expression levels in some cases.) The suspension was added to the culture medium (10 ml), which was then incubated under standard conditions. 5 h later, medium was changed. On the next day, cells were transferred to the required culture vessels according to the desired application and cultivated again for 24 h. Generally cells were used for assays about 48 h after transfection.

5.3.5 Transfection by electroporation

Transfection of GPR55-HEK cells with cDNA coding for dominant-negative Gα13 (Gα13dn) was performed using an electroporation method described previously (Pantaloni, 1996, JBC). In brief: for transfection, cells were trypsinized, centrifuged (3 min, 120 g) and resuspended in an adequate volume of EP (1x) buffer. Cells were counted, and for each transfection 6 million cells were placed into a tube and centrifuged (3 min, 120 g). Subsequently the supernatant was aspirated and cells were resuspended in EP (1x) buffer at a total volume of 60 µM. 50 µl were transferred to a 1.5 ml tube containing the previously prepared transfection mix:

20 µl EB (5x)
4 µl MgSO4 (1M)
x µl vector: pcDNA3.1+ (4µg)
x µl cDNA in pcDNA3.1+ (1µg)
ad 100µl deionized H2O

After 15 min of incubation at room temperature the transfection mix was transferred into a 0.4 cm electroporation cuvette (BioRad®) and pulsed using the Gene Pulser Xcell (BioRad®).

Settings of Gene Pulser Xcell:

Program:	exponential decay
voltage:	250 (V)
capacity:	500 (µF)
resistence:	∞ (Ω)
cuvette:	4 (mm)

Cells were then plated into a 6 cm dish. On the next day, cells were harvested, plated in the requested culture vessels according to the desired application and cultivated for another 24 h.

5.4 Cell based assays

5.4.1 Dynamic mass redistribution (DMR) assay

For DMR measurements the label-free Epic® System (Corning®) was used. The functional principle is described in the introduction (1.4.1).

Cells were seeded onto fibronectin-coated 384-well Epic® biosensor microplates and cultured for 20-24 h under standard conditions to obtain confluent monolayers, using the following cell numbers (cells/well): HEK-293, CRTH2-HEK, DP1-HEK and FFA1-HEK: 15,000; HaCaT: 10,000; keratinocytes: 12,500.

Before the assay, the medium was removed using a manifold and cells were washed two times with assay buffer (HBSS, 20 ml HEPES, pH 7,2) containing the same percentage of DMSO as the compound dilutions, which were later added in the assay. This is important since some solvents can induce bulk refraction index differences. After washing, a total volume of 30 µl assay buffer was left in every well and the microplate was kept for 1 h in the Epic® incubator at a constant temperature of 28°C. Compound dilutions were prepared and applied to a 384 well compound plate, which was also loaded into the Epic® incubator for 1 h.

Hereafter, the assay was started and the sensor plate was scanned, recording a baseline optical signature. Subsequently compound solutions were transferred into the sensor plate by the on-board robotic liquid handling device and DMR was monitored for at least 3600 seconds.

The incubation time for pretreatment with pertussis toxin (PTX) or cholera toxin (CTX) was 18 hours, for YM254890 2.5 hours and for antagonists and forskolin 1 hour.

For GPR55-AD-HEK and AD-HEK cells a starvation protocol was used: 48 h before the assay cells were seeded at a density of 7,500 cells per well on to a 384-well Epic® microplate and cultivated at 37°C and CO_2-humidified atmosphere. 24 h later, cells were washed three times with assay buffer and were further cultivated in this buffer for again 20-24 h under standard conditions. The assay was then performed as described above, using assay buffer supplemented with 0.1% bovine serum albumin (BSA).

5.4.2 Enzyme-linked immunosorbent assay (ELISA)

Coating of tissue culture vessels with poly-D-lysine (PDL)

To obtain an increased adherence of the cells, the bottom of the tissue vessels was coated with poly-D-Lysine (PDL). This avoids the loss of cells due to repeated washing steps as implemented in the ELISA.

A PDL solution (0.1 mg/ml) was applied to the according tissue vessel. The volume should be suitable to cover the bottom e.g. 100 µl per well for 96 well plates. Plates were incubated for 30 min at 37°C. Then the solution was aspirated, followed by two washing steps with PBS.

Assay protocol

ELISA was performed to detect the surface expression levels of CRTH2 or GPR55. For each receptor a slightly different protocol was used for treatment and cultivation before the assay:

Determination of cell surface expression levels of GPR55 containing an N-terminal HA-tag was performed using stable GPR55-AD-HEK cells transiently cotransfected with either Gα13dn cDNA or pcDNA3.1+ as a control. 24 h after transfection, cells were seeded in PDL-coated 96-well tissue culture plates at a density of 50,000 cells per well and cultivated for 6 h under standard conditions. Cells were then washed three times in HBSS with 20 mM HEPES and serum starved for about 16 h.

Surface expression levels of CRTH2 were determined in HEK293 cells transiently transfected with either CRTH2 cDNA or pcDNA3.1+ as a control. Additionally the stable transfected CRTH2-HEK cell line was used and as a control native HEK293 were used. Transfected cells were seeded 24 hours after transfection into PDL-coated 96 well tissue plates at a density of 50,000 cells/well.

Approximately 48 h after transfection (transiently transfected cells) and 24 h after seeding in 96 well PDL-coated assay plates, cells were washed once with PBS. For fixation, a 4% PFA

solution (100 µl/well) was added and incubated for 30 min at room temperature. Cells were washed three times with PBS (200 µl/well). Then blocking solution (100 µl/well) was added and cells were incubated for 1 h at 37°C. Subsequently, cells were incubated with the primary antibody diluted in blocking buffer for 1 h at room temperature followed by three washes and an incubation with the secondary antibody in blocking buffer for 1 h at room temperature. After three washes, the secondary antibody was detected by adding 100 µl/well of the colorimetric horseradish peroxidase substrate 3,3′,5,5′-tetramethylbenzidine (TMB). After about 5 min, when adequate color change was reached, the reaction was terminated by adding of 0.5 M H_2SO_4 (50 µl/well). The supernatants were then transferred to a new 96-well plate with clear bottom, and colorimetric readings were obtained at 450 nm using an ELISA reader (Sunrise, Tecan).

Used antibody dilutions for detection of GPR55:

- primary antibody: 1:400 (mouse anti-HA antibody)
- secondary antibody: 1:1,000 (goat anti-mouse conjugated to horseradish peroxidase)

Used antibody dilutions for detection of CRTH2:

- primary antibody: 1:1,000 (rat anti-CRTH2 antibody)
- secondary antibody: 1:10,000 (goat anti-rat conjugated to horseradish peroxidase)

Antibodies are further specified at 5.1.7.

5.4.3 HitHunter™ cAMP accumulation assay (for endogenously expressed receptors)

Measurement of cAMP accumulation at cell lines with endogenously expressed receptors was performed using the HitHunter™ cAMP-HS+ assay kit (DiscoveRx Corporation) according to the manufacturer's instruction. This assay kit was used for native HEK293 cells, HaCaTs and primary keratinocytes.

Assay principle

The method is a competitive immunoassay combined with enzyme complementation technique: free cAMP from cell lysates competes for antibody binding to labeled enzyme donor-cAMP (ED-cAMP). Unbound ED-cAMP is free to complement enzyme acceptor (EA) to form an active β-galactosidase enzyme by enzyme fragment complementation. Active β-galactosidase hydrolyzes an added substrate producing a chemiluminescence signal. Detected signals are directly proportional to the amount of free cAMP.

The kit includes following buffers and reagents:

- lysis buffer:	cAMP HS+ Lysis Buffer (pH 6.9) containing 10 mM phosphate, 10 mM NaCl, 1 mM IBMX, lysing agent, and other proprietary components.
- enzyme acceptor (EA)	cAMP HS+ EA reagent
- enzyme donor (ED)	cAMP HS+ ED reagent
- antibody reagent (Ab)	cAMP HS+ Ab reagent
- CL-substrate	Galacton-*Star* + Emerald-II™ CL substrate

Assay protocol

20 h before the assay cells were seeded into a 384 well microplate at a density of 2,500 cells/well for HEK293 cells and 5,000 cells/well for HaCaTs and keratinocytes. Medium was replaced by assay buffer (HBSS, 20 mM HEPES, 1 mM 3-isobutyl-1-methylxanthine (IBMX)) and cells were incubated with agonist for 30 min. The reaction was stopped by addition of lysis buffer containing cAMP-HS+ antibody reagent. After 1 h of incubation the cAMP-HS+ ED reagent was added and the microplate was incubated again for further 1 h. Then, cAMP-HS+ EA reagent was added and chemiluminescence signals were detected after 3 h of incubation at room temperature using the Mithras LB 940 multimode reader (Berthold Technologies) at 1 sec/well. Data analysis was performed based on the relative light units of chemiluminescence signals.

5.4.4 Homogeneous Time-Resolved Fluorescence (HTRF®) assays for cAMP or IP-1 (for overexpressed receptors)

Assay principle and data calculation:

The principle of this method herein is described for cAMP detection, but IP-1 detection functions accordingly.

The HTRF® assay is a competitive immunoassay. Native free cAMP produced by cells and cAMP labeled with the dye d2 compete for binding to a labeled cAMP antibody (europium cryptate anti-cAMP conjugate). Light excitation (320 nm) at anti-cAMP conjugates leads to fluorescence caused emission of light (620 nm). When the cAMP-d2 molecule binds to the anti cAMP conjugate, fluorescence resonance energy transfer (FRET) between the europium cryptate and the dye d2 occurs, resulting in fluorescence caused emission of light (655 nm).

Emitted fluorescence is detected at both wavelengths in parallel and the fluorescence ratio (655 nm/620 nm) is calculated. The obtained ratio values were corrected by a negative control containing only europium cryptate but not d2 (and no test compounds) in accordance with the following formula:

$$\text{Delta F} = \frac{\text{Ratio}_{\text{sample}} - \text{Ratio}_{\text{neg}}}{\text{Ratio}_{\text{neg}}} * 100$$

Generation and accumulation of native cAMP leads to replacement of cAMP-d2. As a result less emission at 655 nm is detected in favor of the detected emission at 620 nm, leading to decreased Delta F values. For this reason the specific signal is inversely proportional to the generated cAMP (or respectively IP-1). To obtain proportional relationships, values were inverted by calculating the differences to the basal (buffer) value (for $G\alpha_s$) and the forskolin value (for inhibitory $G\alpha_i$ approaches).

HTRF®cAMP accumulation assay

Activation and inhibition of cAMP accumulation in CRTH2-HEK293 cells was performed using the HTRF®-cAMP dynamic kit (Cisbio) as per manufacturer's instruction and described previously (Schröder, et al., 2009). This assay kit was used for cell lines with overexpressed receptors as there are CRTH2-HEK, FFA1-HEK, and GPR55-AD-HEK cells.

The kit includes the following buffers and reagents:

- lysis buffer (50 mM phosphate buffer (pH 7.0), 1 M KF and 1.25% Triton X-100)
- europium cryptate-labeled anti-cAMP antibody (cAMP-conjugate)
- d2-labeled cAMP (cAMP-d2)

Assay protocol

Cells were washed (HBSS, 20 mM HEPES), resuspended in assay buffer (HBSS, 20 mM HEPES, 1 mM 3-isobutyl-1-methylxanthine (IBMX)) and dispensed in 384-well microplates at a density of 50,000 cells/5 µl per well and settled by centrifugation (1 min, 120 g). After preincubation in assay buffer for 30 min at 37°C, cells were stimulated for 30 min at room temperature with 5 µl agonist diluted in assay buffer alone or for inhibition approaches with agonist in the presence of the indicated concentrations of forskolin,. The reactions were stopped by addition of lysis buffer containing HTRF® assay reagents: anti-cAMP conjugate

and cAMP-d2, 5 µl each. After incubation for 1 h at room temperature, FRET signals were detected at λ_{ex} 320 nm and λ_{em} 665 nm (d2) and λ_{em} 620 (europium cryptate) using the Mithras LB 940 multimode reader (Berthold Technologies). Data analysis was performed as described and according to the formula depicted above.

HTRF®IP one assay

Accumulation of inositol phosphates was detected according to the HTRF®-IP-One kit (Cisbio) instructions and was used for FFA1-HEK and GPR55-AD-HEK cells.

The kit includes the following buffers and reagents:

- lysis buffer (50 mM phosphate buffer (pH 7.0), 1 M KF and 1.25% Triton X-100)
- europium cryptate-labeled anti-IP-1 antibody (IP-1-conjugate)
- d2-labeled IP-1 (IP-1-d2)

Assay protocol

Cells were harvested, counted and the required amount of cells was collected and washed (HBSS + 20 mM HEPES). Cells were then resuspended in assay buffer (HBSS, 20 mM HEPES, 50 mM LiCl), plated at 100,000 cells/7µl per well in a 384-well microplate, settled by a short centrifugation step (1 min, 120g) and incubated for 30 min at 37°C. Receptors were challenged by the addition of 7 µl compound solution solved in assay buffer. Reaction takes place within 30 min at room temperature and was terminated by addition of lysis buffer containing HTRF® assay reagents: anti-IP-1 conjugate and IP-1-d2, 3 µl each. After incubation for 1 h at room temperature, FRET signals were detected at λ_{ex} 320 nm, λ_{em} 665 nm (d2) and λ_{em} 620 (europium cryptate) using the Mithras LB 940 multimode reader (Berthold Technologies). Data analysis was made based on the fluorescence ratio emitted by d2-labeled cAMP (665 nm) over the light emitted by the europium cryptate-labeled anti-cAMP (620 nm). Data analysis was performed as described and according to the formula depicted above.

5.4.5 Calcium assays in CRTH2-HEK cells

CRTH2-HEK cells were transiently transfected to co-express the chimeric G□qi5 protein (see also 5.2.1), engineered to funnel signaling of Gαi sensitive receptors to the Gαq signaling pathway, using the calcium phosphate precipitation method as described above (5.3.3.1). 24 h after transfection cells were detached and plated into 96 well assay plates at a density of 80,000 cells per well. After 24 h cells were washed twice with KHB buffer, and 50 µl of Ca4 solution (Calcium 4 assay kit, Molecular Devices) were applied. Cells were incubated for 30 min prior to challenge with the respective compounds. Fluorescence output was measured in a Novostar® microplate reader with a built-in pipetor (BMG LabTech). Detection of fluorescence at λex 485 nm and λem 520 nm was initiated by injecting 20 µl of the respective agonist solution sequentially into separate wells.

5.4.6 Internalization assay

Assays were performed by Dr. Lene Martini from the Ernest Gallo Clinic & Research Centre, University of California, San Fransisco, Emeryville, CA 94608, US as described previously (Schröder, et al., 2009). See also chapter 2.3, legend at **figure 29**.

5.4.7 Functional assays in primary human leukocytes

Assays at human eosinophils and T helper type 2 (Th2) cells were performed by Dr. Luzheng Xue and Dr. Roy Pettipher from the Oxagen Ltd, 91 Milton Park, Abingdon Oxon, OX14 4RY, UK.

Eosinophile shape change assay

Assays with primary human eosinophils were performed as described previously (Sabroe, et al., 1999). See also the legend of **figure 30** (chapter 2.3.2).

T-helper 2 (Th2) cell migration assay

Assays with primary human Th2 cells were performed as described previously (Vinall, et al., 2007). See also the legend of **figure 29** (chapter 2.3.3).

Th2 calcium flux assay

Calcium flux assays in primary human Th2 cells were performed as described previously (Hirai, et al., 2001). See also the legend of **figure 30** (chapter 2.3.3).

5.4.8 Calculations and data analysis

Data calculation and EC_{50} value determination by nonlinear regression was accomplished using Prism® 4.02 (Graph Pad). Quantification of DMR signals for concentration effect curves was performed as indicated: (i) for $G\alpha_i$ coupling events with a clear maximum peak, this maximum response value was used in the range of 300 and 1200 s, (ii) for all other response profiles the area under the curve (AUC) was calculated in the range of 0 and 3600 s. All optical DMR recordings were buffer corrected. For data normalization, indicated as relative response (%), top levels of concentration effect curves were set 100% and bottom levels 0%. DMR signatures were normalized by setting the maximum response of the depicted time frame to 100 %.

Where appropriate, differences in means were examined by two way analysis of variance (ANOVA) with Bonferroni's multiple comparison post-hoc testing using Prism® 4.02. P values were considered as significant (*) if $p < 0.05$, as very significant (**) if $p < 0.01$ and as extremely significant (***) if $p < 0.001$.

6. Abbreviations

°C	degrees Celsius
µ	10^{-6}
λ	lambda, wavelength (nm)
AlF	aluminium fluoride (AlF_4^-)
ANOVA	analysis of variance
AUC	area under curve
BRET	bioluminescence resonance energy transfer
BSA	bovine serum albumin
cAMP	cyclic 3'-5'-adenosine monophosphate
Cch	carbachol
cDNA	complementary DNA
CHO	Chinese hamster ovary (cells)
COX	cyclo oxygenase
CRTH2	chemo attractant receptor homologous molecule expressed on T-helper type 2 cells
CTX	cholera toxin
DAG	diacylglycerol
DMEM	Dulbecco's modified eagle medium
DMR	dynamic mass redistribution
DMSO	dimethyl sulfoxide
DNA	deoxyribonucleic acid
DP	D-prostanoid receptor
E. coli	*Escherichia coli*
EDTA	diethylenediaminetetraacetic acid
EP	E-prostanoid receptor
EPAC	exchange protein activated by cAMP
FCS	fetal calf (bovine) serum
FFA1	free fatty acid receptor 1
FRET	fluorescence resonance energy transfer
Fsk	foskolin
FU	fluorescence units
g	gram
g	acceleration by gravity
G418	geneticin
GDP	guanosine-5′-diphosphate

GEF	guanine nucleotide exchange factor
GPCR	G protein-coupled receptor
G protein	guanine nucleotide-binding protein
GTP	guanosine-5′-triphosphate
GRK	G protein-coupled receptor kinase
h	human
h	hours
HBSS	Hanks' balanced salt solutions
HEK	human embryonic kidney (cells)
HEPES	4-(2-Hydroxyethyl)-1-piperazineethane sulfonic acid
HRP	horseradish peroxidase
IBMX	3-Isobutyl-1-methylxanthine
IP1	inositol-4-phosphate
IP3	inositol-1,3,4-triphosphate
KHB	Krebs-HEPES-buffer
l	liter
LB-medium	Luria Bertani medium
m	meter
m	milli
MAPK	mitogen-activated protein kinase
min	minutes
M	molar (mol/l)
n	nano (10^{-9})
n	number
p	pico (10^{-12})
p	p-value, probability
pEC_{50}	negative logarithm (base 10) of half maximal effect concentration (EC_{50})
PBS	phosphate buffered saline
PG	prostaglandin
PGDS	prostaglandin D synthase
PGES	prostaglandin E synthase
PKA	protein kinase A
pH	the negative logarithm (base 10) of the molar concentration of dissolved hydronium ions (H_3O^+)
PKC	protein kinase C
PLC	phospholipase C
PTX	Pertussis toxin

RFU	relative fluorescence units
rpm	revolutions per minute
RPMI	Roswell Park Memorial Institute
s	second
siRNA	short interference ribonucleic acid
SEM	standard error of the mean
TP	thromboxane receptor
TX	thromboxane
U	units
UV	ultraviolet
YM	YM254890 ($G\alpha_q$ protein inhibitor)

7. References

1. Antony, J., Kellershohn, K., Mohr-Andra, M., Kebig, A., Prilla, S., Muth, M., Heller, E., Disingrini, T., Dallanoce, C., Bertoni, S., Schrobang, J., Trankle, C., Kostenis, E., Christopoulos, A., Holtje, H.D., Barocelli, E., De Amici, M., Holzgrabe, U., and Mohr, K. (2009) Dualsteric GPCR targeting: a novel route to binding and signaling pathway selectivity. *FASEB J.* 23:442-450.
2. Aritake, K., Kado, Y., Inoue, T., Miyano, M., and Urade, Y. (2006) Structural and functional characterization of HQL-79, an orally selective inhibitor of human hematopoietic prostaglandin D synthase. *J. Biol. Chem.* 281:15277-15286.
3. Asano, H., Shimizu, K., Muramatsu, M., Iwama, Y., Toki, Y., Miyazaki, Y., Okumura, K., Hashimoto, H., and Ito, T. (1994) Prostaglandin H2 as an endothelium-derived contracting factor modulates endothelin-1-induced contraction. *J. Hypertens.* 12:383-390.
4. Barren, B., and Artemyev, N.O. (2007) Mechanisms of dominant negative G-protein alpha subunits. *J. Neurosci. Res.* 85:3505-3514.
5. Bell, J.G., Tocher, D.R., and Sargent, J.R. (1994) Effect of supplementation with 20:3(n-6), 20:4(n-6) and 20:5(n-3) on the production of prostaglandins E and F of the 1-, 2- and 3-series in turbot (Scophthalmus maximus) brain astroglial cells in primary culture. *Biochim. Biophys. Acta*1211:335-342.
6. Bigay, J., Deterre, P., Pfister, C., and Chabre, M. (1987) Fluoride complexes of aluminium or beryllium act on G-proteins as reversibly bound analogues of the gamma phosphate of GTP. *EMBO J.* 6:2907-2913.
7. Böhm, E., Sturm, G.J., Weiglhofer, I., Sandig, H., Shichijo, M., McNamee, A., Pease, J.E., Kollroser, M., Peskar, B.A., and Heinemann, A. (2004) 11-Dehydro-thromboxane B2, a stable thromboxane metabolite, is a full agonist of chemoattractant receptor-homologous molecule expressed on TH2 cells (CRTH2) in human eosinophils and basophils. *J. Biol. Chem.* 279:7663-7670.
8. Boie, Y., Sawyer, N., Slipetz, D.M., Metters, K.M., and Abramovitz, M. (1995) Molecular cloning and characterization of the human prostanoid DP receptor. *J. Biol. Chem.* 270:18910-18916.
9. Bokoch, G.M., Katada, T., Northup, J.K., Ui, M., and Gilman, A.G. (1984) Purification and properties of the inhibitory guanine nucleotide-binding regulatory component of adenylate cyclase. *J. Biol. Chem.* 259:3560-3567.
10. Bonacci, T.M., Mathews, J.L., Yuan, C., Lehmann, D.M., Malik, S., Wu, D., Font, J.L., Bidlack, J.M., and Smrcka, A.V. (2006) Differential targeting of Gbetagamma-subunit signaling with small molecules. *Science* 312:443-446.
11. Boukamp, P., Petrussevska, R.T., Breitkreutz, D., Hornung, J., Markham, A., and Fusenig, N.E. (1988) Normal keratinization in a spontaneously immortalized aneuploid human keratinocyte cell line. *J. Cell. Biol.* 106:761-771.
12. Boulvain, M., Kelly, A., and Irion, O. (2008) Intracervical prostaglandins for induction of labour. *Cochrane Database Syst. Rev.* 23;(1):CD006971.
13. Briscoe, C.P., Tadayyon, M., Andrews, J.L., Benson, W.G., Chambers, J.K., Eilert, M.M., Ellis, C., Elshourbagy, N.A., Goetz, A.S., Minnick, D.T., Murdock, P.R., Sauls, H.R., Jr., Shabon, U., Spinage, L.D., Strum, J.C., Szekeres, P.G., Tan, K.B., Way, J.M., Ignar, D.M., Wilson, S., et al. (2003) The orphan G protein-coupled receptor GPR40 is activated by medium and long chain fatty acids. *J. Biol. Chem.* 278:11303-11311.
14. Cabrera-Vera, T.M., Vanhauwe, J., Thomas, T.O., Medkova, M., Preininger, A., Mazzoni, M.R., and Hamm, H.E. (2003) Insights into G protein structure, function, and regulation. *Endocr. Rev.* 24:765-781.
15. Calebiro, D., Nikolaev, V.O., Persani, L., and Lohse, M.J. (2010) Signaling by internalized G-protein-coupled receptors. *Trends Pharmacol. Sci.* 31:221-228.

16. Camacho, M., Lopez-Belmonte, J., and Vila, L. (1998) Rate of vasoconstrictor prostanoids released by endothelial cells depends on cyclooxygenase-2 expression and prostaglandin I synthase activity. *Circ. Res.* 83:353-365.
17. Cameron, L., Depner, M., Kormann, M., Klopp, N., Illig, T., von Mutius, E., and Kabesch, M. (2009) Genetic variation in CRTh2 influences development of allergic phenotypes. *Allergy* 64:1478-1485.
18. Chilton, F.H., Rudel, L.L., Parks, J.S., Arm, J.P., and Seeds, M.C. (2008) Mechanisms by which botanical lipids affect inflammatory disorders. *Am. J. Clin. Nutr.* 87:498S-503S.
19. Christiansen, E., Urban, C., Merten, N., Liebscher, K., Karlsen, K.K., Hamacher, A., Spinrath, A., Bond, A.D., Drewke, C., Ullrich, S., Kassack, M.U., Kostenis, E., and Ulven, T. (2008) Discovery of potent and selective agonists for the free fatty acid receptor 1 (FFA(1)/GPR40), a potential target for the treatment of type II diabetes. *J. Med. Chem.* 51:7061-7064.
20. Chung, S., Funakoshi, T., and Civelli, O. (2008) Orphan GPCR research. *Br. J. Pharmacol.* 153 Suppl 1:S339-346.
21. Cockcroft, S., and Gomperts, B.D. (1985) Role of guanine nucleotide binding protein in the activation of polyphosphoinositide phosphodiesterase. *Nature* 314:534-536.
22. Conklin, B.R., Farfel, Z., Lustig, K.D., Julius, D., and Bourne, H.R. (1993) Substitution of three amino acids switches receptor specificity of Gq alpha to that of Gi alpha. *Nature* 363:274-276.
23. Corey, E.J., Nicolaou, K.C., Machida, Y., Malmsten, C.L., and Samuelsson, B. (1975) Synthesis and biological properties of a 9,11-azo-prostanoid: highly active biochemical mimic of prostaglandin endoperoxides. *Proc. Natl. Acad. Sci. U S A* 72:3355-3358.
24. de Souza, N.J., Dohadwalla, A.N., and Reden, J. (1983) Forskolin: a labdane diterpenoid with antihypertensive, positive inotropic, platelet aggregation inhibitory, and adenylate cyclase activating properties. *Med. Res. Rev.* 3:201-219.
25. Dodgson, K., Gedge, L., Murray, D.C., and Coldwell, M. (2009) A 100K well screen for a muscarinic receptor using the Epic label-free system--a reflection on the benefits of the label-free approach to screening seven-transmembrane receptors. *J. Recept. Signal Transduct. Res.* 29:163-172.
26. Eardley, I., Donatucci, C., Corbin, J., El-Meliegy, A., Hatzimouratidis, K., McVary, K., Munarriz, R., and Lee, S.W. (2010) Pharmacotherapy for erectile dysfunction. *J. Sex. Med.* 7:524-540.
27. Fang, Y. (2007) Non-Invasive Optical Biosensor for Probing Cell Signaling. *Sensors* 7:2316-2329.
28. Fang, Y., and Ferrie, A.M. (2007) Optical biosensor differentiates signaling of endogenous PAR1 and PAR2 in A431 cells. *BMC Cell Biol* 8:24.
29. Ferguson, S.S. (2001) Evolving concepts in G protein-coupled receptor endocytosis: the role in receptor desensitization and signaling. *Pharmacol. Rev.* 53:1-24.
30. Folco, G., and Murphy, R.C. (2006) Eicosanoid transcellular biosynthesis: from cell-cell interactions to in vivo tissue responses. *Pharmacol. Rev.* 58:375-388.
31. Fredriksson, R., Lagerstrom, M.C., Lundin, L.G., and Schioth, H.B. (2003) The G-protein-coupled receptors in the human genome form five main families. Phylogenetic analysis, paralogon groups, and fingerprints. *Mol. Pharmacol.* 63:1256-1272.
32. Galandrin, S., and Bouvier, M. (2006) Distinct signaling profiles of beta1 and beta2 adrenergic receptor ligands toward adenylyl cyclase and mitogen-activated protein kinase reveals the pluridimensionality of efficacy. *Mol. Pharmacol.* 70:1575-1584.
33. Galandrin, S., Oligny-Longpre, G., and Bouvier, M. (2007) The evasive nature of drug efficacy: implications for drug discovery. *Trends Pharmacol. Sci.* 28:423-430.
34. Gazi, L., Gyles, S., Rose, J., Lees, S., Allan, C., Xue, L., Jassal, R., Speight, G., Gamble, V., and Pettipher, R. (2005) Delta12-prostaglandin D2 is a potent and selective CRTH2 receptor agonist and causes activation of human eosinophils and Th2 lymphocytes. *Prostaglandins Other Lipid Mediat.* 75:153-167.
35. Gervais, F.G., Cruz, R.P., Chateauneuf, A., Gale, S., Sawyer, N., Nantel, F., Metters, K.M., and O'Neill G, P. (2001) Selective modulation of chemokinesis, degranulation, and apoptosis in eosinophils through the PGD2 receptors CRTH2 and DP. *J. Allergy Clin. Immunol.* 108:982-988.

36. Gill, D.M., and Meren, R. (1978) ADP-ribosylation of membrane proteins catalyzed by cholera toxin: basis of the activation of adenylate cyclase. *Proc Natl. Acad. Sci. U S A* 75:3050-3054.
37. Gloerich, M., and Bos, J.L. (2010) Epac: defining a new mechanism for cAMP action. *Annu. Rev. Pharmacol. Toxicol.* 50:355-375.
38. Hamberg, M., and Fredholm, B.B. (1976) Isomerization of prostaglandin H2 into prostaglandin D2 in the presence of serum albumin. *Biochim. Biophys. Acta* 431:189-183.
39. Hamberg, M., Svensson, J., and Samuelsson, B. (1974a) Prostaglandin endoperoxides. A new concept concerning the mode of action and release of prostaglandins. *Proc. Natl. Acad. Sci., U S A* 71:3824-3828.
40. Hamberg, M., Svensson, J., Wakabayashi, T., and Samuelsson, B. (1974b) Isolation and structure of two prostaglandin endoperoxides that cause platelet aggregation. *Proc. Natl. Acad. Sci. U S A* 71:345-349.
41. Hara, S., Kamei, D., Sasaki, Y., Tanemoto, A., Nakatani, Y., and Murakami, M. (2010) Prostaglandin E synthases: Understanding their pathophysiological roles through mouse genetic models. *Biochimie* 92:651-659.
42. Hata, A.N., and Breyer, R.M. (2004) Pharmacology and signaling of prostaglandin receptors: multiple roles in inflammation and immune modulation. *Pharmacol, Ther,* 103:147-166.
43. Heilker, R., Wolff, M., Tautermann, C.S., and Bieler, M. (2009) G-protein-coupled receptor-focused drug discovery using a target class platform approach. *Drug, Discov, Today* 14:231-240.
44. Hein, L., Meinel, L., Pratt, R.E., Dzau, V.J., and Kobilka, B.K. (1997) Intracellular trafficking of angiotensin II and its AT1 and AT2 receptors: evidence for selective sorting of receptor and ligand. *Mol, Endocrinol,* 11:1266-1277.
45. Heinemann, A., Schuligoi, R., Sabroe, I., Hartnell, A., and Peskar, B.A. (2003) Delta 12-prostaglandin J2, a plasma metabolite of prostaglandin D2, causes eosinophil mobilization from the bone marrow and primes eosinophils for chemotaxis. *J. Immunol.* 170:4752-4758.
46. Henstridge, C.M., Balenga, N.A., Ford, L.A., Ross, R.A., Waldhoer, M., and Irving, A.J. (2009) The GPR55 ligand L-alpha-lysophosphatidylinositol promotes RhoA-dependent Ca2+ signaling and NFAT activation. *FASEB J.* 23:183-193.
47. Henstridge, C.M., Balenga, N.A., Schroder, R., Kargl, J.K., Platzer, W., Martini, L., Arthur, S., Penman, J., Whistler, J.L., Kostenis, E., Waldhoer, M., and Irving, A.J. (2010) GPR55 ligands promote receptor coupling to multiple signalling pathways. *Br. J. Pharmacol.* 160:604-614.
48. Hirai, H., Tanaka, K., Yoshie, O., Ogawa, K., Kenmotsu, K., Takamori, Y., Ichimasa, M., Sugamura, K., Nakamura, M., Takano, S., and Nagata, K. (2001) Prostaglandin D2 selectively induces chemotaxis in T helper type 2 cells, eosinophils, and basophils via seven-transmembrane receptor CRTH2. *J. Exp. Med.* 193:255-261.
49. Hoffmann, C., Gaietta, G., Bunemann, M., Adams, S.R., Oberdorff-Maass, S., Behr, B., Vilardaga, J.P., Tsien, R.Y., Ellisman, M.H., and Lohse, M.J. (2005) A FlAsH-based FRET approach to determine G protein-coupled receptor activation in living cells. *Nat. Methods* 2:171-176.
50. Hohwy, M., Spadola, L., Lundquist, B., Hawtin, P., Dahmen, J., Groth-Clausen, I., Nilsson, E., Persdotter, S., von Wachenfeldt, K., Folmer, R.H., and Edman, K. (2008) Novel prostaglandin D synthase inhibitors generated by fragment-based drug design. *J. Med. Chem.* 51:2178-2186.
51. Huang, J.L., Gao, P.S., Mathias, R.A., Yao, T.C., Chen, L.C., Kuo, M.L., Hsu, S.C., Plunkett, B., Togias, A., Barnes, K.C., Stellato, C., Beaty, T.H., and Huang, S.K. (2004) Sequence variants of the gene encoding chemoattractant receptor expressed on Th2 cells (CRTH2) are associated with asthma and differentially influence mRNA stability. *Hum. Mol. Genet.* 13:2691-2697.
52. Inoue, T., Okano, Y., Kado, Y., Aritake, K., Irikura, D., Uodome, N., Okazaki, N., Kinugasa, S., Shishitani, H., Matsumura, H., Kai, Y., and Urade, Y. (2004) First determination of the inhibitor complex structure of human hematopoietic prostaglandin D synthase. *J. Biochem.* 135:279-283.

53. Irikura, D., Aritake, K., Nagata, N., Maruyama, T., Shimamoto, S., and Urade, Y. (2009) Biochemical, functional, and pharmacological characterization of AT-56, an orally active and selective inhibitor of lipocalin-type prostaglandin D synthase. *J. Biol. Chem.* 284:7623-7630.
54. Itoh, Y., Kawamata, Y., Harada, M., Kobayashi, M., Fujii, R., Fukusumi, S., Ogi, K., Hosoya, M., Tanaka, Y., Uejima, H., Tanaka, H., Maruyama, M., Satoh, R., Okubo, S., Kizawa, H., Komatsu, H., Matsumura, F., Noguchi, Y., Shinohara, T., Hinuma, S., et al. (2003) Free fatty acids regulate insulin secretion from pancreatic beta cells through GPR40. *Nature* 422:173-176.
55. Jacoby, E., Bouhelal, R., Gerspacher, M., and Seuwen, K. (2006) The 7 TM G-protein-coupled receptor target family. *ChemMedChem* 1:761-782.
56. Jiang, J., Ganesh, T., Du, Y., Thepchatri, P., Rojas, A., Lewis, I., Kurtkaya, S., Li, L., Qui, M., Serrano, G., Shaw, R., Sun, A., and Dingledine, R. (2010) Neuroprotection by selective allosteric potentiators of the EP2 prostaglandin receptor. *Proc. Natl. Acad. Sci. U S A* 107:2307-2312.
57. Kanaoka, Y., Ago, H., Inagaki, E., Nanayama, T., Miyano, M., Kikuno, R., Fujii, Y., Eguchi, N., Toh, H., Urade, Y., and Hayaishi, O. (1997) Cloning and crystal structure of hematopoietic prostaglandin D synthase. *Cell* 90:1085-1095.
58. Kanaoka, Y., and Urade, Y. (2003) Hematopoietic prostaglandin D synthase. *Prostaglandins Leukot. Essent. Fatty Acids* 69:163-167.
59. Kaslow, H.R., Lim, L.K., Moss, J., and Lesikar, D.D. (1987) Structure-activity analysis of the activation of pertussis toxin. *Biochemistry* 26:123-127.
60. Kato, T., Iwama, Y., Okumura, K., Hashimoto, H., Ito, T., and Satake, T. (1990) Prostaglandin H2 may be the endothelium-derived contracting factor released by acetylcholine in the aorta of the rat. *Hypertension* 15:475-481.
61. Kebig, A., Kostenis, E., Mohr, K., and Mohr-Andra, M. (2009) An optical dynamic mass redistribution assay reveals biased signaling of dualsteric GPCR activators. *J. Recept. Signal Transduct. Res.* 29:140-145.
62. Kenakin, T. (1995) Agonist-receptor efficacy. I: Mechanisms of efficacy and receptor promiscuity. *Trends Pharmacol. Sci.* 16:188-192.
63. Kenakin, T. (2010) Functional Selectivity and Biased Receptor Signaling. *J Pharmacol. Exp. Ther.* (Epub ahead of print)
64. Kenakin, T.P. (2009) Cellular assays as portals to seven-transmembrane receptor-based drug discovery. *Nat. Rev. Drug Discov.* 8:617-626.
65. Kim, H.Y., Kim, J.R., and Kim, H.S. (2008) Upregulation of lipopolysaccharide-induced interleukin-10 by prostaglandin A1 in mouse peritoneal macrophages. *J. Microbiol. Biotechnol.* 18:1170-1178.
66. Konger, R.L., Scott, G.A., Landt, Y., Ladenson, J.H., and Pentland, A.P. (2002) Loss of the EP2 prostaglandin E2 receptor in immortalized human keratinocytes results in increased invasiveness and decreased paxillin expression. *Am. J. Pathol.* 161:2065-2078.
67. Kostenis, E., Martini, L., Ellis, J., Waldhoer, M., Heydorn, A., Rosenkilde, M.M., Norregaard, P.K., Jorgensen, R., Whistler, J.L., and Milligan, G. (2005a) A highly conserved glycine within linker I and the extreme C terminus of G protein alpha subunits interact cooperatively in switching G protein-coupled receptor-to-effector specificity. *J. Pharmacol. Exp. Ther.* 313:78-87.
68. Kostenis, E., and Ulven, T. (2006) Emerging roles of DP and CRTH2 in allergic inflammation. *Trends Mol. Med.* 12:148-158.
69. Kostenis, E., Waelbroeck, M., and Milligan, G. (2005b) Techniques: promiscuous Galpha proteins in basic research and drug discovery. *Trends Pharmacol. Sci.* 26:595-602.
70. Kramarenko, II, Bunni, M.A., Morinelli, T.A., Raymond, J.R., and Garnovskaya, M.N. (2009) Identification of functional bradykinin B(2) receptors endogenously expressed in HEK293 cells. *Biochem. Pharmacol.* 77:269-276.
71. Kunkel, S.L., Thrall, R.S., Kunkel, R.G., McCormick, J.R., Ward, P.A., and Zurier, R.B. (1979) Suppression of immune complex vasculitis in rats by prostaglandin. *J. Clin. Invest.* 64:1525-1529.
72. Lagerström, M.C., and Schioth, H.B. (2008) Structural diversity of G protein-coupled receptors and significance for drug discovery. *Nat. Rev. Drug. Discov.* 7:339-357.

73. Lander, E.S., Linton, L.M., Birren, B., Nusbaum, C., Zody, M.C., Baldwin, J., Devon, K., Dewar, K., Doyle, M., FitzHugh, W., Funke, R., Gage, D., Harris, K., Heaford, A., Howland, J., Kann, L., Lehoczky, J., LeVine, R., McEwan, P., McKernan, K., et al. (2001) Initial sequencing and analysis of the human genome. *Nature* 409:860-921.
74. Leduc, M., Breton, B., Gales, C., Le Gouill, C., Bouvier, M., Chemtob, S., and Heveker, N. (2009) Functional selectivity of natural and synthetic prostaglandin EP4 receptor ligands. *J. Pharmacol. Exp. Ther.* 331:297-307.
75. Lee, P.H., Gao, A., van Staden, C., Ly, J., Salon, J., Xu, A., Fang, Y., and Verkleeren, R. (2008) Evaluation of dynamic mass redistribution technology for pharmacological studies of recombinant and endogenously expressed g protein-coupled receptors. *Assay. Drug. Dev. Technol.* 6:83-94.
76. Lefkowitz, R.J. (2007) Seven transmembrane receptors: something old, something new. *Acta Physiol. (Oxf)* 190:9-19.
77. Levin, G., Duffin, K.L., Obukowicz, M.G., Hummert, S.L., Fujiwara, H., Needleman, P., and Raz, A. (2002) Differential metabolism of dihomo-gamma-linolenic acid and arachidonic acid by cyclo-oxygenase-1 and cyclo-oxygenase-2: implications for cellular synthesis of prostaglandin E1 and prostaglandin E2. *Biochem. J.* 365:489-496.
78. Liu, B., and Wu, D. (2004) Analysis of the coupling of G12/13 to G protein-coupled receptors using a luciferase reporter assay. *Methods Mol. Biol.* 237:145-149.
79. Lukacs, N.W., Berlin, A.A., Franz-Bacon, K., Sasik, R., Sprague, L.J., Ly, T.W., Hardiman, G., Boehme, S.A., and Bacon, K.B. (2008) CRTH2 antagonism significantly ameliorates airway hyperreactivity and downregulates inflammation-induced genes in a mouse model of airway inflammation. *Am. J. Physiol. Lung Cell Mol. Physiol.* 295:L767-779.
80. Luster, A.D., and Tager, A.M. (2004) T-cell trafficking in asthma: lipid mediators grease the way. *Nat. Rev. Immunol.* 4:711-724.
81. Ma, Y.C., Huang, J., Ali, S., Lowry, W., and Huang, X.Y. (2000) Src tyrosine kinase is a novel direct effector of G proteins. *Cell* 102:635-646.
82. Mandal, A.K., Zhang, Z., Kim, S.J., Tsai, P.C., and Mukherjee, A.B. (2005) Yin-yang: balancing act of prostaglandins with opposing functions to regulate inflammation. *J. Immunol.* 175:6271-6273.
83. Marchese, A., Sawzdargo, M., Nguyen, T., Cheng, R., Heng, H.H., Nowak, T., Im, D.S., Lynch, K.R., George, S.R., and O'Dowd B, F. (1999) Discovery of three novel orphan G-protein-coupled receptors. *Genomics* 56:12-21.
84. Marullo, S., and Bouvier, M. (2007) Resonance energy transfer approaches in molecular pharmacology and beyond. *Trends Pharmacol. Sci.* 28:362-365.
85. Mathiesen, J.M., Christopoulos, A., Ulven, T., Royer, J.F., Campillo, M., Heinemann, A., Pardo, L., and Kostenis, E. (2006) On the mechanism of interaction of potent surmountable and insurmountable antagonists with the prostaglandin D2 receptor CRTH2. *Mol. Pharmacol.* 69:1441-1453.
86. Mathiesen, J.M., Ulven, T., Martini, L., Gerlach, L.O., Heinemann, A., and Kostenis, E. (2005) Identification of indole derivatives exclusively interfering with a G protein-independent signaling pathway of the prostaglandin D2 receptor CRTH2. *Mol. Pharmacol.* 68:393-402.
87. McConnell, H.M., Owicki, J.C., Parce, J.W., Miller, D.L., Baxter, G.T., Wada, H.G., and Pitchford, S. (1992) The cytosensor microphysiometer: biological applications of silicon technology. *Science* 257:1906-1912.
88. Meyer, B.H., Freuler, F., Guerini, D., and Siehler, S. (2008) Reversible translocation of p115-RhoGEF by G(12/13)-coupled receptors. *J. Cell Biochem.* 104:1660-1670.
89. Millar, R.P., and Newton, C.L. (2010) The year in G protein-coupled receptor research. *Mol. Endocrinol.* 24:261-274.
90. Milligan, G. (2003) Principles: extending the utility of [35S]GTP gamma S binding assays. *Trends Pharmacol. Sci.* 24:87-90.
91. Milligan, G. (2009) G protein-coupled receptor hetero-dimerization: contribution to pharmacology and function. *Br. J. Pharmacol.* 158:5-14.
92. Milligan, G., and Kostenis, E. (2006) Heterotrimeric G-proteins: a short history. *Br. J. Pharmacol.* 147 Suppl 1:S46-55.

93. Monneret, G., Gravel, S., Diamond, M., Rokach, J., and Powell, W.S. (2001) Prostaglandin D2 is a potent chemoattractant for human eosinophils that acts via a novel DP receptor. *Blood* 98:1942-1948.
94. Monneret, G., Li, H., Vasilescu, J., Rokach, J., and Powell, W.S. (2002) 15-Deoxy-delta 12,14-prostaglandins D2 and J2 are potent activators of human eosinophils. *J. Immunol.* 168:3563-3569.
95. Müllershausen, F., Zecri, F., Cetin, C., Billich, A., Guerini, D., and Seuwen, K. (2009) Persistent signaling induced by FTY720-phosphate is mediated by internalized S1P1 receptors. *Nat. Chem. Biol.* 5:428-434.
96. Murota, H., Kotobuki, Y., Umegaki, N., Tani, M., and Katayama, I. (2008) New aspect of anti-inflammatory action of lipo-prostaglandinE1 in the management of collagen diseases-related skin ulcer. *Rheumatol. Int.* 28:1127-1135.
97. Nagata, K., Hirai, H., Tanaka, K., Ogawa, K., Aso, T., Sugamura, K., Nakamura, M., and Takano, S. (1999a) CRTH2, an orphan receptor of T-helper-2-cells, is expressed on basophils and eosinophils and responds to mast cell-derived factor(s). *FEBS Lett.* 459:195-199.
98. Nagata, K., Tanaka, K., Ogawa, K., Kemmotsu, K., Imai, T., Yoshie, O., Abe, H., Tada, K., Nakamura, M., Sugamura, K., and Takano, S. (1999b) Selective expression of a novel surface molecule by human Th2 cells in vivo. *J. Immunol.* 162:1278-1286.
99. Nishimura, A., Kitano, K., Takasaki, J., Taniguchi, M., Mizuno, N., Tago, K., Hakoshima, T., and Itoh, H. (2010) Structural basis for the specific inhibition of heterotrimeric Gq protein by a small molecule. *Proc. Natl. Acad. Sci. U S A* 107:13666-13671.
100. Nomiya, R., Okano, M., Fujiwara, T., Maeda, M., Kimura, Y., Kino, K., Yokoyama, M., Hirai, H., Nagata, K., Hara, T., Nishizaki, K., and Nakamura, M. (2008) CRTH2 plays an essential role in the pathophysiology of Cry j 1-induced pollinosis in mice. *J. Immunol.* 180:5680-5688.
101. Northup, J.K., Sternweis, P.C., Smigel, M.D., Schleifer, L.S., Ross, E.M., and Gilman, A.G. (1980) Purification of the regulatory component of adenylate cyclase. *Proc. Natl. Acad. Sci. U S A* 77:6516-6520.
102. Oldham, W.M., and Hamm, H.E. (2008) Heterotrimeric G protein activation by G-protein-coupled receptors. *Nat. Rev. Mol. Cell Biol.* 9:60-71.
103. Overington, J.P., Al-Lazikani, B., and Hopkins, A.L. (2006) How many drug targets are there? *Nat. Rev. Drug. Discov.* 5:993-996.
104. Peters, M.F., Vaillancourt, F., Heroux, M., Valiquette, M., and Scott, C.W. (2009) Comparing label-free biosensors for pharmacological screening with cell-based functional assays. *Assay Drug Dev. Technol.* 8:219-227.
105. Pettipher, R. (2008) The roles of the prostaglandin D(2) receptors DP(1) and CRTH2 in promoting allergic responses. *Br. J. Pharmacol.* 153 Suppl 1:S191-199.
106. Pierce, K.L., and Lefkowitz, R.J. (2001) Classical and new roles of beta-arrestins in the regulation of G-protein-coupled receptors. *Nat. Rev. Neurosci.* 2:727-733.
107. Pierce, K.L., Premont, R.T., and Lefkowitz, R.J. (2002) Seven-transmembrane receptors. *Nat. Rev. Mol. Cell Biol.* 3:639-650.
108. Prezeau, L., Rives, M.L., Comps-Agrar, L., Maurel, D., Kniazeff, J., and Pin, J.P. (2010) Functional crosstalk between GPCRs: with or without oligomerization. *Curr. Opin. Pharmacol.* 10:6-13.
109. Radmark, O., and Samuelsson, B. (2010) Microsomal prostaglandin E synthase-1 and 5-lipoxygenase: potential drug targets in cancer. *J. Intern. Med.* 268:5-14.
110. Rocheville, M., and Jerman, J.C. (2009) 7TM pharmacology measured by label-free: a holistic approach to cell signalling. *Curr. Opin. Pharmacol.* 9:643-649.
111. Ross, E.M., and Gilman, A.G. (1980) Biochemical properties of hormone-sensitive adenylate cyclase. *Annu. Rev. Biochem.* 49:533-564.
112. Ross, R.A. (2009) The enigmatic pharmacology of GPR55. *Trends Pharmacol. Sci.* 30:156-163.
113. Rossi, A., Kapahi, P., Natoli, G., Takahashi, T., Chen, Y., Karin, M., and Santoro, M.G. (2000) Anti-inflammatory cyclopentenone prostaglandins are direct inhibitors of IkappaB kinase. *Nature* 403:103-108.

114. Ryberg, E., Larsson, N., Sjogren, S., Hjorth, S., Hermansson, N.O., Leonova, J., Elebring, T., Nilsson, K., Drmota, T., and Greasley, P.J. (2007) The orphan receptor GPR55 is a novel cannabinoid receptor. *Br. J. Pharmacol.* 152:1092-1101.
115. Sabroe, I., Hartnell, A., Jopling, L.A., Bel, S., Ponath, P.D., Pease, J.E., Collins, P.D., and Williams, T.J. (1999) Differential regulation of eosinophil chemokine signaling via CCR3 and non-CCR3 pathways. *J. Immunol.* 162:2946-2955.
116. Saito, M., Tanabe, Y., Kudo, I., and Nakayama, K. (2003) Endothelium-derived prostaglandin H2 evokes the stretch-induced contraction of rabbit pulmonary artery. *Eur. J. Pharmacol.* 467:151-161.
117. Samama, P., Cotecchia, S., Costa, T., and Lefkowitz, R.J. (1993) A mutation-induced activated state of the beta 2-adrenergic receptor. Extending the ternary complex model. *J. Biol. Chem.* 268:4625-4636.
118. Samuelsson, B., Goldyne, M., Granstrom, E., Hamberg, M., Hammarstrom, S., and Malmsten, C. (1978) Prostaglandins and thromboxanes. *Annu. Rev. Biochem.* 47:997-1029.
119. Sandig, H., Andrew, D., Barnes, A.A., Sabroe, I., and Pease, J. (2006) 9alpha,11beta-PGF2 and its stereoisomer PGF2alpha are novel agonists of the chemoattractant receptor, CRTH2. *FEBS Lett.* 580:373-379.
120. Sawyer, N., Cauchon, E., Chateauneuf, A., Cruz, R.P., Nicholson, D.W., Metters, K.M., O'Neill, G.P., and Gervais, F.G. (2002) Molecular pharmacology of the human prostaglandin D2 receptor, CRTH2. *Br. J. Pharmacol.* 137:1163-1172.
121. Schröder, R., Janssen, N., Schmidt, J., Kebig, A., Merten, N., Hennen, S., Muller, A., Blattermann, S., Mohr-Andra, M., Zahn, S., Wenzel, J., Smith, N.J., Gomeza, J., Drewke, C., Milligan, G., Mohr, K., and Kostenis, E. (2010) Deconvolution of complex G protein-coupled receptor signaling in live cells using dynamic mass redistribution measurements. *Nat. Biotechnol.* 28:943-949.
122. Schröder, R., Merten, N., Mathiesen, J.M., Martini, L., Kruljac-Letunic, A., Krop, F., Blaukat, A., Fang, Y., Tran, E., Ulven, T., Drewke, C., Whistler, J., Pardo, L., Gomeza, J., and Kostenis, E. (2009) The C-terminal tail of CRTH2 is a key molecular determinant that constrains Galphai and downstream signaling cascade activation. *J. Biol. Chem.* 284:1324-1336.
123. Schuligoi, R., Sedej, M., Waldhoer, M., Vukoja, A., Sturm, E.M., Lippe, I.T., Peskar, B.A., and Heinemann, A. (2009) Prostaglandin H2 induces the migration of human eosinophils through the chemoattractant receptor homologous molecule of Th2 cells, CRTH2. *J. Leukoc. Biol.* 85:136-145.
124. Scott, C.W., and Peters, M.F. (2010) Label-free whole-cell assays: expanding the scope of GPCR screening. *Drug Discov. Today* 15:704-716.
125. Shiraishi, Y., Asano, K., Niimi, K., Fukunaga, K., Wakaki, M., Kagyo, J., Takihara, T., Ueda, S., Nakajima, T., Oguma, T., Suzuki, Y., Shiomi, T., Sayama, K., Kagawa, S., Ikeda, E., Hirai, H., Nagata, K., Nakamura, M., Miyasho, T., and Ishizaka, A. (2008) Cyclooxygenase-2/prostaglandin D2/CRTH2 pathway mediates double-stranded RNA-induced enhancement of allergic airway inflammation. *J. Immunol.* 180:541-549.
126. Shirasaki, H., Kikuchi, M., Kanaizumi, E., and Himi, T. (2009) Accumulation of CRTH2-positive leukocytes in human allergic nasal mucosa. *Ann. Allergy Asthma Immunol.* 102:110-115.
127. Siehler, S. (2009) Regulation of RhoGEF proteins by G12/13-coupled receptors. *Br. J. Pharmacol.* 158:41-49.
128. Simon, M.I., Strathmann, M.P., and Gautam, N. (1991) Diversity of G proteins in signal transduction. *Science* 252:802-808.
129. Smyth, E.M., Grosser, T., Wang, M., Yu, Y., and FitzGerald, G.A. (2009) Prostanoids in health and disease. *J. Lipid Res.* 50 Suppl:S423-428.
130. Soler, M., Camacho, M., Sola, R., and Vila, L. (2001) Mesangial cells release untransformed prostaglandin H2 as a major prostanoid. *Kidney Int.* 59:1283-1289.
131. Sorkin, A., and von Zastrow, M. (2009a) Endocytosis and signalling: intertwining molecular networks. *Nat. Rev. Mol. Cell Biol.* 10:609-622.
132. Sorkin, A., and von Zastrow, M. (2009b) Endocytosis and signalling: intertwining molecular networks. *Nat. Rev. Mol. Cell Biol.* 10:609-622.

133. Sprang, S.R. (1997) G proteins, effectors and GAPs: structure and mechanism. *Curr. Opin. Struct. Biol.* 7:849-856.
134. Sternweis, P.C., and Robishaw, J.D. (1984) Isolation of two proteins with high affinity for guanine nucleotides from membranes of bovine brain. *J. Biol. Chem.* 259:13806-13813.
135. Stoddart, L.A., Brown, A.J., and Milligan, G. (2007) Uncovering the pharmacology of the G protein-coupled receptor GPR40: high apparent constitutive activity in guanosine 5'-O-(3-[35S]thio)triphosphate binding studies reflects binding of an endogenous agonist. *Mol. Pharmacol.* 71:994-1005.
136. Strathmann, M.P., and Simon, M.I. (1991) G alpha 12 and G alpha 13 subunits define a fourth class of G protein alpha subunits. *Proc. Natl. Acad. Sci. U S A* 88:5582-5586.
137. Stubbs, V.E., Schratl, P., Hartnell, A., Williams, T.J., Peskar, B.A., Heinemann, A., and Sabroe, I. (2002) Indomethacin causes prostaglandin D(2)-like and eotaxin-like selective responses in eosinophils and basophils. *J. Biol. Chem.* 277:26012-26020.
138. Sturm, E.M., Schratl, P., Schuligoi, R., Konya, V., Sturm, G.J., Lippe, I.T., Peskar, B.A., and Heinemann, A. (2008) Prostaglandin E2 inhibits eosinophil trafficking through E-prostanoid 2 receptors. *J. Immunol.* 181:7273-7283.
139. Sugimoto, Y., and Narumiya, S. (2007) Prostaglandin E receptors. *J. Biol. Chem.* 282:11613-11617.
140. Svensson, J., Hamberg, M., and Samuelsson, B. (1975) Prostaglandin endoperoxides IX. Characterization of rabbit aorta contracting substance (RCS) from guinea pig lung and human platelets. *Acta Physiol. Scand.* 94:222-228.
141. Tajima, T., Murata, T., Aritake, K., Urade, Y., Hirai, H., Nakamura, M., Ozaki, H., and Hori, M. (2008) Lipopolysaccharide induces macrophage migration via prostaglandin D(2) and prostaglandin E(2). *J Pharmacol. Exp. Ther.* 326:493-501.
142. Takasaki, J., Saito, T., Taniguchi, M., Kawasaki, T., Moritani, Y., Hayashi, K., and Kobori, M. (2004) A novel Galphaq/11-selective inhibitor. *J. Biol. Chem.* 279:47438-47445.
143. Uller, L., Mathiesen, J.M., Alenmyr, L., Korsgren, M., Ulven, T., Hogberg, T., Andersson, G., Persson, C.G., and Kostenis, E. (2007) Antagonism of the prostaglandin D2 receptor CRTH2 attenuates asthma pathology in mouse eosinophilic airway inflammation. *Respir. Res.* 8:16.
144. Ulven, T., and Kostenis, E. (2010) Novel CRTH2 antagonists: a review of patents from 2006 to 2009. *Expert. Opin. Ther. Pat.* 20(11):1505-30
145. Urade, Y., and Hayaishi, O. (2000) Biochemical, structural, genetic, physiological, and pathophysiological features of lipocalin-type prostaglandin D synthase. *Biochim. Biophys. Acta* 1482:259-271.
146. Venter, J.C., Adams, M.D., Myers, E.W., Li, P.W., Mural, R.J., Sutton, G.G., Smith, H.O., Yandell, M., Evans, C.A., Holt, R.A., Gocayne, J.D., Amanatides, P., Ballew, R.M., Huson, D.H., Wortman, J.R., Zhang, Q., Kodira, C.D., Zheng, X.H., Chen, L., Skupski, M., et al. (2001) The sequence of the human genome. *Science* 291:1304-1351.
147. Vinall, S.L., Townsend, E.R., and Pettipher, R. (2007) A paracrine role for chemoattractant receptor-homologous molecule expressed on T helper type 2 cells (CRTH2) in mediating chemotactic activation of CRTH2+ CD4+ T helper type 2 lymphocytes. *Immunology* 121:577-584.
148. Wang, H., Deng, J.L., Yue, J., Li, J., and Hou, Y.B. (2010) Prostaglandin E1 for preventing the progression of diabetic kidney disease. *Cochrane. Database Syst. Rev.* 12;(5):CD006872.
149. Wei, H., Ahn, S., Shenoy, S.K., Karnik, S.S., Hunyady, L., Luttrell, L.M., and Lefkowitz, R.J. (2003) Independent beta-arrestin 2 and G protein-mediated pathways for angiotensin II activation of extracellular signal-regulated kinases 1 and 2. *Proc. Natl. Acad. Sci. U S A* 100:10782-10787.
150. Whistler, J.L., Gerber, B.O., Meng, E.C., Baranski, T.J., von Zastrow, M., and Bourne, H.R. (2002) Constitutive activation and endocytosis of the complement factor 5a receptor: evidence for multiple activated conformations of a G protein-coupled receptor. *Traffic* 3:866-877.
151. Woehler, A., and Ponimaskin, E.G. (2009) G protein--mediated signaling: same receptor, multiple effectors. *Curr Mol Pharmacol* 2:237-248.
152. Worzfeld, T., Wettschureck, N., and Offermanns, S. (2008) G(12)/G(13)-mediated signalling in mammalian physiology and disease. *Trends Pharmacol. Sci.* 29:582-589.

153. Xue, L., Barrow, A., and Pettipher, R. (2009) Novel function of CRTH2 in preventing apoptosis of human Th2 cells through activation of the phosphatidylinositol 3-kinase pathway. *J. Immunol.* 182:7580-7586.
154. Xue, L., Gyles, S.L., Barrow, A., and Pettipher, R. (2007) Inhibition of PI3K and calcineurin suppresses chemoattractant receptor-homologous molecule expressed on Th2 cells (CRTH2)-dependent responses of Th2 lymphocytes to prostaglandin D(2). *Biochem. Pharmaco.l* 73:843-853.
155. Xue, L., Gyles, S.L., Wettey, F.R., Gazi, L., Townsend, E., Hunter, M.G., and Pettipher, R. (2005) Prostaglandin D2 causes preferential induction of proinflammatory Th2 cytokine production through an action on chemoattractant receptor-like molecule expressed on Th2 cells. *J. Immunol.* 175:6531-6536.
156. Yahara, H., Satoh, T., Miyagishi, C., and Yokozeki, H. (2010) Increased expression of CRTH2 on eosinophils in allergic skin diseases. *J. Eur. Acad. Dermatol. Venereol.* 24:75-76.
157. Yoshimura-Uchiyama, C., Iikura, M., Yamaguchi, M., Nagase, H., Ishii, A., Matsushima, K., Yamamoto, K., Shichijo, M., Bacon, K.B., and Hirai, K. (2004) Differential modulation of human basophil functions through prostaglandin D2 receptors DP and chemoattractant receptor-homologous molecule expressed on Th2 cells/DP2. *Clin. Exp. Allergy* 34:1283-1290.
158. Yu, B., and Simon, M.I. (1998) Interaction of the xanthine nucleotide binding Goalpha mutant with G protein-coupled receptors. *J. Biol. Chem.* 273:30183-30188.
159. Zhang, J.Z., Maruyama, K., Iwatsuki, K., Ono, I., and Kaneko, F. (1994) Effects of prostaglandin E1 on human keratinocytes and dermal fibroblasts: a possible mechanism for the healing of skin ulcers. *Exp. Dermatol.* 3:164-170.
160. Zurier, R.B. (1982) Prostaglandins, immune responses, and murine lupus. *Arthritis Rheum.* 25:804-809.
161. Zurier, R.B., and Quagliata, F. (1971) Effect of prostaglandin E 1 on adjuvant arthritis. *Nature* 234:304-305.

9. Publications

Research articles:

Schröder, R., Merten, N., Mathiesen, J. M., Martini, L., Kruljac-Letunic, A., Krop, F., Blaukat, A., Fang, Y., Tran, E., Ulven, T., Drewke, C., Whistler, J.L., Pardo, L., Gomeza, J., and Kostenis, E.
(2009) The C-terminal tail of CRTH2 is a key molecular determinant that constrains Gαi- and downstream-signaling cascade activation. *The Journal of Biological Chemistry* 284(2), 1324-1336 (IF 5.3)

Henstridge, C.M., Balenga, N.A.B., Schröder, R., Kargl, J.K., Platzer, W., Martini, L., Arthur, S., Whistler, J.L., Kostenis, E., Waldhoer, M., and Irving, A.
(2010) GPR55 ligands promote receptor coupling to multiple signalling pathways. *British Journal of Pharmacology* 160:604-614 (IF 5.2)

Schröder, R., Janssen, N., Schmidt, J., Kebig, A., Merten, N., Hennen, S., Müller, A., Blättermann, S., Mohr-Andrä, M., Zahn, S., Wenzel, J., Smith, N.J., Gomeza, J., Drewke, C., Milligan, G., Mohr, K., and Kostenis, E.
(2010) Deconvolution of complex G protein coupled receptor signaling in live cells using dynamic mass redistribution measurements. *Nature Biotechnology* 28(9):943-949 (IF 29.5)

Balenga, N.A.B., Aflaki, E., Julia Kargl, J., Schröder, R., Stefanie Blättermann, S., Kostenis, K., Brown, A., Heinemann, A., and Maria Waldhoer, M.
(in revision) GPR55 regulates cannabinoid 2 receptor-mediated responses in human neutrophils. *Cell Research* (IF 8.2)

Schröder, R., Martini, L., Xue, L., Whistler, J.L., Uven, T., Pettipher, R. and Kostenis, E.
(submitted) PGH_1 the precursor for the anti-inflammatory prostaglandins of the 1-series is a potent activator of the pro-inflammatory receptor CRTH2/DP2. *The Journal of Biological Chemistry* (IF 5.3)

Oral presentation:

Schröder, R., Müller, A., Zahn, S., Wenzel, J., and Kostenis, E.
(2009) Utilizing dynamic mass redistribution to record signaling of endogenous E prostanoid (EP) receptors in immortalized and primary human cells. 51. Jahrestagung der Deutschen Gesellschaft für Experimentelle und Klinische Pharmakologie und Toxikologie (DGPT), Mainz, *Naunyn-Schmiedeberger's Archives of Pharmacology* 381 (Supplement 1): 15

Poster presentations:

Schröder, R. and Kostenis, E.
(2009) Utilizing dynamic mass redistribution, a novel label-free technology to quantify activation and inhibition of CRTH2 signaling in living cells. *Gordon Research Conference:* Molecular Pharmacology, Barga, Italy

Schröder, R., Müller, A., Zahn, S., Wenzel, J., and Kostenis, E.
(2009) Utilizing dynamic mass redistribution to record signaling of E prostanoid (EP) receptores in immortalized and primary human cells. *Corning Label-Free-Summit,* Fontainebleau, France

10. Acknowledgements

First and foremost I am especially grateful to my supervisor Prof. Dr. Evi Kostenis who gave me the possibility to carry out a very exciting Ph.D. and introduced me to the fascinating field of G protein coupled receptor research. She provides an excellent guidance and support and I would like to thank her for the contributions of time and valuable discussions. Superlatively appears her talent to inspire for this field of research.

I would also like to thank Prof. Dr. Gabriele König for officiating as second referee and for the pleasant collaboration in teaching matters with regard to the course "Biology for Pharmacists III / Biologie für Pharmazeuten III".

I would like to express my sincere thanks to Prof. Dr. Klaus Mohr for the very pleasant and successful cooperation and support particularly with regard to the DMR validation project. I am also grateful for his participation in the examination committee.

I wish to express my gratitude to Prof. Dr. Heinz Bönisch for participation in the evaluation committee.

Some special tasks involved in this study were performed in cooperation with other research groups. For this work thanks go to:
Dr. Lene Martini and Prof. Dr. Jennifer Whistler, Department of Neurology, Ernest Gallo Clinic & Research Centre, University of California, San Fransisco, Emeryville, CA 94608, US, for contributing the CRTH2 internalization assays.
Dr. Luzheng Xue and Dr. Roy Pettipher from the Oxagen Ltd, 91 Milton Park, Abingdon Oxon, OX14 4RY, UK, for providing the assays in primary human eosinophils and Th2 cells.

I would like to thank Dr. Christel Drewke and Dr. Jesus Gomeza for constructive contributions in many concerns. Especially many thanks to Christel for proof-reading the first version of my thesis and the nice collaboration in the course "Biology for Pharmacists III / Biologie für Pharmazeuten III"

I would also like to thank very much all my colleagues for providing a very enjoyable atmosphere accomplished with constructive mutual assistance. I am especially grateful to Marianne Vasmer-Ehses for the pleasant and successful interaction and her experimental support.

I would like to thank all members of the Institute for Pharmaceutical Biology, University of Bonn, for cooperation and support.

Many thanks go to the members of the working group of Prof. Dr. Mohr for the pleasant and successful cooperation.